

4.75
48

Petrology of the Noritic and
Gabbro-noritic Rocks below the
J-M Reef in the Mountain View Area,
Stillwater Complex, Montana

U.S. GEOLOGICAL SURVEY BULLETIN 1674-C



Chapter C

Petrology of the Noritic and Gabbronoritic Rocks below the J–M Reef in the Mountain View Area, Stillwater Complex, Montana

By NORMAN J PAGE and BARRY C. MORING

U.S. GEOLOGICAL SURVEY BULLETIN 1674

CONTRIBUTIONS ON ORE DEPOSITS IN THE EARLY MAGMATIC ENVIRONMENT

DEPARTMENT OF THE INTERIOR

MANUEL LUJAN, JR., Secretary

U.S. GEOLOGICAL SURVEY

Dallas L. Peck, Director



Any use of trade, product, or firm names in this publication is for descriptive purposes only and does not imply endorsement by the U.S. Government

UNITED STATES GOVERNMENT PRINTING OFFICE, WASHINGTON : 1990

For sale by the Books and
Open-File Reports Section,
U.S. Geological Survey
Federal Center, Box 25425
Denver, CO 80225

Library of Congress Cataloging-in-Publication Data

Page, Norman, J

Petrology of the noritic and gabbro-noritic rocks below the J-M Reef in the Mountain View area, Stillwater Complex, Montana / by Norman J Page and Barry C. Moring.

p. cm. — (U.S. Geological Survey bulletin ; 1674-C) (Contributions on ore deposits in the early magmatic environment

Includes bibliographical references.

Supt. of Docs. no.: I 19.3: 1674-C

1. Petrology—Beartooth Mountains Region (Mont. and Wyo.) 2. Geology—Beartooth Mountains Region (Mont. and Wyo.) I. Moring, Barry C. II. Title. III. Title: Stillwater Complex, Montana. IV. Series. V. Series: Contributions on ore deposits in the early magmatic environment ; ch. C.

QE75.B9 no. 1674-C

557.3 s—dc20

89-600286

[QE445.M9]

[552.09786'6]

CIP

CONTENTS

Abstract	C1
Introduction and previous studies	C1
Acknowledgments	C2
Generalized geologic history of the Stillwater Complex and adjacent rocks	C2
Terminology and stratigraphic considerations	C3
Methods and techniques	C6
Geology and stratigraphy of the Lower Banded series	C6
Geologic setting in the Mountain View area	C7
Stratigraphic characteristics of the lower part of the Lower Banded series	C10
Definition, distribution, and thickness of the subzones and zones	C10
Norite I zone	C10
Subzone 1	C10
Subzone 2	C10
Subzone 3	C10
Gabbronorite I zone	C12
Subzone 1	C12
Subzone 2	C13
Subzone 3	C14
Subzone 4	C14
Olivine-bearing I zone	C14
Norite II zone	C16
Structures in the rocks below Olivine-bearing I zone	C16
Modal and phase layering	C16
Fabric of layers from subzone 2 of the Gabbronorite I zone	C18
Size-graded layering	C20
Layering similar to current types (irregular layering)	C20
Syn depositional deformation structures	C22
Petrography of the Norite I and Gabbronorite I zones	C25
Plagioclase cumulate	C25
Plagioclase-bronzite cumulates	C28
Plagioclase-bronzite-augite cumulate	C30
Plagioclase-bronzite-chromite cumulate	C33
Modal mineralogy	C33
Mineral composition	C36
Sulfide mineral variation in subzone 4 of the Gabbronorite I zone	C37
Rock geochemistry of subzone 4 of the Gabbronorite I zone	C39
Environments of magmatic accumulation below the J-M Reef	C41
Discussion and development of a model for the genesis of the Norite I and Gabbronorite I zones	C44
References cited	C45

PLATE

[Plate is in pocket]

1. Geologic map showing the lower part of the Lower Banded series, west side of Stillwater canyon, Mountain View area, Stillwater Complex, Montana.

FIGURES

1. Simplified geologic map of Beartooth Mountains **C3**
2. Correlation chart of nomenclature used for subdividing rock succession in Stillwater Complex **C5**
3. Geologic map of part of Mountain View area **C8**
4. Generalized schematic composite columnar section and rock description of part of Lower Banded series **C11**
5. Columnar section of subzone 1 of Norite I zone **C12**
6. Photograph of contact between subzones 1 and 2 of Norite I zone **C14**
- 7–10. Columnar sections showing stratigraphy, modal mineralogy, and plagioclase and bronzite compositions
 7. Subzone 2 of Norite I zone **C15**
 8. Subzone 3 of Norite I zone **C16**
 9. Subzone 1 of Gabbronorite I zone **C18**
 10. Subzone 2 of Gabbronorite I zone **C19**
11. Photographs of plagioclase cumulate layers in subzone 2 of Gabbronorite I zone **C20**
12. Columnar section showing stratigraphy, modal mineralogy, and plagioclase and bronzite compositions, subzone 3 of Gabbronorite I zone **C21**
13. Columnar sections showing stratigraphy, modal mineralogy, and plagioclase and bronzite compositions, subzone 4 of Gabbronorite I zone **C22**
14. Columnar sections showing stratigraphy, modal mineralogy, and plagioclase and bronzite compositions, Norite II zone **C24**
15. Photograph of two rock slabs from subzone 2 of Gabbronorite I zone **C25**
16. Plot of microprobe analyses of bronzite and plagioclase compositions in layers of samples 60EDJ1 and 60EDJ2 from subzone 2 of Gabbronorite I zone **C26**
17. Petrofabric diagrams of bronzite from bronzite-plagioclase cumulates of subzone 2 of the Gabbronorite I zone **C27**
18. Histogram of size of bronzite crystals in single samples **C28**
19. Columnar section of upper part of subzone 4 of Gabbronorite I zone and variation in size of bronzite crystals and cumulate color index **C28**
20. Photographs of crosslamination **C29**
21. Photograph of wispy layering near contact of subzone 2 with subzone 3 of Norite I zone **C29**
22. Schematic sketch map of “Snoopy’s Doghouse” area **C30**
23. Photograph of bronzite plagioclase and plagioclase cumulate layers in basinlike structure from “Snoopy’s Doghouse” area **C31**
24. Photograph of ramp structure at locality A on plate 1 **C31**
25. Photograph of slump structure at “Snoopy’s Doghouse” area **C31**
26. Photomicrograph of bronzite with spiderweb overgrowth in plagioclase-bronzite cumulate **C32**
27. Triangular diagrams of mode of bronzite, augite, and plagioclase for plagioclase-bronzite cumulates **C32**
28. Photomicrograph of plagioclase overgrowth poikilitically enclosing augite in plagioclase-bronzite-augite cumulate **C32**
29. Columnar section based on core from drill hole DS-2/WD-6 showing textural grading **C32**
30. Textural categories and their variations shown schematically **C33**
31. Triangular diagrams of plagioclase-bronzite-augite cumulates **C34**
32. Photomicrograph of plagioclase-bronzite-chromite cumulate from subzone 1 of Norite I zone **C34**
- 33–36. Graphs comparing:
 33. Weighted-average plagioclase, bronzite, and augite modes by subzone and zone **C34**

34. Average total and cumulus modes for plagioclase-bronzite cumulate by subzone and zone **C35**
35. Average mode of plagioclase-bronzite-augite cumulates by subzone and zone **C36**
36. Average plagioclase and bronzite compositions by subzone and zone **C37**
37. Generalized composite columnar sections for lower part of Banded series in Mountain View area **C38**
38. Columnar section and graphs comparing estimated sulfide mineral abundance and silicate stratigraphy in subzone 4 of Gabbonorite I zone **C40**
39. Graphs of standard residuals from regressions of several elements against total pyroxene mode, plotted against stratigraphic position, in subzone 4 of Gabbonorite I zone **C43**

TABLES

1. Generalized geologic history of the Stillwater Complex, Montana **C4**
2. Weighted-average modes by subzone and zone **C34**
3. Average total and cumulus modes for plagioclase-bronzite cumulates by subzone and zone **C35**
4. Average total and cumulus modes for plagioclase-bronzite-augite cumulates by subzone and zone **C36**
5. Average, range, and standard deviations of mineral compositions of plagioclase and bronzite by subzone and zone **C37**
6. Trace element analyses of rock samples from subzone 4 of the Gabbonorite I zone **C41**
7. Correlation coefficients of log-transformed concentrations of selected trace elements in rocks from subzone 4 of the Gabbonorite I zone **C42**
8. Average concentrations of selected trace elements in rocks from subzone 4 of the Gabbonorite I zone based on analyses in table 5 **C42**
9. Correlation coefficients of log-transformed concentrations of selected elements, total pyroxene mode, and En content of bronzite for rocks from subzone 4 of the Gabbonorite I zone **C42**

Petrology of the Noritic and Gabbronoritic Rocks below the J-M Reef in the Mountain View Area, Stillwater Complex, Montana

By Norman J. Page and Barry C. Moring

Abstract

Field, petrologic, and geochemical investigations of part of the Lower Banded series of the Stillwater Complex, Montana, indicate that the cumulates forming the Norite I and Gabbronorite I zones can be divided into subzones and environments of deposition. The outcrops along the west side of the Stillwater River that contain units above the Bronzite zone of the Ultramafic series and below the Olivine-bearing I zone, containing the J-M Reef, are the focus of this investigation. The Norite I zone is divided into three subzones that tend to have cumulates with bronzite-rich bases and plagioclase-rich tops with unconformities between the subzones. The Gabbronorite I zone is divided into four subzones with bases enriched in bronzite and augite and tops enriched in plagioclase. Rock sequences are plagioclase-bronzite to plagioclase cumulates and plagioclase-bronzite-augite to plagioclase-bronzite to plagioclase cumulates. Two extremes of different depositional environments are reflected in the subzones. One, found in the lower parts of the subzones, produced cumulates with monotonous-appearing characteristics that vary only slightly over relatively large distances; the other, occurring mainly in the upper parts of subzones, produced cumulates that have highly variable characteristics over relatively short distances.

Characteristics of the monotonous-appearing cumulates include relatively thick modal and phase layers within which there is slight variation in the modal composition of the cumulates. Nevertheless, the layers exhibit pyroxene-enriched bases and plagioclase-enriched tops and are therefore mineral graded. Cryptic layering is limited; bronzite and plagioclase show only small changes in En and An content. Textural layering is rare.

Characteristics of the rocks representing the environment that produced highly variable cumulates include thin modal and phase layering, variable modal proportions, and variable bronzite and plagioclase compositions. Mineral, size, cryptic, and textural layering are well developed. Syndepositional structures, such as slump and ramp structures, and irregular layering such as crossbeds and basinlike structures are common. Changes take place rapidly up stratigraphic section and along strike.

Overall characteristics of the zones constrain models for the processes and include the following: (1) The average modal composition of plagioclase-bronzite and

plagioclase-bronzite-augite cumulates approaches hypothetical eutectoid compositions, although few individual samples do; (2) average bronzite and plagioclase compositions change by about only 3 percent in En and An contents, although they tend to change to lower En and An contents upward through the zones in a relatively regular fashion; (3) layer sequences most commonly are one- or two-pyroxene-plagioclase cumulates followed by plagioclase-bronzite and plagioclase cumulates or one-pyroxene-plagioclase followed by plagioclase cumulates; and (4) monotonous-appearing cumulates dominate the stratigraphic section in the Norite I zone, and the cumulates with variable characteristics have a progressively increasing dominance in the upper part of the Gabbronorite I zone as the Olivine-bearing I zone is approached.

One possible model for the development of these cumulate packages in the Lower Banded series consists of the following sequence of events: (1) Equilibrium crystallization of basaltic magma in approximately eutectoid proportions with the crystals suspended throughout the magma followed by settling, floating, or both of the cumulus crystals to produce the monotonous-appearing lower parts of the subzones; (2) continual changes in the orientation of the floor, perhaps related to the introduction of new magma into the chamber, that produced mechanical instability and initiated currents, convective cells, and instability in the crystal pile to produce the highly variable cumulates of the upper parts of subzones; (3) introduction of new magma either from an external source or by variable depth convection within the Stillwater chamber; and (4) return to mechanical stability and repetition of the processes. The progressive increasing dominance of cumulates with variable properties up section as the Olivine-bearing I zone is approached suggests that mechanical instability reached a maximum just before and perhaps during the deposition of the Olivine-bearing I zone and the J-M Reef.

INTRODUCTION AND PREVIOUS STUDIES

The glaciated outcrops of norite on the west side of the Stillwater River valley have attracted the attention of many investigators in the Stillwater Complex in southwestern Montana. These outcrops have been given a variety of

names: "westside of the Stillwater Valley" by Hess (1938a, 1960); "back of the home of M. W. Mouat" by Jones and others (1960); "Hjelsvik outcrop" in Anaconda Minerals Company informal usage; "Minneapolis Adit area" by Anaconda Minerals Company; and "Snoopy's Doghouse" in U.S. Geological Survey informal usage. Hess (1938a) developed his early observations and ideas concerning the origin of banding in norite and gabbro on the basis of these outcrops and later expanded these ideas and observations with detailed cross sections and sketches of structural features (Hess, 1960). Jones and others (1960) used observations from these outcrops as examples of the variation in layer thickness in the Banded series and as examples of gravity stratification. The discovery and exploration of the J-M Reef, a platinum-group-element mineralized zone, in the Mountain View area and elsewhere in the Stillwater Complex revived the interest in these outcrops and adjacent ones as representing the results of precursor processes to the development of the platinum-bearing zone. Before and during the period of exploration for platinum-group mineralization, other investigators studied rocks from the equivalent stratigraphic levels of the complex along strike and added geologic and mineralogic information for those areas (Hess, 1960; McCallum and others, 1980; Segerstrom and Carlson, 1982; Todd and others, 1982). This report focuses on stratigraphic, structural, mineralogic, petrologic, and geochemical details of these and adjacent outcrops that form the Lower Banded series below the J-M Reef in the Mountain View area.

Without the accumulated information base on the Stillwater Complex and adjacent rocks built since 1920 by several overlapping comprehensive investigations of structure, stratigraphy, geochemistry, and petrology of the complex, the present investigation would lack a framework. The stratigraphic nomenclature used in this report is that of Zientek and others (1985), who in addition to making stratigraphic recommendations summarized the previous usages. In the Lower Banded series, the usage in the report parallels that of McCallum and others (1980). The extensive studies of the bottom part of the complex, the Basal series, and the overlying Ultramafic series done up to 1984 are summarized and referenced in a guide to the Stillwater Complex edited by Czamanske and Zientek (1985). Peoples (1932, 1933, 1936), Hess (1936, 1938a, b; 1939, 1941, 1940, 1960), Hess and Phillips (1938, 1940), McCallum and others (1982), Segerstrom and Carlson (1982), Todd and others (1982), Lambert (1982), LeRoy (1985), and Foote (1985) concentrated on the Banded series. Isotopic studies include those of Nunes and Tilton (1971), DePaolo and Wasserberg (1979), Coffrant and others (1980), Nunes (1981), and Lambert and others (1985). Studies on sulfide minerals and platinum-group metals include those of Howland (1933), Howland and others (1936), Roby (1949), Page (1971a, b, 1972, 1979), Page and Jackson (1967), Page, Riley, and Haffty (1969, 1971, 1972), Page, Rowe, and Haffty (1976), Fuchs and Rose (1974), Cabri (1981),

Leonard and others (1969), Conn (1979), Barnes (1982), Boudreau (1982), Bow and others (1982), Todd and others (1982), Barnes and others (1982), Humphreys (1983), Barnes and Naldrett (1985), Turner and others (1985), and Mann and Lin (1985). Page (1977) summarized the information on the succession of rocks, metamorphism, and structure of the Stillwater Complex and adjacent rocks.

ACKNOWLEDGMENTS

During the previous studies, W.J. Nokleberg initiated a study of these norite outcrops under the guidance of E.D. Jackson. Subsequently, he has contributed unpublished maps and data on cumulate mineral analysis, fabric, and structure to this study. Without the cooperation of Anaconda Minerals Company and their personnel, including Richard N. Miller, Alistair Turner, Craig Bow, Diane Wolfgram, Jerry Dorherthy, and Roger Cooper, this project would not have been possible. The able field assistance of Lars D. Page during the summers of 1980 and 1981 is much appreciated. Numerous discussions over many years with Stan G. Todd of Manville Corporation have unclouded much fuzzy thinking.

GENERALIZED GEOLOGIC HISTORY OF THE STILLWATER COMPLEX AND ADJACENT ROCKS

The geologic history of the Stillwater Complex and associated rocks that crop out along a northwest-southeast trend on the north margin of the Beartooth Mountains in southwestern Montana (fig. 1) extends back over 3,140 m.y. (million years) and contains at least two mountain-building events. Page (1977) and Page and Zientek (1985) summarized the Precambrian events, and Jones and others (1960) described the post-Middle Cambrian events for the Stillwater area. Segerstrom and Carlson (1979) described some of the Cenozoic events. Foote and others (1961), Casella (1969), and Mueller and others (1985) gave summaries of the geology of the encircling Beartooth Mountain region. The geologic history of the area is summarized in table 1. Five major groups of rocks are present: (1) regionally metamorphosed rocks consisting of granitic gneiss and associated metasedimentary rocks of Precambrian or Archean age; (2) hornfelsed metasedimentary rocks associated with the Stillwater Complex; (3) stratiform mafic and ultramafic rocks of the Stillwater Complex; (4) an intrusive sequence of quartz monzonitic rocks of Precambrian age or Late Archean; and (5) sedimentary rocks of Paleozoic and Mesozoic age.

The events listed in table 1 that are the most significant in the generation of the Lower Banded series in its present position and attitude are (1) the fractionation and accumulation of magmatic sediments from the Stillwater magma(s); (2) low-grade regional metamorphism with possible thrust and normal faulting in the Early Proterozoic;

(3) faulting, rotation, tilting, and erosion before Middle Cambrian time; and (4) thrust, normal, and strike-slip faulting accompanying major Laramide uplift and deformation in early Paleocene through early Eocene time. Most of this report focuses on the first event, describing the resultant rocks and investigating the possible mechanisms and processes of formation of the Norite I and Gabbronorite I zones of the Lower Banded series.

TERMINOLOGY AND STRATIGRAPHIC CONSIDERATIONS

The subdivision of Stillwater Complex into the three major series, Basal, Ultramafic, and Banded, is based on the early publications of Jones and others (1960), Hess (1960), and Jackson (1961a) and many subsequent studies.

In recent years, several slightly different subdivisions of these series have been made (see summary diagrams in Zientek and others, 1985, for the details of each series). The various subdivisions proposed for the units immediately below, above, and within the J–M Reef are shown in figure 2. Each of the previous nomenclatures has its own attractions; however, we prefer to use the nomenclature shown in the righthand column, which parallels that of McCallum and others (1982), but is divided into subzones recognized in the Mountain View area.

The Norite I zone is defined to include all the rocks above the first appearance of cumulus plagioclase and below where the major amount of cumulus pyroxene through a relatively large stratigraphic section is augite. Below the Norite I zone is the Bronzite zone of the Ultramafic series, and above the Norite I zone are the Gabbronorite I, Olivine-bearing I, and Norite II zones. The

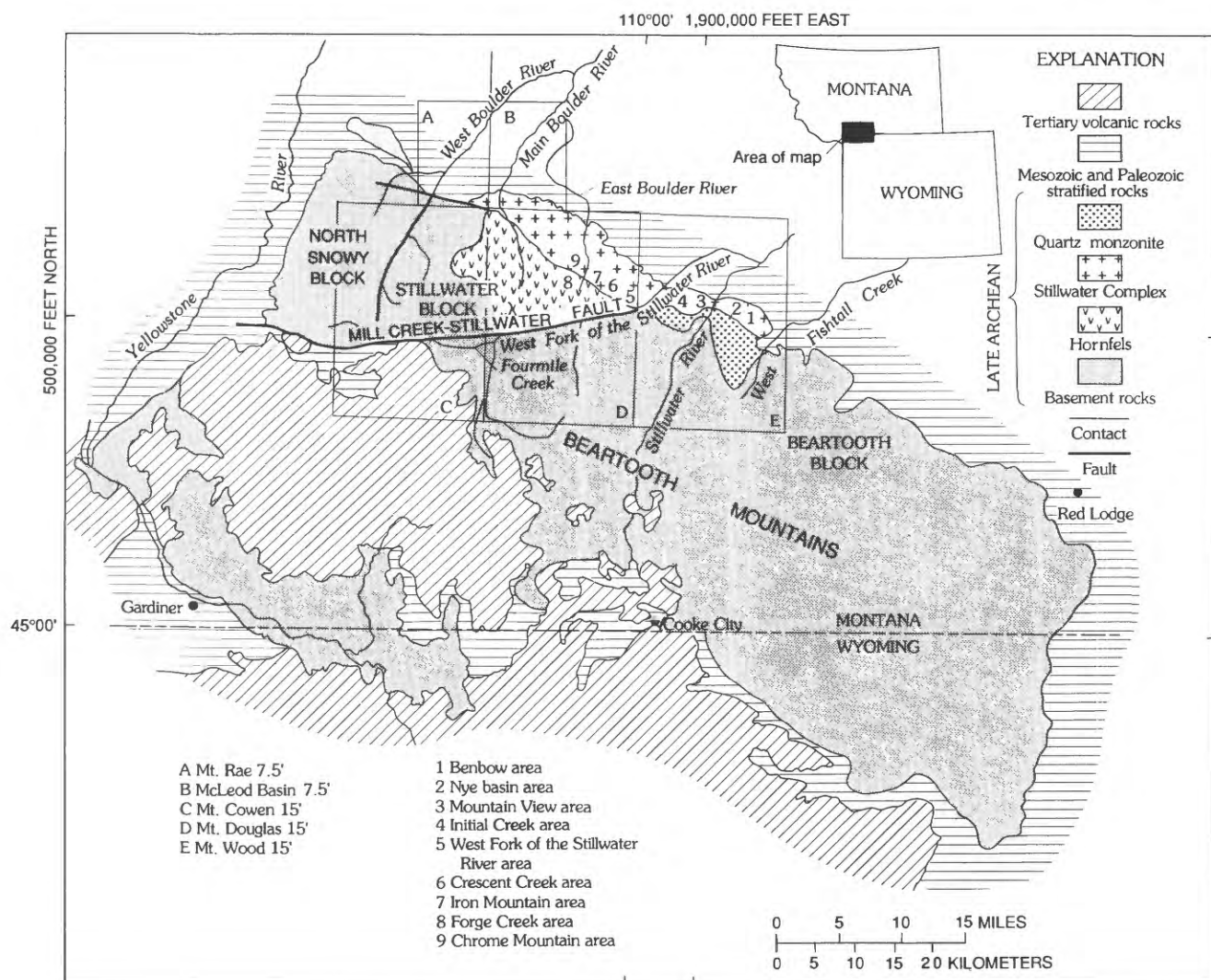


Figure 1. Simplified geologic map of Beartooth Mountains showing location of Stillwater Complex and areas discussed in report.

Table 1. Generalized geologic history of the Stillwater Complex, Montana

[From Page (1977), Jones and others (1960), Foose and others (1961), and Page and Zientek (1985)]

Age	Event
Middle Archean (before 3,270 Ma)	1. Presence of a terrane containing mafic, ultramafic, and intermediate composition rocks that were being actively eroded. 2. Deposition of clastic and chemically precipitated magnesium- and iron-enriched sediments including iron formation: deposition of a diamictite—possible local glaciation. 3. Complex folding of magnesium- and iron-enriched sediments, possible regional metamorphism.
Middle to Late Archean (2,750–3,140 Ma)	Strike-slip faulting, fractionation, and accumulation of magmatic sediments from Stillwater magma; intrusion of Stillwater magma and contact metamorphism of older rocks.
Late Archean (2,750±60 Ma)	Intrusion of quartz monzonitic rocks; contact metamorphism of older rocks.
Early Proterozoic (1,600–1,800 Ma)	Intrusion of mafic dikes, penetrative deformation, low-grade regional metamorphism, possible thrust and normal faulting.
Pre-Middle Cambrian	Faulting, rotation, tilting, and erosion.
Middle Cambrian	Subsidence of Stillwater Complex.
Middle Cambrian through Early Cretaceous	Deposition of 2,400–3,000 m of marine and continental sedimentary rocks with breaks in the Silurian and Permian.
Late Cretaceous	Extrusion of volcanic rocks: initiation of Laramide deformation.
Early Paleocene through early Eocene	Thrust, normal, and strike-slip faulting; major uplift and deformation; folding; intrusion of siliceous and intermediate sills, dikes, and stocks; extrusion of volcanic rocks (Laramide orogeny).
Middle Eocene through early Miocene	Erosion.
Miocene through Pliocene	Erosion and uplift.
Pleistocene through Holocene	Erosion and glaciation, minor faulting.

rocks are composed of various combinations of plagioclase, bronzite, augite, and olivine as cumulus phases. In the Mountain View area, the Norite I zone can be divided into three mappable units and the Gabbronorite I zone into four mappable units on the basis of textural and mineralogic variations (pl. 1; fig. 2). Other mappable units include the Olivine-bearing I and Norite II zones.

Subzones 1, 2, and 3 (listed in ascending order) of the Norite I zone consist of cumulates containing varying proportions of cumulus plagioclase and bronzite; augite is oikocrystic or interstitial. Each unit has modal layering caused by the variation in amounts of cumulus minerals and local phase layering caused by absence of cumulus bronzite; however, within a unit the overall amount of cumulus bronzite tends to decrease upward. These units would correspond to the Norite zone I subdivision of McCallum and others (1980) and Todd and others (1982, fig. 2) and to Segerstrom and Carlson's (1982) 250 m of plagioclase-bronzite cumulate.

The Gabbronorite I zone, subzones 1, 2, 3, and 4 (listed in ascending order), consists of cumulates containing varying proportions of cumulus plagioclase, bronzite, and augite. Both modal layering and phase layering are more common in these units than in the underlying ones. Within

a unit, the proportion of cumulus pyroxene tends to decrease upward; the amount of cumulus augite decreases more rapidly than bronzite. These units correspond with McCallum and others' (1980) Gabbronorite I and Todd and others' (1982) Gabbro zone I and appears to have been unrecognized by Segerstrom and Carlson (1982).

The Olivine-bearing I zone consists of cumulates characterized by repeating cycles dominated by olivine, olivine-plagioclase, and plagioclase cumulates, locally with pegmatoidal textures. The Olivine-bearing I zone also contains a zone of disseminated to net-textured sulfides enriched in platinum- group elements that is known as the J–M Reef (Todd and others, 1982). Previously the J–M Reef has been called the PGE-zone, zone of interest (zoi), and Howland Reef. The Olivine-bearing I zone corresponds in part with Todd and others' (1982) Troctolite-Anorthosite zone I and with Segerstrom and Carlson's (1982) 100 m of mixed group (fig. 2).

The Norite II zone consists of cumulates with varying proportions of plagioclase, bronzite, and augite; rocks containing cumulus augite are a minor component. The Norite II zone corresponds to the Norite zone II of Todd and others (1982) and may be equivalent to the upper 350 m of the Norite member of Segerstrom and Carlson (1982). The

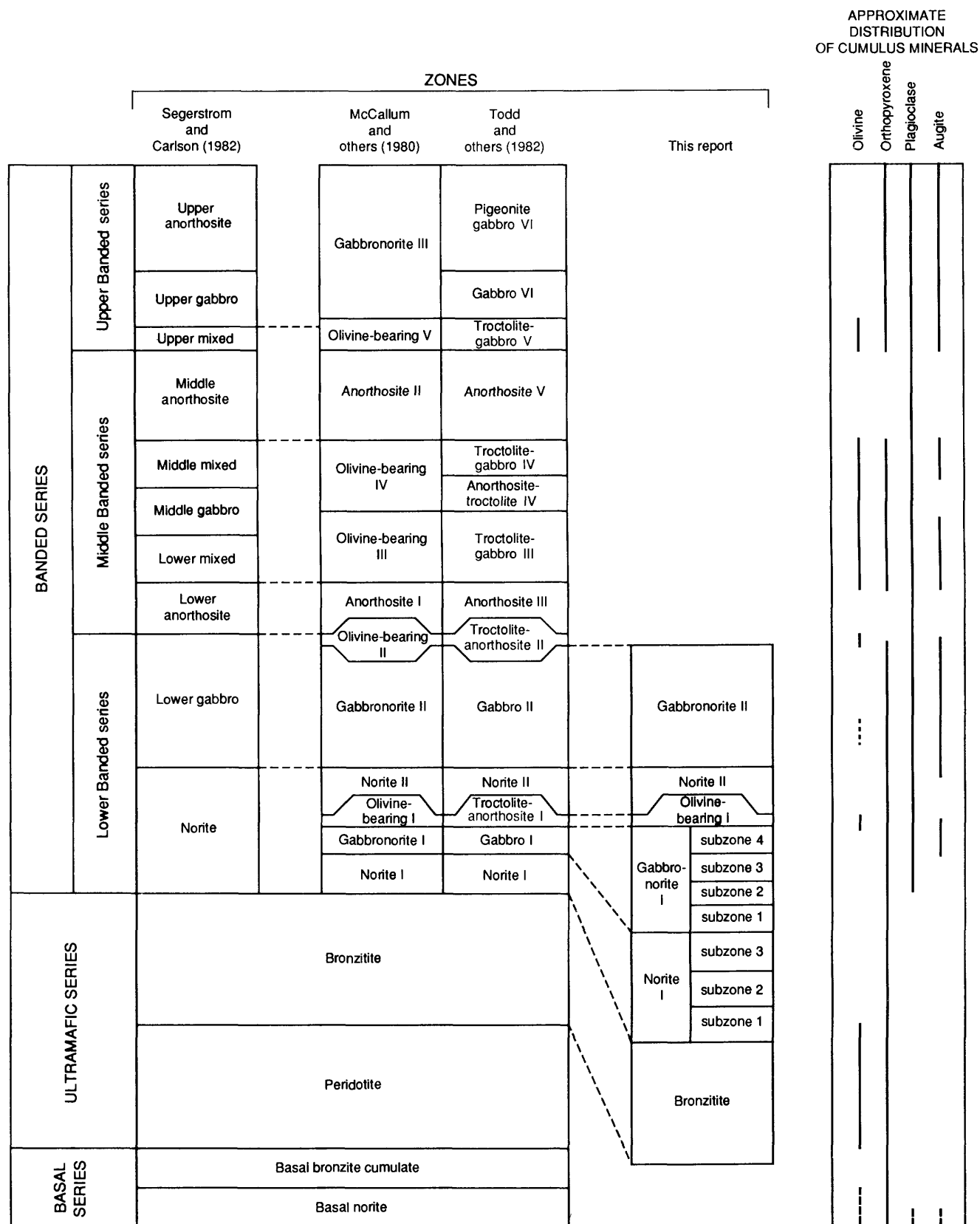


Figure 2. Correlation chart of nomenclature used for subdividing rock succession in Stillwater Complex, Montana (modified from Zientek and others, 1985).

details of the distribution, thickness, structures, fabrics, internal stratigraphy, petrology, mineral compositions, and geochemistry of each unit and synthesis of these data for the Lower Banded series make up most of this report.

Although cumulus terminology which contains the concept of crystal settling as developed by Wager and others (1960) and Jackson (1967) has been questioned on the correctness of the concept (Campbell, 1978; McBirney and Noyes, 1979), cumulus terminology is used in this report without a genetic connotation in the sense of Irvine (1982). Definitions, origins of terminology, and references to examples are adequately discussed by Irvine (1982) and need not be repeated here.

METHODS AND TECHNIQUES

Besides the normal usage of aerial photographs and topographic maps at various scales, stratigraphic sections, measured in detail, constitute a large part of the input into detailed maps. A schematic sketch map, reproduced here as figure 22, was constructed from sections 1.5 to 3 m apart with individual contacts and rock units traced in between sections. Although most of the sections in this report have been adjusted for dip, the reported thicknesses are approximations. A.E. Boudreau (University of Washington) contributed maps of faces and walls of the underground workings in the Minneapolis adit, which were used in conjunction with measured sections to produce the stratigraphic sections from underground workings.

Most of the samples, both hand and drillcore samples, were slabbed, ground, and etched with HF to amplify the plagioclase-pyroxene textural relations and to allow photocopying of slabs for working diagrams. Thin sections were described and for many of the samples polished thin sections were examined. Using grids and a binocular microscope, 500 points were counted on slabs to obtain modes of plagioclase, pyroxene, olivine, spinel, and sulfide and, in some samples, orthopyroxene-to-augite ratios. Modes of 1,000 points were also obtained from thin sections to refine the slab modes. In thin sections, exsolution lamellae in pyroxenes were counted as part of the host pyroxene, and alteration minerals were assigned to parent minerals where possible; otherwise, alteration minerals were counted as such. In some of the thin sections, attempts were made to separate cumulus material from postcumulus material, and the criteria for doing this will be discussed in a later section of the report. Grain sizes, maximum and minimum dimensions, were measured on slabs and in thin section. Usually, 60 to 100 grains were measured in a particular slab or thin section. The technique used is similar to that of Jackson (1961a) and Page (1979). Because the data are used only for internal comparisons, no corrections for sectioning effects were made.

Electron microprobe analyses of plagioclases (Scheidle, 1983; Czamanske and Scheidle, 1985) and of

pyroxenes (Zientek, 1983) have shown large (5 to 10 mole percent) variations in composition within single samples. These studies indicate that to obtain average pyroxene and plagioclase compositions by the microprobe would take an overwhelming effort. Because we wished to average the internal sample variations in composition, X-ray diffraction techniques developed with Stillwater plagioclases and pyroxenes were chosen. Himmelberg and Jackson (1967) developed a method for determining the ionic percentage of magnesium in bronzite, referred to in this report as the En (enstatite) content of bronzite. The precision of the measurements ranges from 0.08 to 2.54 percent En content and averages 1.14, which is well within the two-sigma deviation of ± 1.3 percent assigned to the determinative survey by Himmelberg and Jackson (1967). Many estimates of plagioclase composition were made during examination of thin sections, but all the compositions reported were determined by the X-ray method of Jackson (1961b) developed specifically for plagioclase from the Stillwater Complex. The uncertainty for the determinative curve is ± 2.1 percent An (anorthite) in the range of about An₆₅₋₈₀ and otherwise is ± 2.5 percent An (Jackson, 1961b). Precision of the measurements in this study is within these limits. Measurements between standard and unknown diffraction peaks were made using the computerized techniques described by Moring and Carlson (1985) and Carlson and Moring (1985).

GEOLOGY AND STRATIGRAPHY OF THE LOWER BANDED SERIES

The Norite I, Gabbronorite I, Olivine-bearing I, and Norite II zones crop out along a 40-km strike length between the Bronzite zone of the Ultramafic series and the Gabbronorite II zone of the Lower Banded series, as can be inferred from the maps by Segerstrom and Carlson (1982) or figure 4 of Page and Zientek (1985). At the east end, the complex is covered by glacial moraines in the Fishtail Creek area; it is cut out by faulting at the west end. Locally (for example, at the Benbow area), Paleozoic sedimentary rocks overlie the Banded series on an erosional unconformity. Attitudes of cumulus layering within the units and contacts with the overlying and underlying units strike between about N. 80° W. and N. 60° W. Page (1977, p. 59-62) discussed layering fabrics in the Banded series and pointed out that there is a consistent overall decrease in dip of cumulus layering from nearly vertical to overturned on the east end to near 60° N. on the west end of the complex, with an average strike of N. 78° W. and a dip of 77° N. Locally dips are as low as 30° N. These observations also apply to the Norite I, Gabbronorite I, Olivine-bearing I, and Norite II zones.

The approximate thickness of these zones ranges from about 320 m between the Mountain View and Initial Creek areas, where faulting has structurally thinned the unit, to about 1,067 m north of the Chrome Mountain area,

where faulting has thickened the unit by repetition. Normal thicknesses appear to be between 600 and 900 m where structures have not been recognized. The variation in thickness indicates that there is about 150 to 300 m of variation that is probably due to depositional conditions. North- or south-dipping, westerly striking ramp and thrust faults such as the Brownlee Creek, Iron Creek, and South Prairie fault systems locally alter profoundly the outcrop widths of these zones (see Page, 1977; Jones and others, 1960; Bow and others, 1982; and Turner and others, 1985, for detailed discussions), whereas the northeast-southwest-striking normal faults alter the strike continuity.

The contact between the Norite I zone and the underlying Bronzitite zone appears to be sharp and conformable or concordant, meaning that the attitude of the contact parallels cumulus layering in both zones. Locally, bronzite cumulate xenoliths are found in the Lower Banded series, such as those described by Hess (1960) from the East Boulder Plateau, which he believed were from the Bronzitite zone because of similar bronzite compositions (En_{86}). If his hypothesis is correct, then the contact between the Norite I zone and Bronzitite zone must locally be an unconformity. The contact between the Norite II zone and the overlying Gabbronorite II zone appears to be conformable and varies in nature from gradational, by interstratification of plagioclase-bronzite and plagioclase-bronzite-augite cumulates, to sharp, with the appearance of augite as a persistent cumulus mineral.

Geologic Setting in the Mountain View Area

The area under consideration, shown in figure 3, is part of the Mountain View area (fig. 1). The map units in figure 3 are based on Segerstrom and Carlson's (1982) nomenclature, unlike the rest of this report. Underlying rocks of the Mountain View area are contained within two blocks bounded by thrust faults. One block, bounded by the Lake fault and Bluebird thrust, has been rotated so that cumulus layering within the block is about at right angles to the average trend of cumulus layering in the rest of the complex. Major rock units within this block include the Stillwater Complex units consisting of the Basal series, Ultramafic series, and part of the Norite I zone; metasedimentary rocks below the complex; and quartz monzonites intrusive into the Basal series and the metasedimentary rocks. Geologic, structural, and petrologic problems within this block have been addressed by Jones and others (1960), Jackson (1968, 1969), Page (1977, 1979), Zientek (1983), and Raedeke and McCallum (1984) among many others. The other major block in the Mountain View area is bounded on the south by the Lake fault and on the north by the Horseman thrust. Rock units within this block include the upper part of the Bronzitite zone of the Ultramafic series, and the Lower Banded series. Cumulus layering within this block more closely approximates the average

attitude within the Banded series of the complex (see fabric diagrams of Page (1977, p. 62 for subarea 17). An important structural feature within this block is the South Prairie fault system that causes repetitions within the Lower Banded series (Bow and others, 1982; Turner and others, 1985). Unpublished and published geologic maps of this block have been made at various scales by Howland and Peoples (1940–1950, unpublished, 1:6,000), Jackson (1951–1959, unpublished, 1:12,000), Page and Nokleberg (1974, 1:12,000), and Segerstrom and Carlson (1982, 1:24,000); however, except for the rocks immediately adjacent to and within the J–M Reef (Bow and others, 1982; Barnes and Naldrett, 1983; Turner and others, 1985) and the studies of Hess (1960), few geologic, petrologic, or chemical problems have been addressed.

Mapping of surface outcrops in the Mountain View area allows the lower part of the Lower Banded series to be divided into nine relatively distinctive units. In general, the lower 22 percent of the section is dominated by massive, nonlayered plagioclase-bronzite cumulate followed by plagioclase-bronzite cumulate that is modally layered and contains minor amounts of thin plagioclase cumulate layers for the next 23 percent of the section. The next 21 percent of section is still dominated by modally layered plagioclase-bronzite cumulate but contains minor amounts of plagioclase-bronzite-augite and plagioclase cumulates. About the next 8 percent of section is characterized by cyclic repetition of plagioclase-bronzite and plagioclase-augite-bronzite cumulates with minor plagioclase cumulate layers. The appearance of olivine and olivine-plagioclase cumulates interlayered with plagioclase cumulates marks the next 3 percent of the section. The top 23 percent of the section contains modally graded layers of dominantly plagioclase-bronzite cumulates with minor plagioclase-bronzite-augite cumulates.

Another feature of the lower part of the Lower Banded series in the Mountain View area is the well-developed modal layering, most of which has decreasing amounts of pyroxene upwards. Hess (1960) estimated that two-thirds of the layers were "gravity stratified," that is, showed an increase in the amount of plagioclase upwards. In addition, over 80 percent of the plagioclase cumulate layers have sharp upper contacts and gradational lower contacts.

The composite unit consisting of the Norite I, Gabbronorite I, Olivine-bearing I, and Norite II zones forms a tabular unit in the Mountain View area striking west-northwest and dipping 60° to 80° N. (fig. 3). As exposed in outcrops, it varies in thickness from about 594 m at the east end low in the Stillwater River valley to about 320 m at the western edge of the map area. This variation in thickness is ascribed in part to repetition and removal of section by the South Prairie fault system. Within the Mountain View area, the composite unit does not reach the thickness of 700 m given by Segerstrom and Carlson (1982) or the 835 m estimated by Hess (1960).

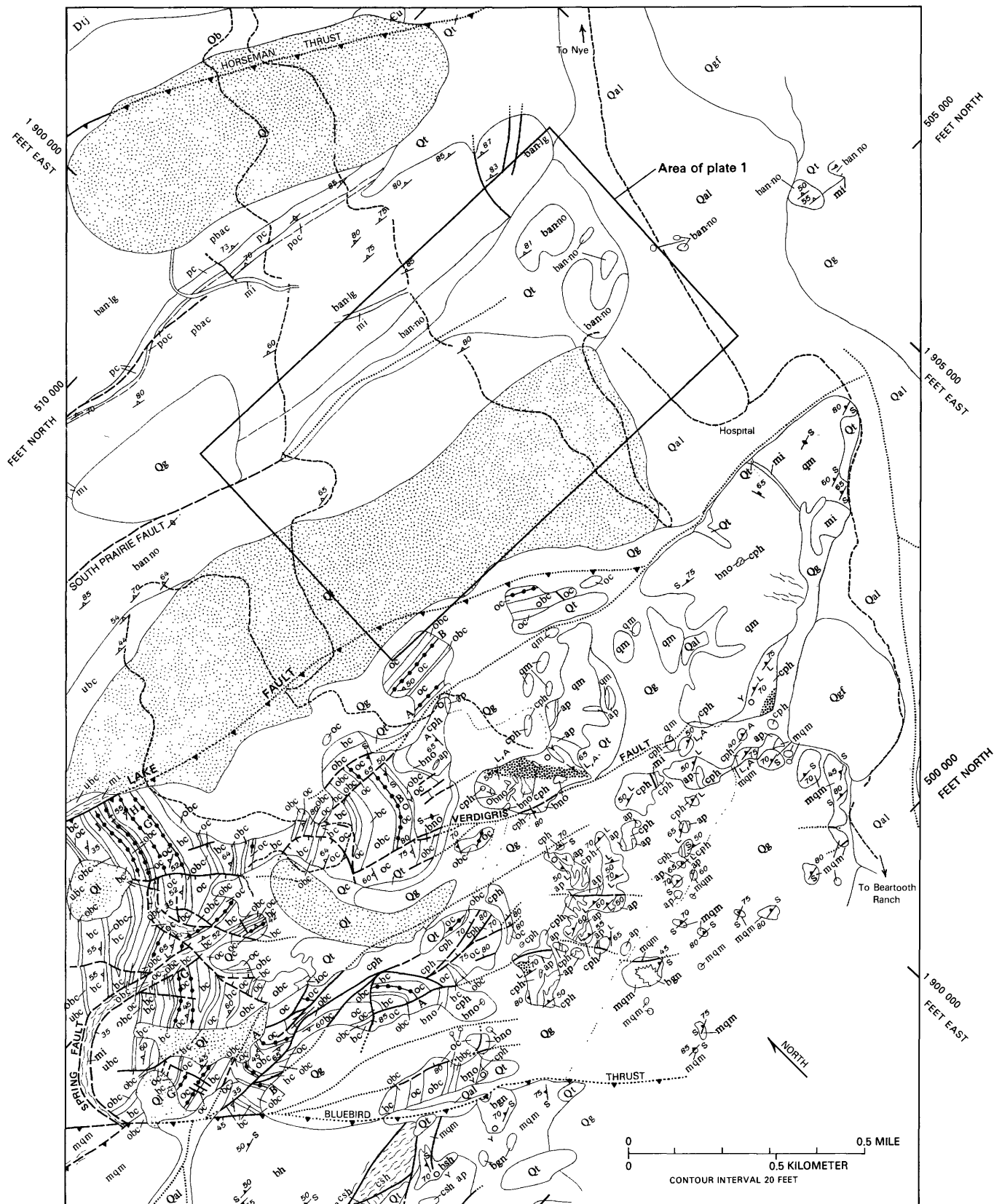


Figure 3. Geologic map of part of Mountain View area, Stillwater Complex, Montana, modified from Page and Nokleberg (1974), using unpublished geologic mapping of Page and Moring (1980–1983), and from Page and others (1985).

EXPLANATION

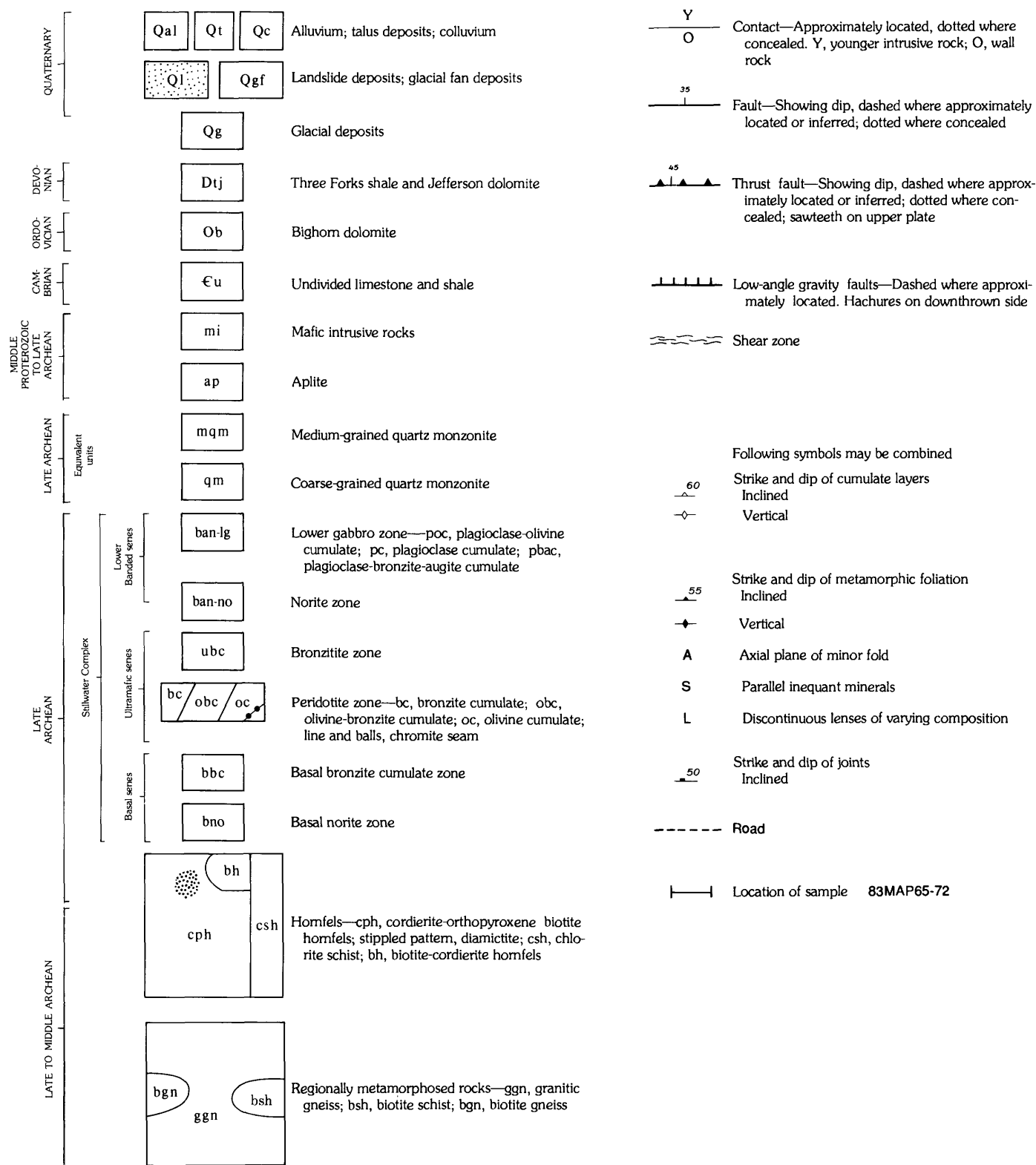


Figure 3. Continued.

Stratigraphic Characteristics of the Lower Part of the Lower Banded Series

The generalized composite columnar section of the lower part of the Lower Banded series, from slightly above the contact of the Bronzite zone with the Norite I zone to the Olivine-bearing I zone, illustrates the complexities and variation in cumulate rocks within this interval (fig. 4). Both the lower and upper contacts of this interval are phase contacts marked by the appearance of plagioclase and olivine as cumulus minerals, respectively. The development of cross-stratification, slump structures, basinlike structures, and onlap and offlap and ramp structures seems to be characteristic of this interval in the Mountain View area, although such features are common in certain parts of the stratigraphic succession above the lower part of the Lower Banded series. The approximate stratigraphic positions and figure number for more detailed columnar sections are shown on the generalized section (fig. 4) and the sample numbers shown on each detailed section are on plate 1. These sections and map form the basis for the discussion of each unit in the lower part of the Lower Banded series. After examining the details of each zone and subzone, the rest of the report will synthesize and interpret the information as related to the generalized section (fig. 4).

Definition, Distribution, and Thickness of the Subzones and Zones

Norite I Zone

The Norite I zone consists predominantly of plagioclase-bronzite cumulates and minor amounts of plagioclase cumulates. It is divided into three subzones described below.

Subzone 1

Subzone 1 consists of monotonous-appearing plagioclase-bronzite cumulates throughout most of its thickness, all with approximately the same modal mineralogy. It overlies the Bronzite zone and near its base locally contains disseminated cumulus chromite (see Page and others, 1985, p. 178). In the upper part of subzone 1, modal variations become common, and thin, discontinuous (on the scale of an outcrop) plagioclase cumulate layers are developed, as well as various layering structures such as basin, slump, and ramplike features. The upper contact of subzone 1 with subzone 2 is marked by beds with an upward-increasing amount of plagioclase, followed by the bronzite-rich base of subzone 2. Subzone 1 is thicker (274 m); in the western part of the area and thins to the east (137 m); its top surface is inferred to be concave down, forming a basinlike shape.

Exposures are not extensive in the area studied; however, the basal part was examined on upper part of the

Mouat mine road, the middle part on the road to the Mountain View Cu-Ni adit, and the upper part in a glaciated outcrop on the lower part of the Mouat mine road (see plate 1). All the locations are shown on figure 4, and the measured columnar sections are presented in figure 5. Modal variations were used to define the beds shown in columnar sections (fig. 5). Because of variations along strike, the thickness and number of beds in a particular column are accurate only for the place where the section was measured, but they are representative of the outcrop in a general way. The measured sections indicate that most of the complications in bedding, rapid variation in modal mineralogy, development of structures, and so forth, occur only in the top part of subzone 1 (fig. 5). Elsewhere in the unit, such features appear not to have developed.

Subzone 2

The base of subzone 2 is a bronzite-rich (40–70 percent)-plagioclase cumulate which has a sharp disconformable contact with upper plagioclase cumulate or plagioclase-rich (80–90 percent)-bronzite cumulate of subzone 1 (fig. 6). From the bronzite-rich base the rocks grade rapidly to plagioclase (80–70 percent)-bronzite (20–30 percent) cumulates within which modal and size-graded layering is rare, especially in the western part of subzone 2. Along strike to the east, the middle part of subzone 2 contains plagioclase-bronzite cumulates with thin (2–30 cm thick) interlayered plagioclase cumulate. Modal layering is common in the plagioclase-bronzite cumulates. Layers are graded from bronzite-rich bases to plagioclase-rich tops. Besides these more common layers, wispy discontinuous (>2 to 5 cm thick) plagioclase cumulate layers are present as are crossbedded structures. The upper part of subzone 2 contains modally graded plagioclase-bronzite cumulates with plagioclase-rich tops with some discontinuous wispy plagioclase cumulate layers. Eventually subzone 2 grades up to plagioclase-bronzite (95–100 percent and 0–5 percent, respectively) cumulate at the top. In the eastern part of the map area subzone 2 is about 76 m thick (fig. 7), and is inferred to wedge out toward the west.

Comparison of the columnar sections (fig. 7) shows that the thick isomodal parts of subzone 2 change along strike to complexly layered plagioclase-bronzite cumulates. This appears to be a characteristic of subzone 2; however, because of poor exposures of other units, it is unknown if similar changes along strike may occur in them too.

Subzone 3

The base of subzone 3 consists of bronzite-rich plagioclase cumulate in its western exposure and in its eastern exposure consists of a thin bronzite-augite-rich-plagioclase cumulate that grades rapidly upward to a bronzite-plagioclase cumulate (fig. 8). These cumulates disconformably overlie, with a sharp contact, the plagioclase or plagioclase-rich bronzite cumulates of subzone 2.

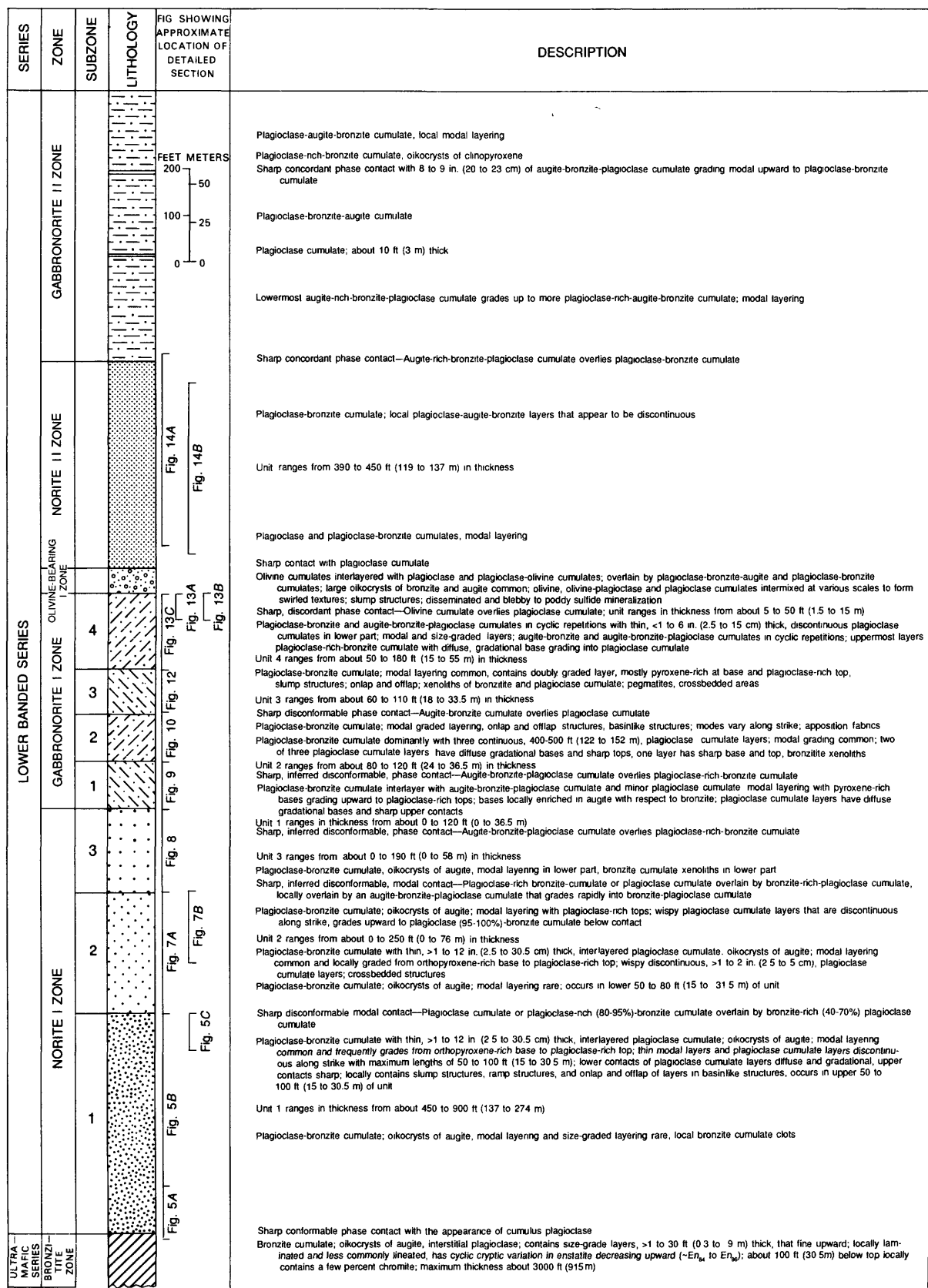


Figure 4. Generalized schematic composite columnar section and rock description of part of Lower Banded series showing position of J-M Reef, Mountain View area, Stillwater Complex, Montana.

Most of subzone 3 consists of isomodal plagioclase-bronzite cumulate that near the top of the unit grades upward into a plagioclase or plagioclase-rich bronzite cumulate.

Subzone 3 is about 58 m thick in its eastern exposures and is inferred to pinch out to the west (pl. 1).

Gabbronorite I Zone

The Gabbronorite I zone marks the appearance of abundant augite as a cumulus mineral and is composed of bronzite-augite-plagioclase, bronzite-plagioclase, and plagioclase cumulates. It is divided into four subzones, described below.

Subzone 1

A bronzite-augite-rich-plagioclase cumulate marks the base of subzone 1 of the Gabbronorite I zone; it overlies the plagioclase-rich upper layer of subzone 3 of the Norite I zone with a sharp and disconformable contact. The unit consists of plagioclase-bronzite cumulate interlayered with plagioclase-bronzite-augite cumulate and minor amounts of plagioclase cumulate. Modal layering characterized by the gradation from pyroxene-rich bases to plagioclase-rich tops is common. Many of these layers have bases that are locally enriched in augite with respect to bronzite and grade upward into plagioclase-bronzite cumulate. Plagioclase cumulate

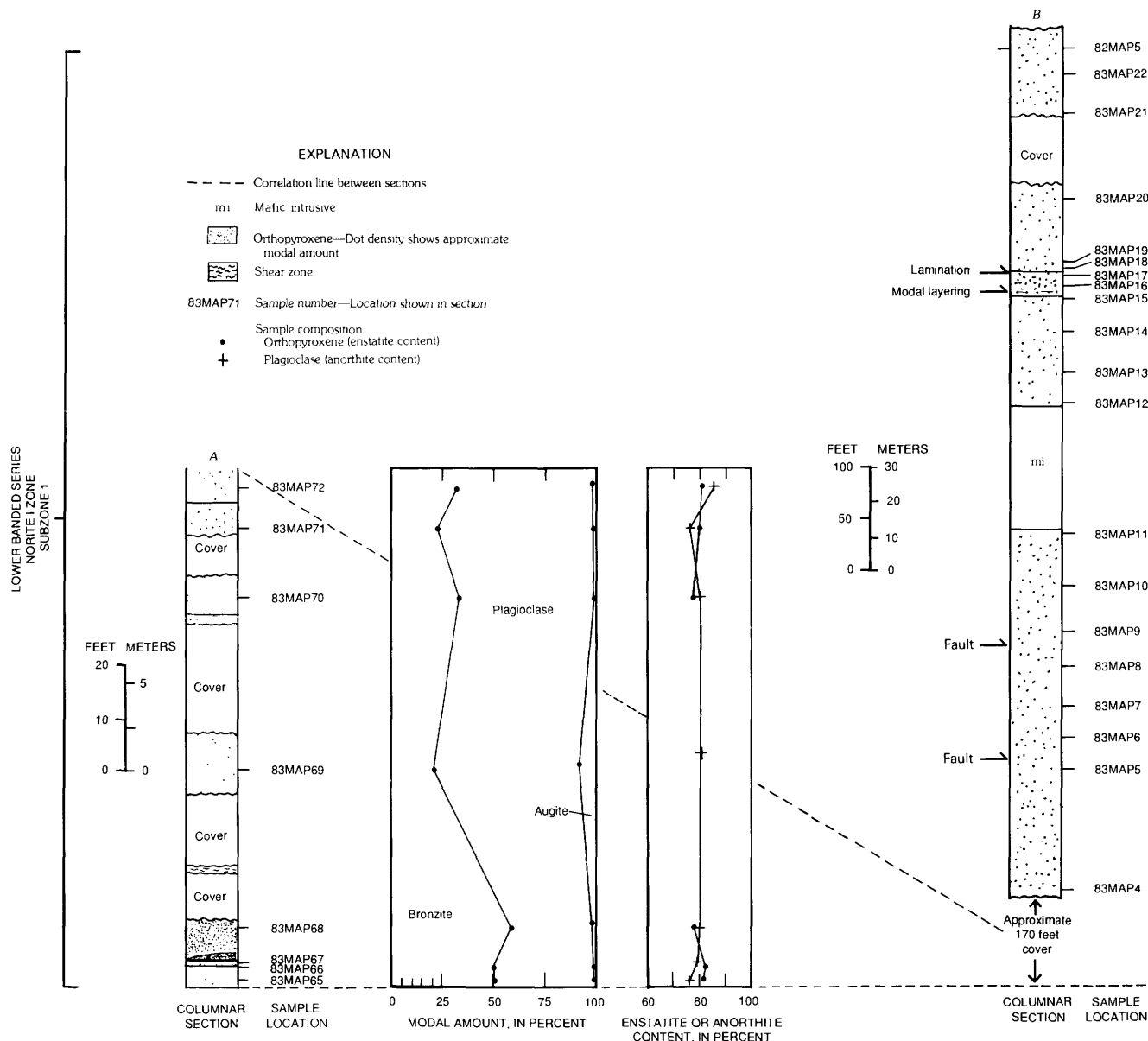


Figure 5. Columnar section of subzone 1 of Norite I zone (located on fig. 4) showing stratigraphy, modal mineralogy, and plagioclase and bronzite compositions in Mountain View area, Stillwater Complex, Montana. A, Basal section, upper part of Mouat Mine Road. B, Middle section, road to Mouat Cu-Ni adit. C, Upper section, lower part of Mouat Mine Road (see pl. 1 for locations).

layers tend to have diffuse gradational bases and sharp upper contacts. The top of subzone 1 is a plagioclase or plagioclase-rich-bronzite cumulate. Two generalized columnar sections in subzone 1 (fig. 9) illustrate the change in thickness from east to west of subzone 1. Subzone 1, as do two of the lower units, pinches out to the west and has a maximum thickness of about 40 m in the eastern part of the map area (pl. 1).

Subzone 2

Bronzite-augite-plagioclase cumulate overlying the plagioclase-rich cumulate at the top of subzone 1 forms the base of subzone 2 of the Gabbronorite I zone (fig. 10). The

basal contact is inferred to be disconformable. The lower parts of subzone 2 contain abundant bronzite-augite-plagioclase cumulates and minor amounts of plagioclase-bronzite cumulate. The upper part dominantly consists of modally layered plagioclase-bronzite-augite-cumulate which, about 9 m from the top of the unit, contains three relatively continuous (120–180 m along strike) plagioclase cumulate layers that range in thickness from 13 to 25 cm. Two of the plagioclase cumulate layers have diffuse gradational basal contacts and sharp upper contacts (fig. 11A); the other has sharp contacts at its base and top (fig. 11B). Modally graded layers with plagioclase-rich tops are common at this level in subzone 2, as are

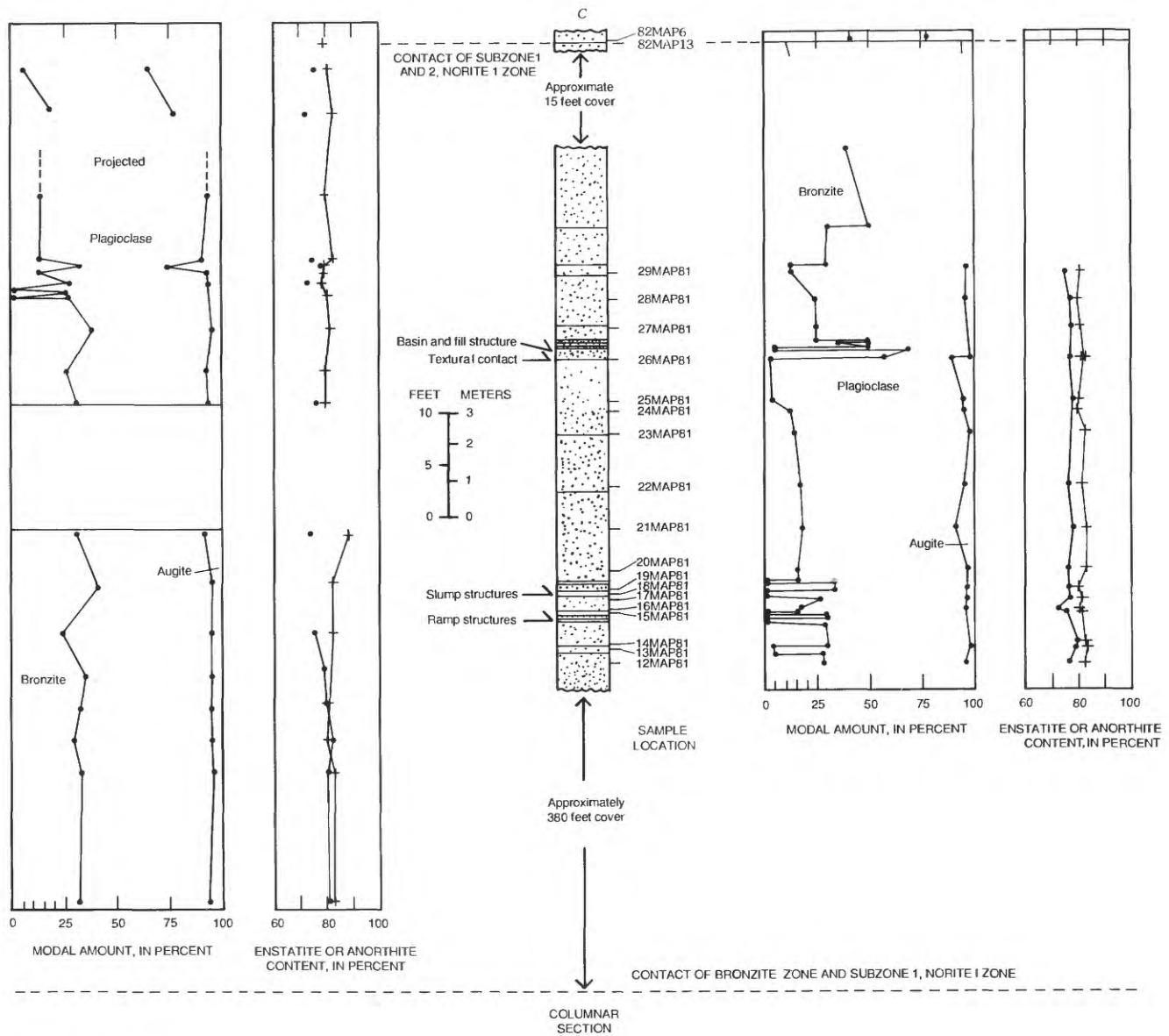


Figure 5. Continued.

bronzitite clots, lenses, and irregular-shaped pieces. The upper part of subzone 2, well exposed in the "Snoopy's Doghouse" area, is dominantly plagioclase-bronzite cumulate with modal graded layers, onlap and offlap structures, basinlike structures, apposition fabrics, and modes that vary along strike. The top of subzone 2 is a plagioclase cumulate. Subzone 2 is continuous in the Mountain View map area (pl. 1) and ranges in thickness from about 24 to 37 m.

Subzone 3

The basal layer of subzone 3 of the Gabbronorite I zone is a bronzite-augite-plagioclase cumulate that has a sharp, disconformable phase contact with the underlying plagioclase cumulate of subzone 2. The basal layer grades upward into plagioclase-bronzite cumulate, which forms the dominant cumulate type of subzone 3 (fig. 12). The unit consists predominantly of modally graded layers of plagioclase-bronzite cumulate with bronzite-rich bases and

plagioclase-rich tops. Also present are symmetrically graded layers with pyroxene-rich bases and tops and two-pyroxene-rich middle parts. Onlap and offlap, slump, and crossbedded structures are present within subzone 3, as are xenoliths of anorthosite and bronzitite. The top of subzone 3 is marked by a plagioclase cumulate 0.3–3 m thick. The unit ranges from 18 to 30 m in thickness in the map area (pl. 1).

Subzone 4

The base of subzone 4 of the Gabbronorite I zone is formed by a thick symmetrical graded plagioclase-bronzite-augite cumulate that overlies the upper plagioclase cumulates of subzone 3. The contact between the units is a conformable, sharp phase contact. Subzone 4 consists of modally graded and phase-graded layers in the sequence plagioclase-bronzite-augite cumulate, plagioclase-bronzite cumulate, and plagioclase cumulate (fig. 13). Symmetrical grading is common, and plagioclase cumulate layers 2–15 cm thick superimposed within the overall cyclic sequences are numerous. Bronzitite xenoliths are found throughout the unit. The contact of subzone 4 with the Olivine-bearing I zone is disconformable, with the Olivine-bearing I zone apparently cutting down through subzone 4 (Bow and others, 1982; Turner and others, 1985). Subzone 4 ranges in thickness from 18 to 60 m in the map area.

Olivine-Bearing I Zone

In the map area (pl. 1), the Olivine-bearing I zone, from base to top, consists of coarse-grained olivine cumulates that have a phase contact with plagioclase-olivine cumulates, in which the olivine content decreases upward to a gradational contact with a plagioclase cumulate, which has a phase contact with a bronzite-plagioclase olivine cumulate. In this upper unit, olivine occurs as corroded cores in cumulus bronzite crystals. Various variants of this idealized section occur along strike (Turner and others, 1985). The platinum-group mineralization of the J-M Reef is associated with this zone. The basal coarse-grained olivine cumulate rests unconformably on subzone 4 of the Gabbronorite I zone in the eastern part of the area and appears to cut down into Norite I zone rocks toward the west. The top plagioclase-bronzite-olivine cumulate has a conformably and locally gradational contact with the Norite II zone. The Olivine-bearing I zone ranges from 4 to 25 m in thickness, although its outcrop width is complicated by faulting. Details of the Olivine-bearing I zone in the Mountain View area have been presented by Bow and others (1982), Turner and others (1985), and Barnes and Naldrett (1985) which can be compared with the stratigraphically regular sections elsewhere in the complex described by Todd and others (1982), Mann and others (1985), Mann and Lin (1985), and LeRoy (1985).



Figure 6. Contact between subzones 1 and 2 of Norite I zone.

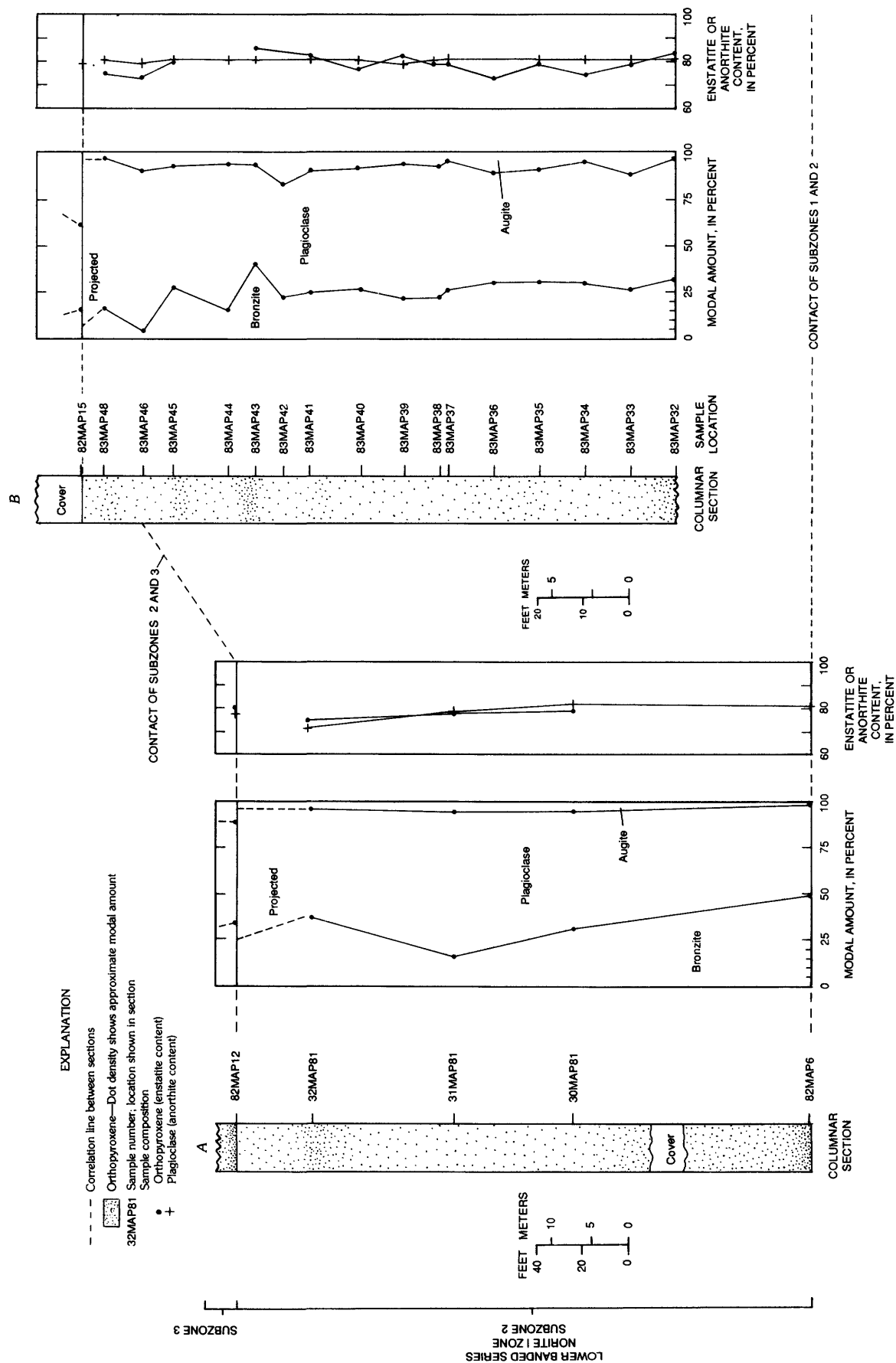


Figure 7. Columnar sections of subzone 2 of Norite I zone showing stratigraphy, modal mineralogy, and plagioclase and bronzite compositions. A, Area B on plate 1. B, Mouat Cu-Ni Adit Road.

Norite II Zone

Modally layered plagioclase-bronzite and plagioclase cumulates with local discontinuous plagioclase-bronzite-augite cumulates in the upper parts compose the Norite II zone (fig. 14). The unit has a sharp, conformable phase contact with the underlying plagioclase cumulates of the Olivine-bearing I zone and a sharp phase contact with the overlying plagioclase-bronzite-augite cumulate of the Gabbronorite II zone. The Norite II zone ranges in thickness from 119 to 137 m within the map area.

STRUCTURES IN THE ROCKS BELOW OLIVINE-BEARING I ZONE

Within the units below the Olivine-bearing I zone, the most visible structural feature is igneous layering formed by variations in various physical and chemical properties of the minerals and thus in the rocks that form the units. Another

type of layering displays characteristics similar to current-formed features in sedimentary rocks. In addition to layering, there are structures that deform the nearly parallel layering and that appear to have formed slightly after the layering formed. These structures will be called syndepositional deformation structures and appear analogous to soft-sediment deformation features.

Modal and Phase Layering

Igneous layering, defined by the abundance, presence, size, or composition of various cumulus minerals, characterizes the units below the Olivine-bearing I zone. Thickness of layers ranges from that of one crystal width to greater than 15 m with the lateral (along strike) extent of individual layers ranging from a few to hundreds of meters. Layers are generally subparallel within the subzones; both concordant and discordant contacts occur between layers.

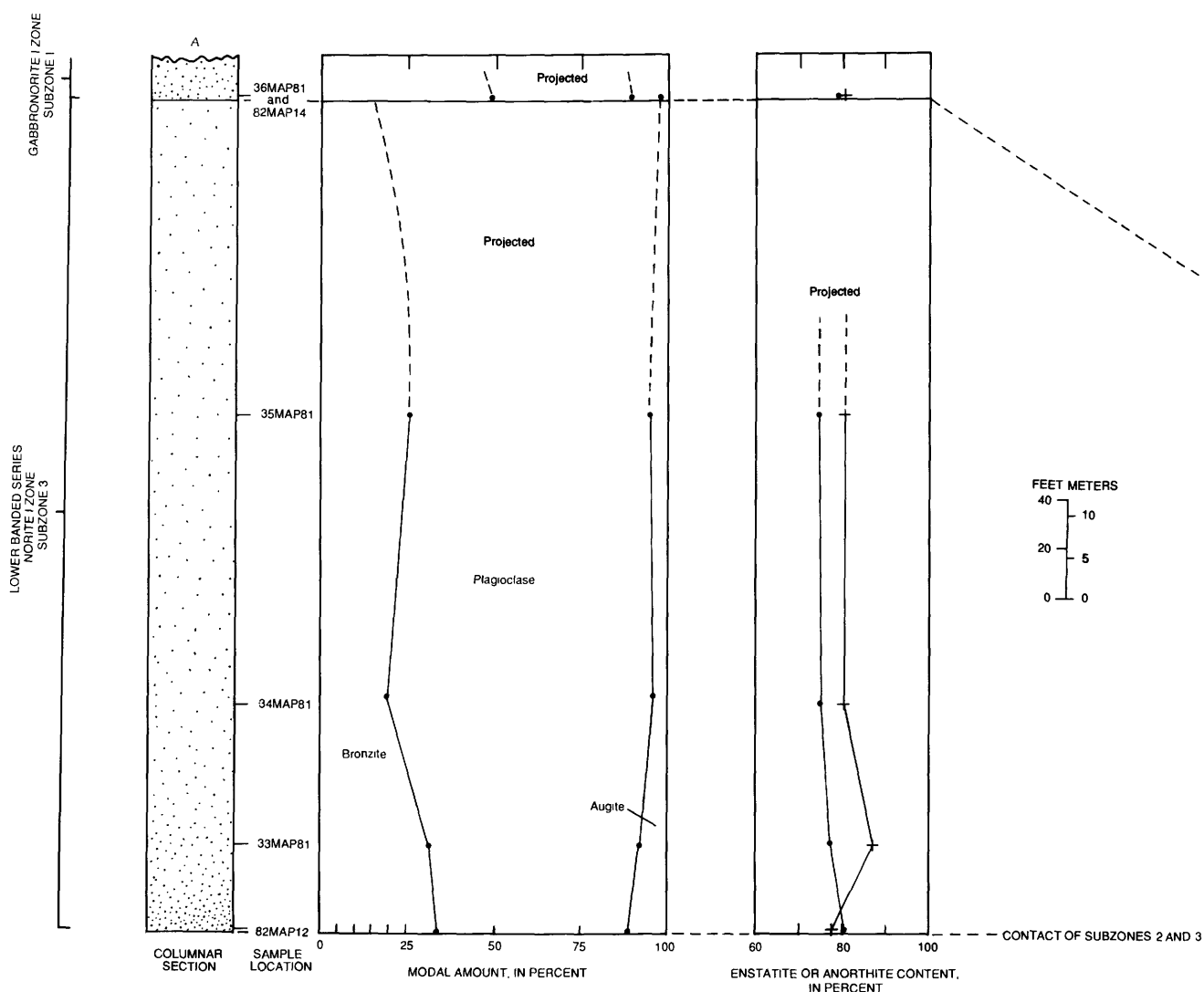


Figure 8. Columnar sections of subzone 3 of Norite I zone showing stratigraphy, modal mineralogy, and plagioclase and bronzite compositions. A, Area B on plate 1. B, Detailed section locality D on plate 1.

Syn depositional deformation ramp and slump structures and currentlike features such as crossbedding, channels, and wispy layering occur locally.

Modal layering, resulting from relative changes in the proportions of cumulus minerals, can form either isomodal or modally graded layers. Normally graded layers—decreasing mafic modes from bottom to top (Irvine, 1982)—are significantly more common than inversely graded layers. Several symmetrically graded layers, ones with inversely graded lower parts and normally graded upper parts, occur in the Gabbro-norite I zone, especially in subzone 3 (for example, see fig. 12).

Phase layers are a special case of modal layers marked by the appearance or discontinuance of a cumulus phase (Irvine, 1982). By definition, all phase contacts are sharp, although cumulus phases may modally grade to a sharp phase contact. Phase layers range in thickness from less than 1 cm to at least 180 m in subzone 1 of the Norite I zone. Plagioclase cumulate layers followed by plagioclase-bronzite or plagioclase-bronzite-augite cumulates form the most common sequence in the section below the Olivine-bearing I zone (fig. 4) and have phase contacts between them.

Layering in subzones 1, 2, and 3 of the Norite I zone consists of modally graded plagioclase-bronzite cumulates

and plagioclase cumulates. Where both lithologies crop out with stratigraphic continuity, the upward sequence is plagioclase-bronzite cumulate going to plagioclase cumulate through loss of bronzite. The change from the lower cumulate layer to the upper one is generally graded over centimeters to meters by the loss of orthopyroxene until a phase contact is reached. With few exceptions, the contacts between plagioclase cumulates and overlying plagioclase-bronzite cumulates are sharp with the base of plagioclase-bronzite layers enriched in bronzite. Rarely, plagioclase cumulate layers are bounded by sharp modal basal and upper contacts.

Subzone 1 is distinguished from the overlying subzones of the Norite I zone by the predominance of massive, indistinct layering. In general, there appears to be a slight upward decrease in cumulus bronzite (fig. 5). Superimposed upon the trend are a few modal and phase layers that are 0.6 to 0.9 m thick near the bottom of the unit and 8 to 30 cm thick near the top of the unit. The phase layers near the base consist of plagioclase-bronzite-chromite cumulates interlayered with plagioclase-bronzite cumulates. These layers extend 3 to 6 stratigraphic meters above the lower contact of subzone 1 of the Norite I zone with the Bronzite zone. The other phase-graded and modally graded layers occur in the upper 15 to 30 m of subzone 1 of the Norite I

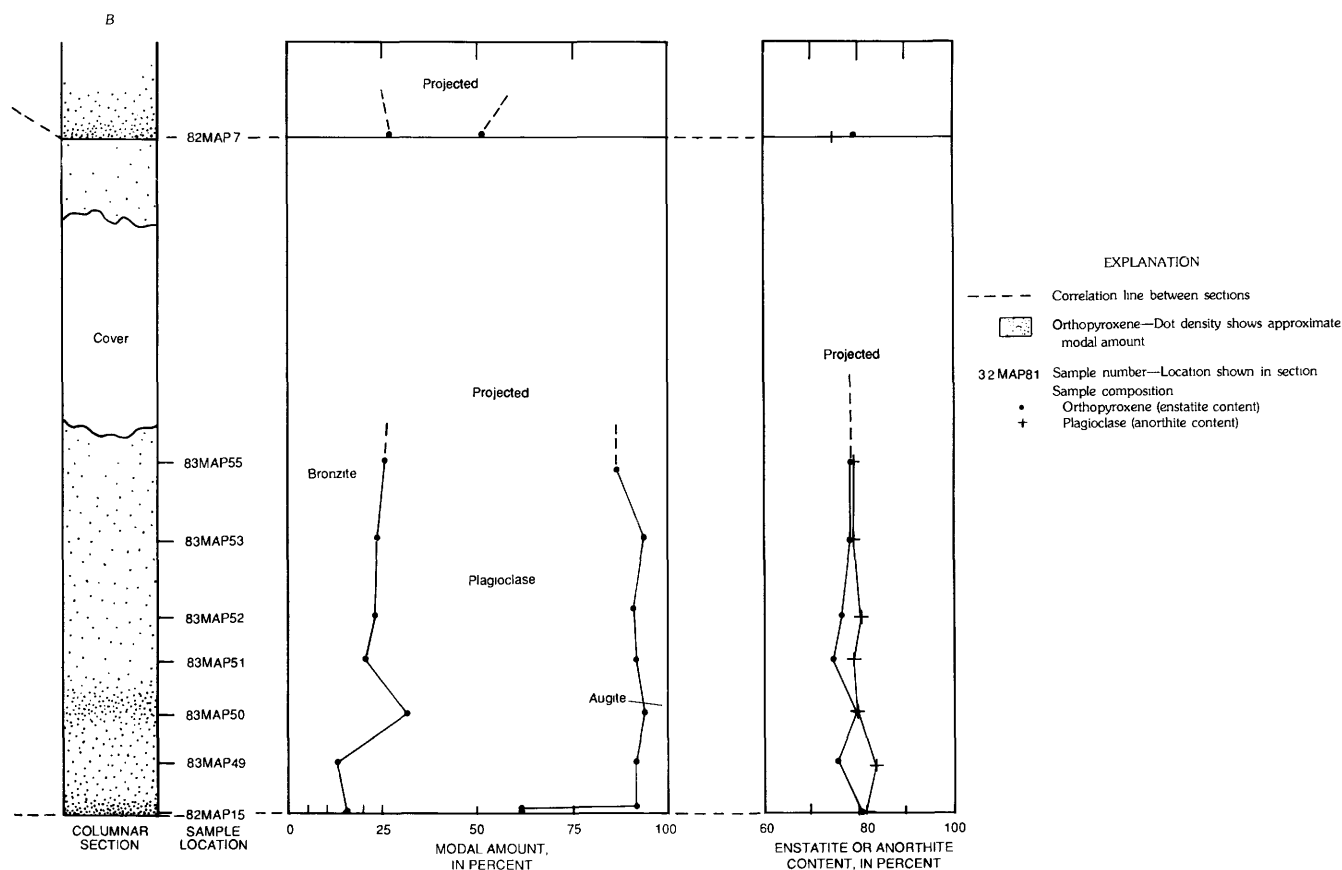


Figure 8. Continued.

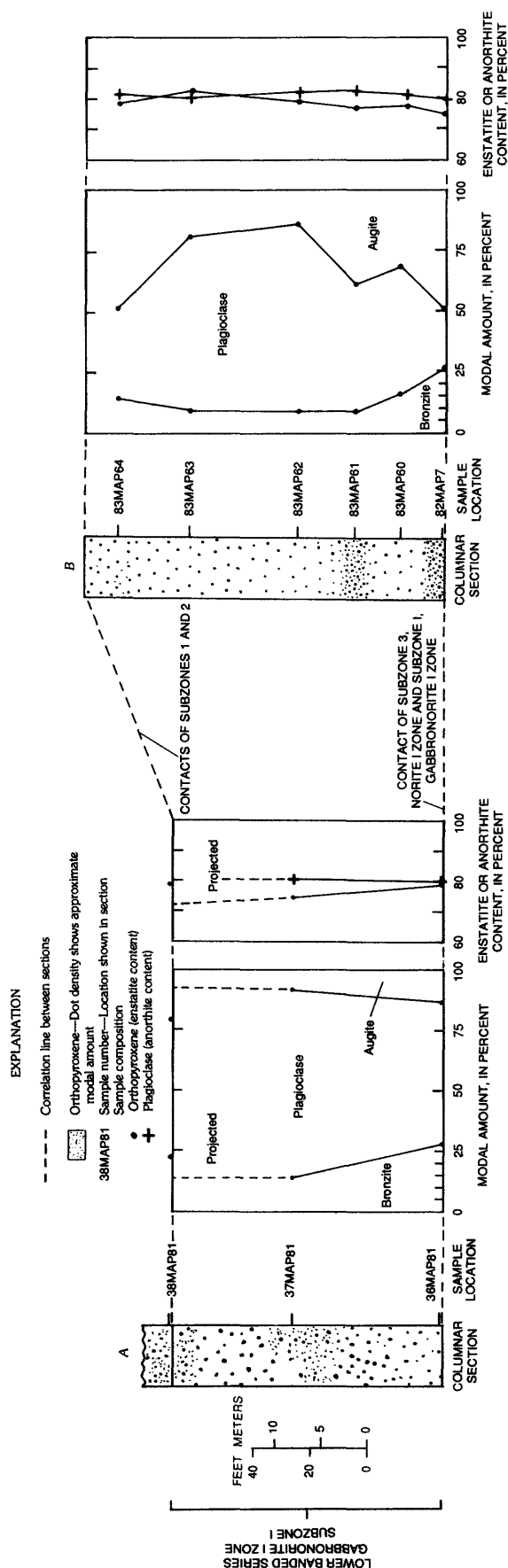


Figure 9. Columnar sections of subzone 1 of Gabbronorite I zone showing stratigraphy, modal mineralogy, and plagioclase and bronzite compositions. A, Area north of area B on plate 1. B, Area north of described section locality D on plate 1.

zone. The phase layers consist of 3- to 15-cm plagioclase cumulate interlayered with plagioclase-bronzite cumulate.

Layering in the subzones of the Gabbronorite I zone consists of modal and phase layers of plagioclase-bronzite-augite cumulate, plagioclase-bronzite cumulate, and plagioclase cumulate. Where all lithologies are present, the complete upward sequence is generally plagioclase-bronzite-augite cumulate grading through loss of augite to plagioclase-bronzite cumulate and to plagioclase cumulate upon the loss of cumulus bronzite. Symmetrically graded layers, common to subzone 4, may begin with a plagioclase-bronzite cumulate and then follow the above sequence. Locally numerous plagioclase cumulate layers 1 to 15 cm thick are superimposed on these cyclic trends but with minimal effect on the overall modal trends (fig. 13).

Fabric of Layers from Subzone 2 of the Gabbronorite I Zone

Petrofabric investigations in the Ultramafic series on bronzite by Jackson (1961a) demonstrated that where the crystals are equidimensional there is little or no preferred orientation, but where the crystals are broad and flat or elongate they tend to lie in the layering plane making an apposition fabric. W.J. Nokleberg gathered information of a similar nature on bronzite-plagioclase cumulates from the "Snoopy's Doghouse" outcrop in order to extend Jackson's (1961a) type of study into the Lower Banded series. He worked on two samples, collected by Jackson, containing seven layers within about 46 cm of section that came from subzone 2 of the Gabbronorite I zone. This section of the report is based on Nokleberg's generously contributed unpublished information.

Slabs of the rock samples used in this study, shown in figure 15, illustrate the layered sequence of plagioclase-bronzite and plagioclase cumulates. The variation in the composition of bronzite and plagioclase, based on electron microprobe analyses of single crystals over the 46-cm stratigraphic interval, is less than 6 atomic percent $Mg/Mg \pm Fe \pm Mn \pm Cr \pm Ca$ and less than 4 atomic percent $Ca/Ca \pm Na \pm K$, respectively (fig. 16). The variation over this short interval is about the same as within the Norite I and Gabbronorite I zones. Calcium in bronzite and potassium in plagioclase show very little variation with stratigraphic position.

The layer from which fabric 1 (fig. 15) of bronzite was determined contains crystals that range in size (along optic axes) from $X=1.5$ mm, $Y=1.3$ mm, and $Z=2.8$ mm to $X=6.1$ mm, $Y=7.9$ mm, and $Z=14.7$ mm. The average size of bronzite is $X=3.61.1$ mm, $Y=4.41.6$ mm, and $Z=8.03.3$ mm. A weighted average was used to calculate a crystallographic axial ratio $a:b:c$ of 0.64:0.57:1, using the bronzite orientation preferred by Hess and Phillips (1940). Fabric diagrams of the principal optic axes directions of 39 crystals are shown in figure 17A, contoured in percent

points per 1 percent areas. The diagrams show 6 percent concentration of X axes perpendicular to the layering, a well developed girdle of Z axes approximately perpendicular to the X maxima, and little or no preferred orientation of Y axes.

Fabric 2 was determined from a slightly more plagioclase-rich layer (fig. 15). The bronzite crystals range in size from X=1.5 mm, Y=1.5 mm, Z=2.3 mm to X=6.8 mm, Y=6.8 mm, Z=10.9 mm. The average size of

bronzite is X = 3.51.4 mm, Y=3.71.5 mm, and Z=6.62.4 mm. A weighted average gives calculated axial ratios of $a:b:c$ of 0.62:0.56:1. Fabric diagrams (fig. 17B) of the principal optic axes directions of 46 crystals show a concentration of X axes perpendicular to layering, a girdle of Z axes in the plane of layering, and little or no preferred orientation of the Y axes.

Fabrics 1 and 2 are almost identical. They indicate that the c -axes of the bronzite crystals lie in the layering

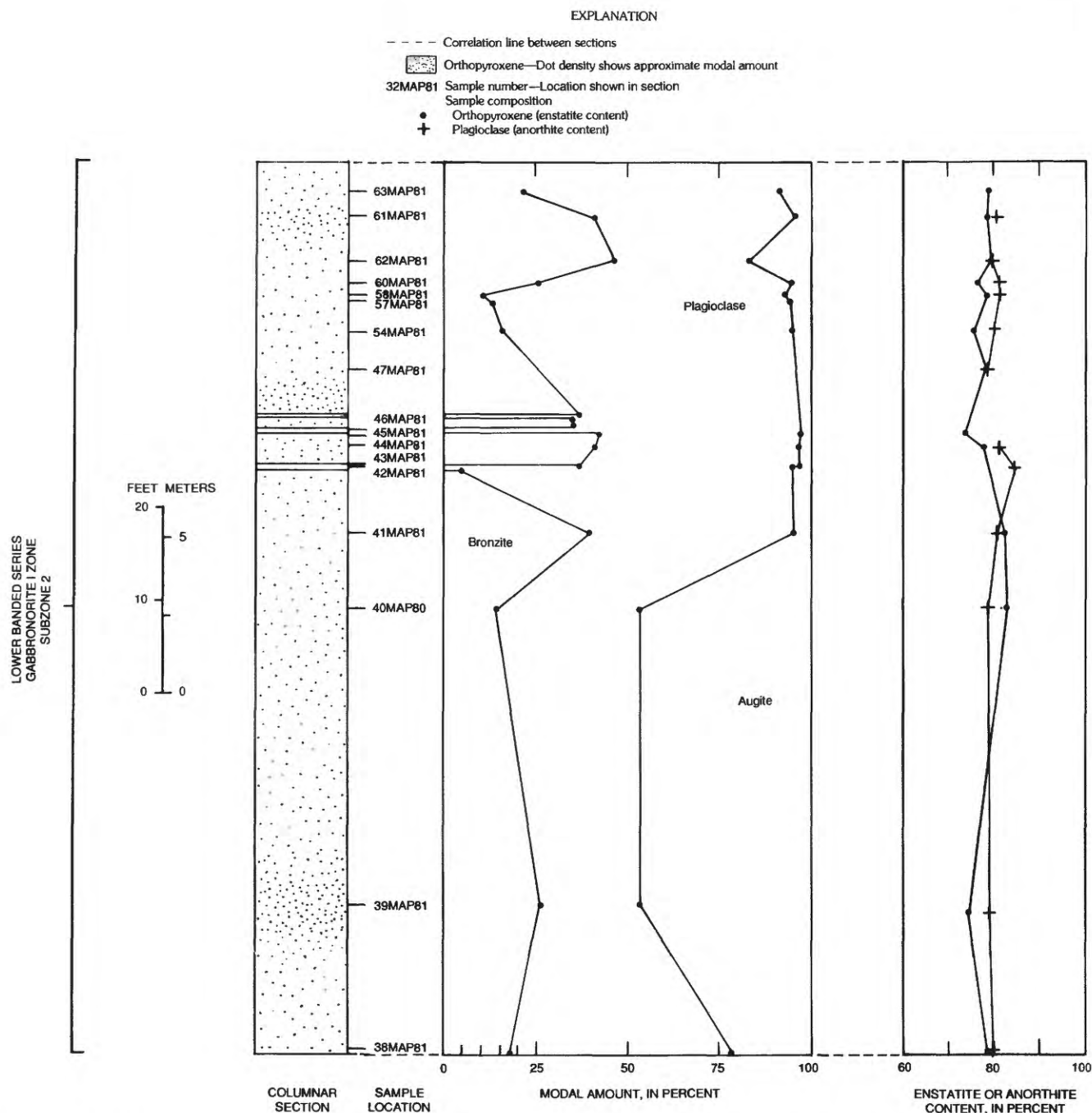


Figure 10. Columnar section of subzone 2 of Gabbronorite I zone showing stratigraphy, modal mineralogy, and plagioclase and bronzite compositions.

plane with little or no orientation, forming well-developed apposition fabrics. These fabrics are similar to those found by Jackson (1961a).

Size-Graded Layering

Variation in the size of cumulus crystals through stratigraphic sections of cumulus rocks has been shown to be important to the study of cumulates in the Stillwater Complex (Jackson, 1961a; Jones and others, 1960; Hess, 1960; Page and others, 1972; Page, 1979; Loferski and Lipin, 1984). Both size-graded units and nongraded layers that correlate with cumulate layers have been recognized. Small variations in crystal sizes are not easy to document in the field, except in a general way, and therefore our studies of size variation were limited to 44 closely spaced samples from a 17-m interval of core taken perpendicular to layering in subzone 4 of the Gabbronorite I zone immediately below the Olivine-bearing I zone. The technique of Jackson (1961a), which involves the measurement of the major and minor axes of crystals in thin sections, was used to gather size data on bronzite crystals. The average crystal size

ranges from 1 to 5 mm, and the population of crystal sizes within an individual sample has a log-normal distribution (fig. 18).

The average size of bronzite crystals for individual samples (fig. 19) varies throughout the section of the cumulates in the upper part of subzone 4 of the Gabbronorite I zone. This variation defines four size-graded units that are bounded by abrupt changes in crystal size (for example at 12.7 m, fig. 19). Two of the four size-graded layers are symmetrically graded: the maximum pyroxene crystal size is approximately one-quarter to one-half the thickness up from the base of the layer.

Layering Similar to Current Types (Irregular Layering)

Perturbations in the subparallel, more regular layering occur locally within the units below the Olivine-bearing I zone and include crosslamination and wavy laminations, wispy layering, channellike or basinlike structures, and onlap and offlap relations. Crosslamination consists of thin bronzite-rich and plagioclase-rich layers that are at an angle



Figure 11. Plagioclase cumulate layers in subzone 2 of Gabbronorite I zone. A, Layers with diffuse bases and sharp tops. B, Layer with sharp top and base. Rock hammer handle is 28 cm.

to attitude of more regular modal layering. Two examples of crosslamination are shown in figure 20.

M.P. Ryan (in Page and others, 1985) described the crosslamination in figure 20B as crossbeds built up of sigmoidally nested members, each suggesting the deposition of successive bronzite-rich, then plagioclase-rich horizons formed, Ryan inferred, in response to bed-load transport in the basal boundary layer. The alternating bronzite-rich and bronzite-poor layers in figure 20A could be interpreted as foreset beds raking toward the east. All of the crosslamination and wavy laminations are suggestive of crystal deposition from currents near the floor of the magma chamber.

Wispy layering occurs in three locations in subzone 2 of the Norite I zone, two of them immediately below the

contact of subzones 2 and 3 (fig. 21) and the third near the middle of the unit associated with slumping and channeling. In each location, the wispy layering forms irregular zones of nonplanar modal and phase layering that are 0.6 to 1.5 m thick. The individual layers range in thickness from one crystal to 1 cm and are discontinuous along strike. These thin layers appear to have no systematic orientation or shape and vary from irregular wave shapes to short discontinuous lenses.

Small-scale (1.5 to 3 m across) and larger scale channel-like or basinlike structures are present in the map area and seem to be more common in subzones 2 through 4 of the Gabbronorite I zone. The area called "Snoopy's Doghouse" contains some of the better exposed basinlike features, thus it was mapped in detail by compiling visual

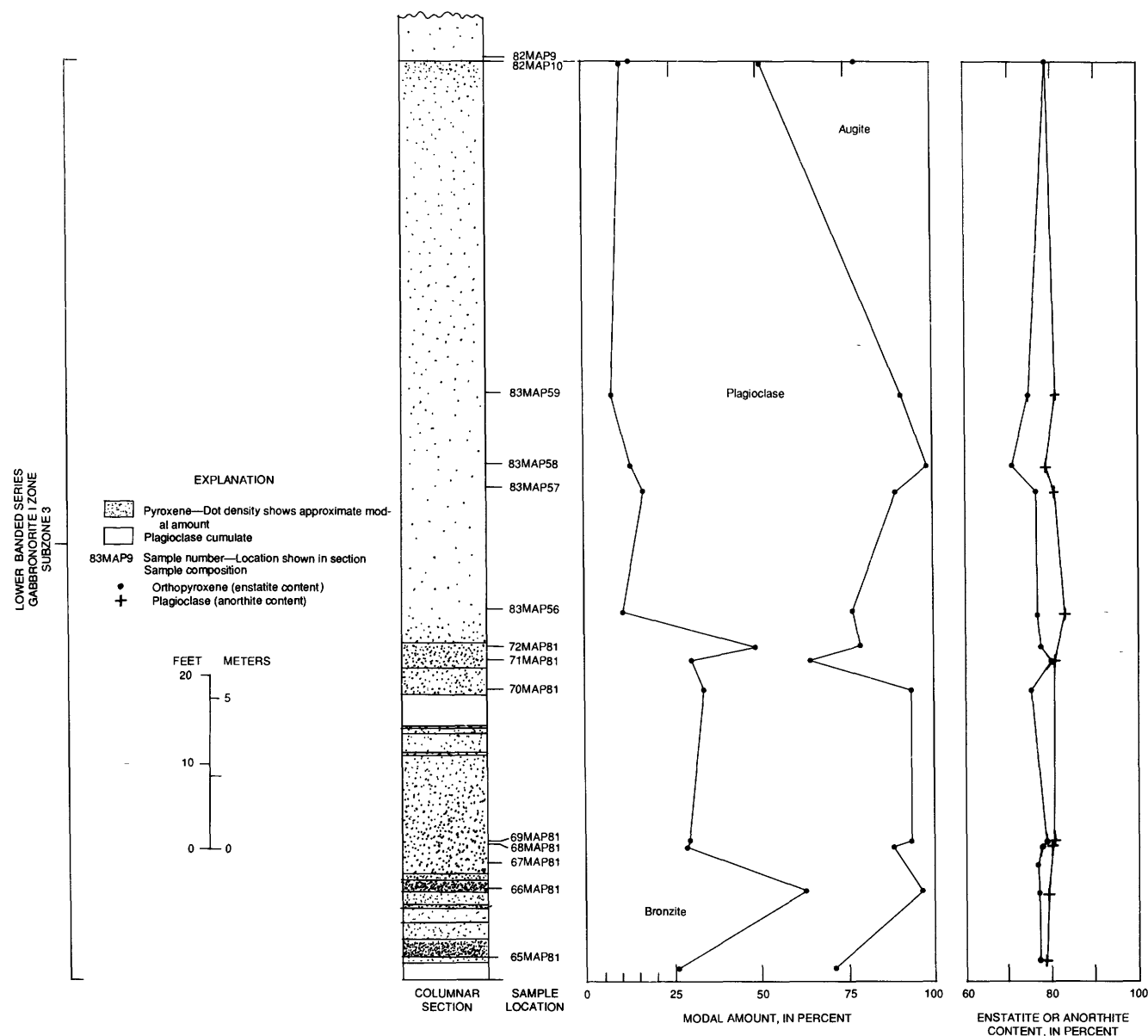


Figure 12. Columnar section of subzone 3 of Gabbronorite I zone showing stratigraphy, modal mineralogy, and plagioclase and bronzite compositions.

estimates of pyroxene modes in 10 sections across the strike of the layering and along the strike between sections. This type of modal mapping shows the shapes and dimensions of two small-scale basinlike features (fig. 22). The structures are concave down with respect to the stratigraphic section and appear to cut out some of the underlying layer. The basins are then filled by thin bronzite- plagioclase and plagioclase cumulate layers (fig. 23) that within the basin are discontinuous. The lowermost infilled layers tend to be enriched in bronzite. The axis of the channels appears to trend toward the northeast and plunge either down the dip direction or up the dip direction. Because of the subflat-tened, glaciated outcrops, making a series of structure measurements and finding a solution for the attitude of the axis was unsuccessful.

Examination of the vertical and lateral variations in the modal layers of the "Snoopy's Doghouse" area (fig. 22) and comparison of these changes with similar changes in modal variation in the small-scale basinlike structures suggests that there are basinlike structures larger than the outcrop exposure. The layer at point A on the plate appears to mark the bottom of a larger basin that deepens eastward. The layer is bronzite-rich with modal bronzite decreasing westward as the layer thins. Above the layer is another one,

containing less bronzite, which also pinches out westward. These examples of offlap and onlap are similar to portions of the smaller basins and in this example suggest a basin axis to the east of the available outcrop. Other examples of onlap and offlap in this area involve layers less than 2 cm thick and others that are much thicker. Such structures suggest that the crystals forming the layers did not fall from great heights above the bottom of the magma chamber and possibly fell no greater distances than the layer containing them, if they fell at all.

SYNDEPOSITIONAL DEFORMATION STRUCTURES

Both ramp and slump structures have long been known to exist in the Stillwater Complex within the Ultramafic and Banded series. Hess (1960) described the slump structures in the Gabbro-norite I zone in the "Snoopy's Doghouse" outcrop, and Jackson (1961a) described similar features in the Ultramafic series. More recently, Foote (1985) described such features in detail in the Contact Mountain area. Descriptions of the J-M Reef in the Mountain View area indicate that similar structures are

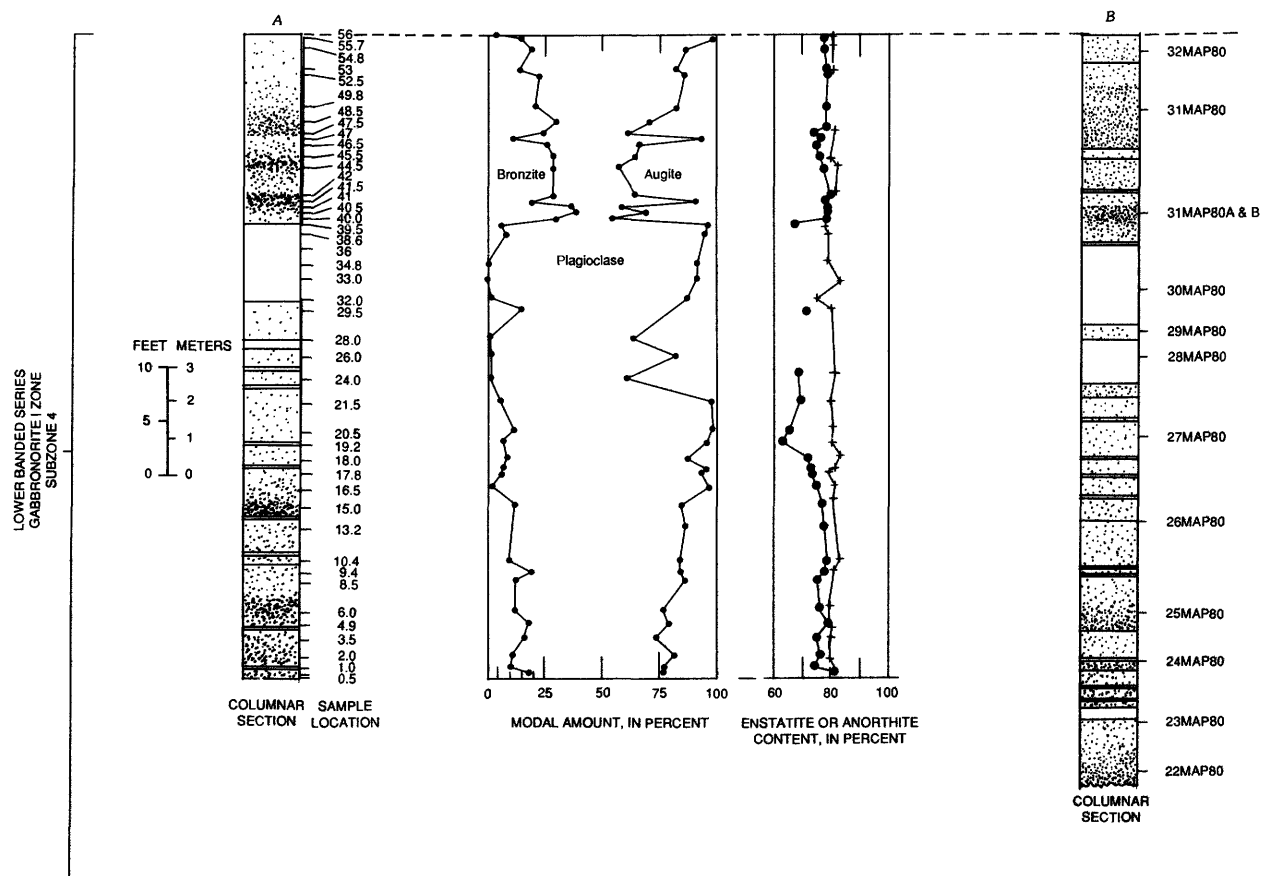


Figure 13. Columnar sections of subzone 4 of Gabbro-norite I zone showing stratigraphy, modal mineralogy, and plagioclase and bronzite compositions. A, Core DS-2/WD-6. B, 5114N crosscut, west rib. C, Surface.

common there (Bow and others, 1982; Turner and others, 1985).

Ramp structures crop out near the top of subzone 1 of the Norite I zone (pl. 1, loc. A) south of the Minneapolis adit and about 150 m east of the adit in subzone 2 of the Norite I zone. The ramp structure (fig. 24) at locality A (pl. 1) consists of plagioclase-bronzite cumulate about 15 cm thick that has been broken and moved about 60 cm (apparent) to the east over itself, as by a small-scale thrust fault. This layer appears to have been brittlely deformed while the more plagioclase rich plagioclase-bronzite cumulate below and above the ramped layer appears to have deformed plastically to accommodate the overthrusting. Immediately above the structure, modal layers of plagioclase-bronzite cumulate continue across the structure and show no evidence of disturbance. In subzone 2 of the Norite I zone at locality B (pl. 1), the upper of two plagioclase-bronzite-augite cumulate layers, which are 5 cm thick and about 30 cm apart stratigraphically, shows a similar ramp structure. The layer failed brittlely and apparently moved westward about 30 cm, because several fragments 15 to 23 cm long from the faulted layer are now lying on top of it.

Both ramp structures are examples of brittle fracture of semisolid, competent, mafic-rich layers in less competent, less mafic plagioclase-bronzite cumulates. Undisturbed modal layers above and below the ramp structures indicate that their formation was a surface feature at the magma-crystal interface and that the process affected layers no more than a few centimeters to meters from this surface.

Slump or roll structures are found in subzone 2 of the Norite I zone about 15 stratigraphic meters below the ramp structures described above and in subzone 1 of the Gabbro-norite I zone in the "Snoopy's Doghouse" area (fig. 22). The slump structure in subzone 2 is an east-facing asymmetric fold in a plagioclase-bronzite, bronzite-plagioclase, plagioclase cumulate sequence that is about 0.6 m thick. Over a strike distance of about 45 cm, the plagioclase-bronzite cumulate thins eastward by about 25 percent; the 15-cm-thick plagioclase cumulate layer thickens slightly in the crest of the fold. One to 3 m east of the fold the plagioclase cumulate interdigitates with a wispy layered wedge that begins at this point and thickens toward the east.

The slump structure mapped in the "Snoopy's Doghouse" area (fig. 25) is the structure originally described by Hess (1960). A sequence of plagioclase-bronzite,

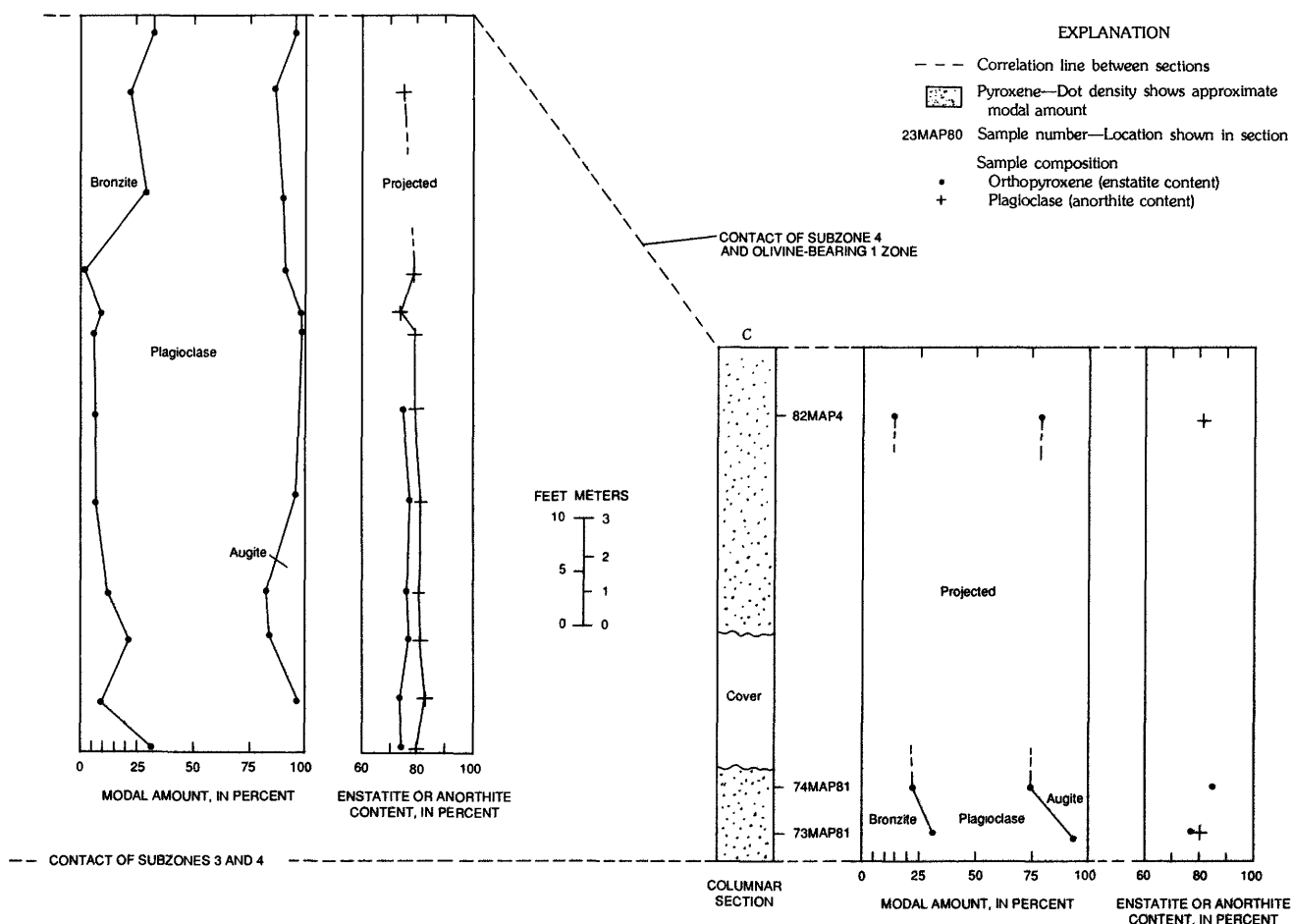


Figure 13. Continued.

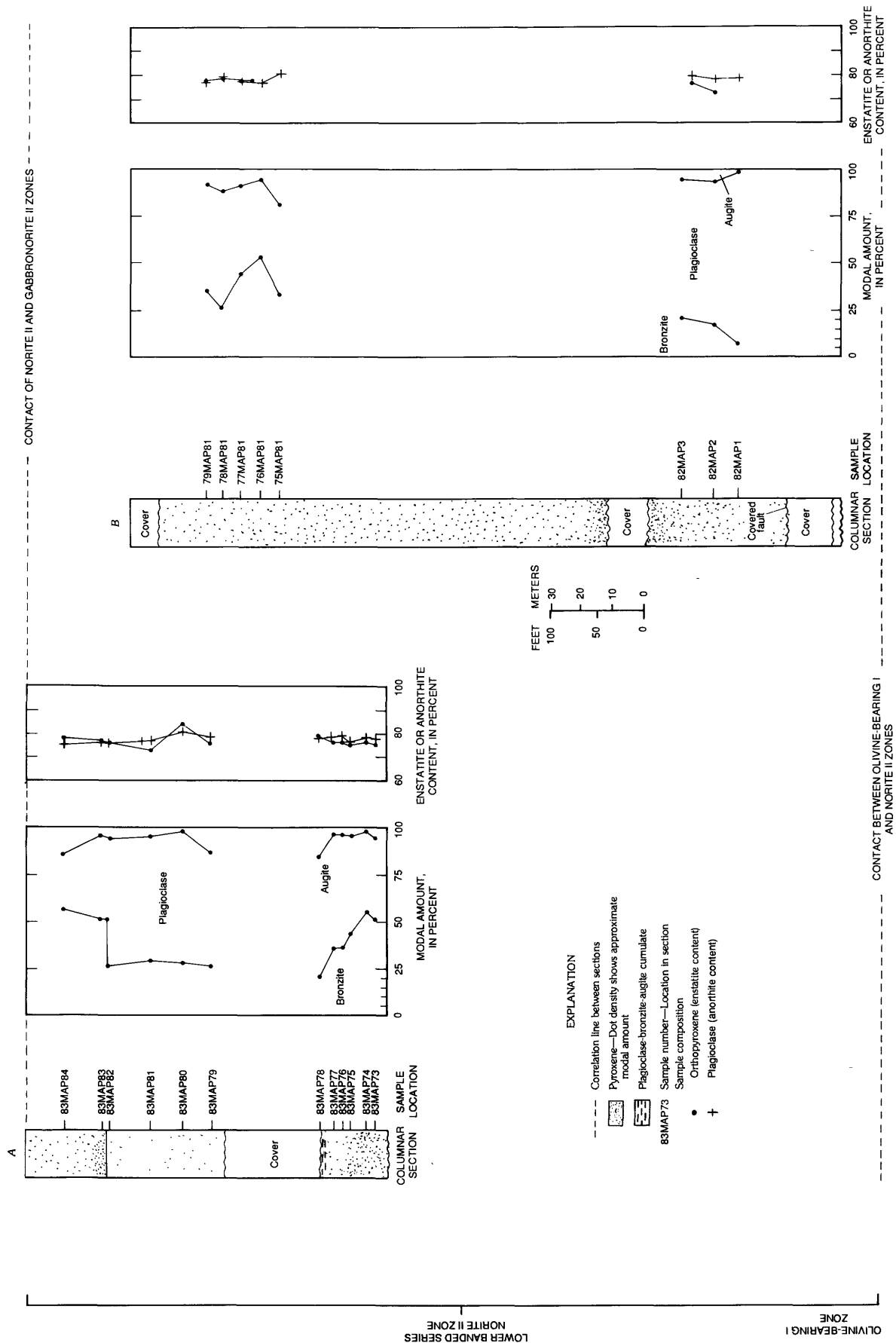


Figure 14. Columnar sections of Norite II zone showing stratigraphy, modal mineralogy, and bronzite compositions. A, Upper part of Mout Mine Road on plate 1. B, Area east of described section locality H on plate 1.

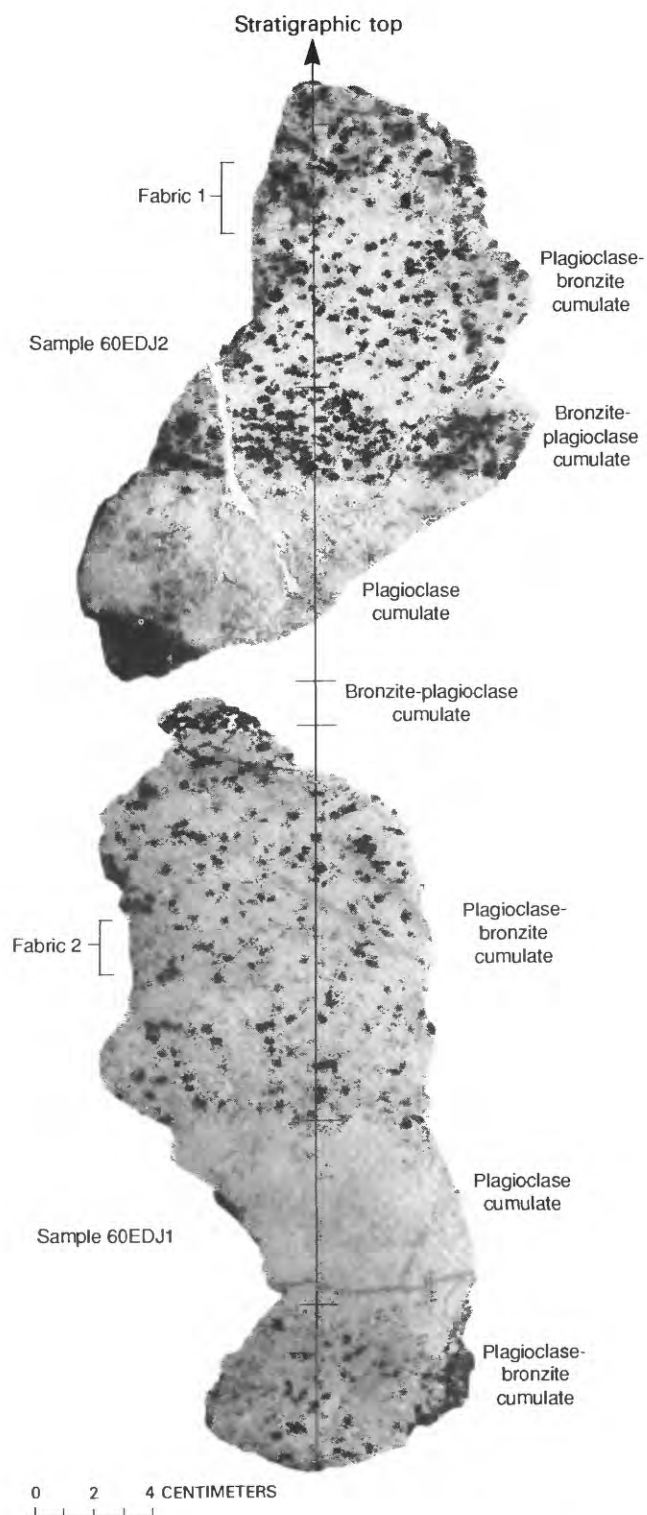


Figure 15. Rock slabs from subzone 2 of Gabbro-norite I zone showing detailed stratigraphy and location of areas where petrofabric studies were done. Sample locality shown on plate 1. See figure 16 for microprobe analyses of samples.

plagioclase-bronzite-augite, and plagioclase cumulates bulges from about 0.6 to 1.5 m in thickness over a strike length of about 7.6 m of outcrop. The structure consists of two asymmetric folds of the plagioclase-bronzite-augite cumulate layer with significant thickening in the hinge. The overlying plagioclase cumulate has attitudes subparallel to the regional trend with no evidence of folding or draping over the folded layers beneath.

The slump structures are best explained by plastic deformation of narrow zones of cumulate layers at or near the crystal pile-magma interface. Both examples suggest a floor of the magma chamber sloping to the east and thus a possible basin to the east of the outcrops. The infilling of the slump structure by overlying layers without those layers draping over the structure suggests that crystal accumulation was by bottom crystallization and that the crystals did not fall from great heights in the magma chambers.

Locally within the modal and phase layers, blocks of rocks that do not have the modal mineralogy of their host layer are found. These are most common in subzones of the Gabbro-norite I zone and in general consist of bronzite fragments, lenses, and schlieren-shaped clasts and locally anorthosite fragments. Figure 22 shows several of these fragments in the "Snoopy's Doghouse" area. The fragments can all be identified as parts of the Stillwater Complex, some from nearby lithologies, others, such as those described by Todd and others (1982), probably from farther removed lithologies.

PETROGRAPHY OF THE NORITE I AND GABBRO-NORITE I ZONES

The major cumulate rocks of the Norite I and Gabbro-norite I zones are described in terms of texture and mineralogy and by their variations in mode. Plagioclase, bronzite, augite, olivine, and chromite form the cumulus phases and occur in various combinations, as discussed below. Intercumulus phases include the same minerals, except chromite and rarely olivine, as well as phlogopite, amphibole, quartz, rutile, and sulfide and Fe-Ti oxide minerals. Secondary or alteration minerals include chlorite, sericite, tremolite-actinolite, epidote-clinzoisite, prehnite, serpentine, and magnetite. The sequence in which rocks are described in this section is from one- to two- to three-phase cumulates and is not the sequence in which rocks occur within units.

Plagioclase Cumulate

By definition, plagioclase is the only cumulus phase in plagioclase cumulates. Augite, bronzite, or both may occur as oikocrysts or as interstitial material to cumulus plagioclase in the plagioclase cumulates. Plagioclase has two habits in plagioclase cumulates; most commonly as intergrown subhedral to anhedral crystals ranging from 2 to

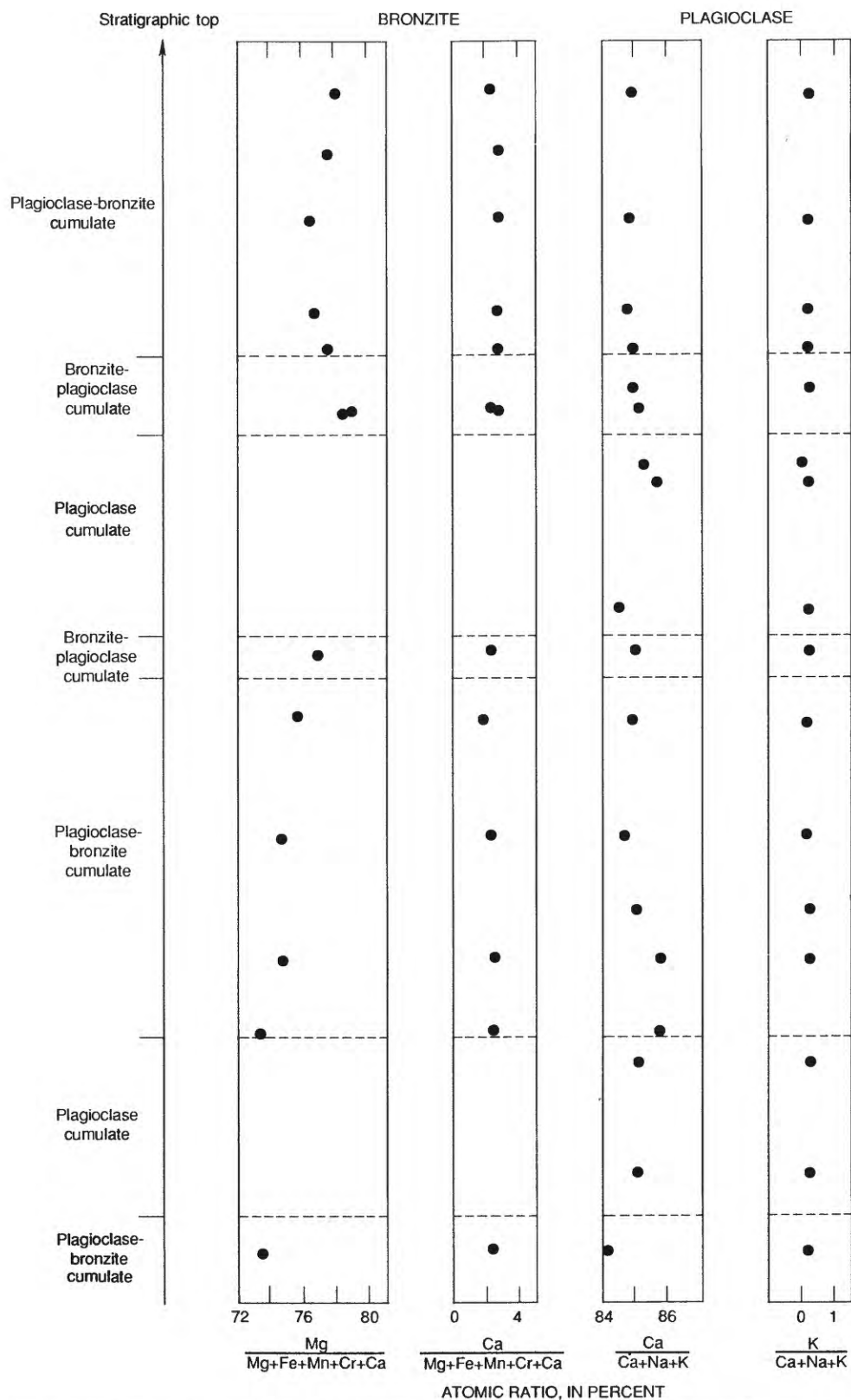


Figure 16. Microprobe analyses of bronzite and plagioclase compositions in layers of samples 6OEDJ1 and 6OEDJ2 (shown in fig. 15) from subzone 2 of Gabbonorite I zone.

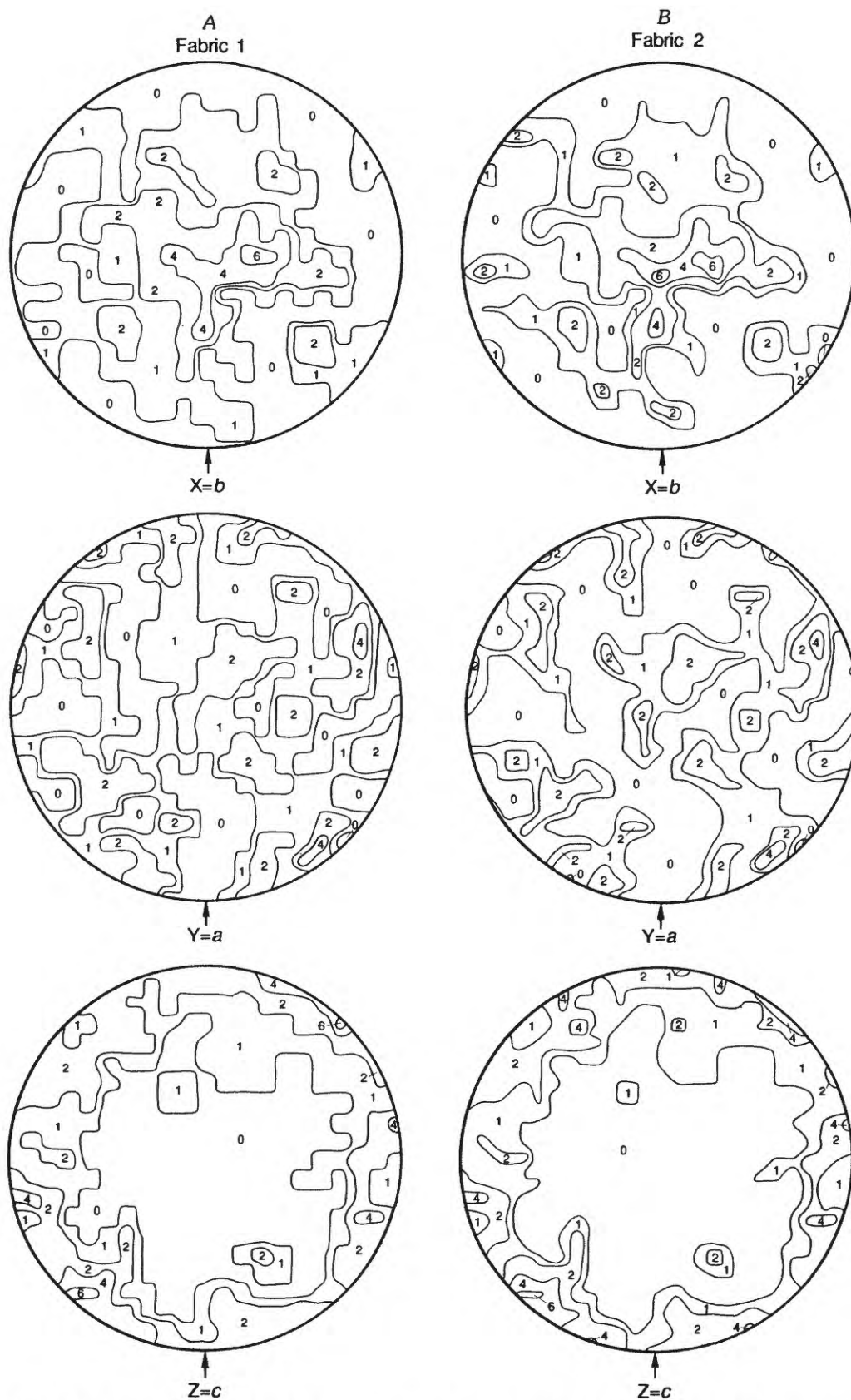


Figure 17. Petrofabric diagrams of bronzite from bronzite-plagioclase cumulates of subzone 2 of Gabbonorite I zone. *A*, Fabric 1. *B*, Fabric 2. 100 prismatic bronzite grains for each fabric. Contours in percent points per 1-percent area. Sections parallel to layering. Axial ratios $a:b:c=0.64:0.57:1$.

5 mm long and 1 to 3 mm wide with sutured to angular mutual boundaries. Less common are smaller, nearly euhedral crystals of plagioclase with rounded corners enclosed by a pyroxene oikocryst; for these crystals, the pyroxene oikocryst appears to have limited overgrowth on the original cumulus crystal. Zoning, common but never obvious, ranges from patchy to normal and oscillatory. This slight degree of zoning is consistent with Scheidle's (1983) and Czamanske and Scheidle's (1985) study of the Lower Anorthosite I zone, where An content ranged by several percent, in a single sample even though zoning was never distinct. Pyroxene oikocrysts range from 0.5 to 5 cm in diameter, are irregularly distributed, and show no preferred crystallographic orientation. No textural differences in the plagioclase cumulates of the various units was noted.

Plagioclase-Bronzite Cumulates

Within the Norite I zone, plagioclase-bronzite cumulate is the dominant rock type. Cumulus plagioclase and

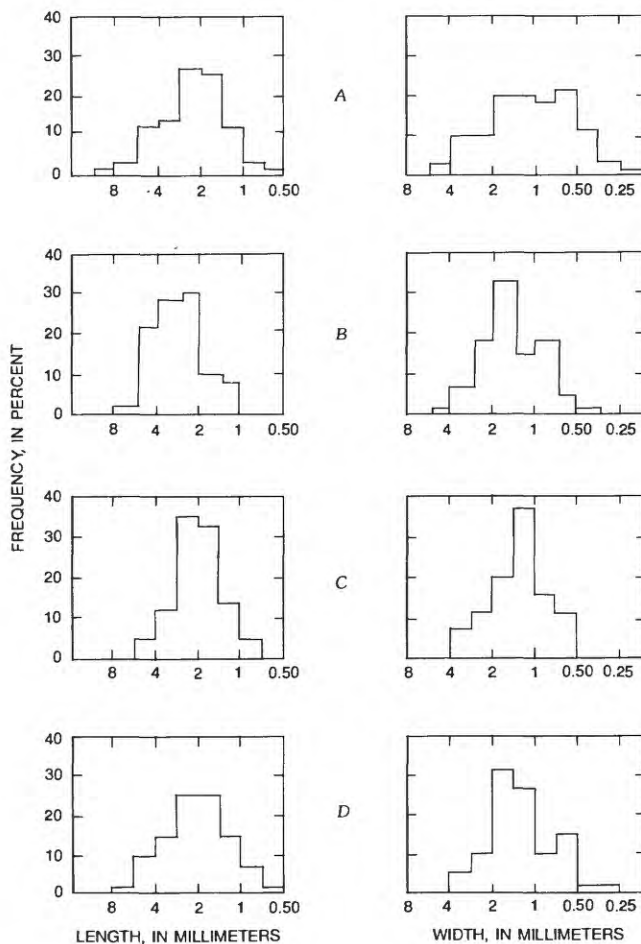


Figure 18. Histograms of size (length and width) of bronzite crystals in single samples showing their log-normal characteristics. A, Sample 48.0. B, Sample 47.5. C, Sample 13.2. D, Sample 9.4.

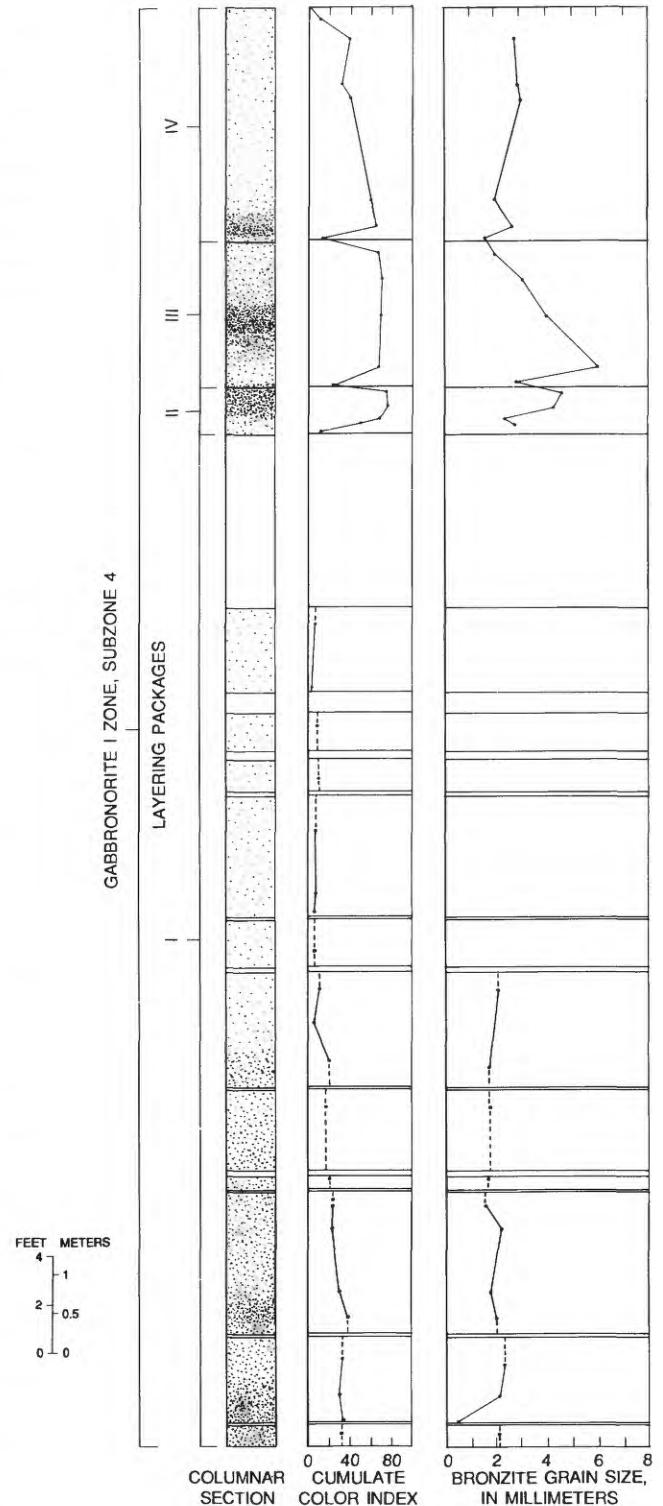


Figure 19. Columnar section of upper part of subzone 4 of Gabbro-norite I zone and variations in size of bronzite crystals and cumulate color index (dots represent individual samples; dashed lines represent projected trends). Dot density in section shows approximate modal amount of pyroxene.

bronzite both commonly have overgrowths, and augite is interstitial and locally replaces bronzite. Plagioclase is typically blocky in shape with angular to sutured grain boundaries but also occurs as inclusions with simple albite or Carlsbad twins within cumulus bronzite. Diffuse, patchy zoning of plagioclase crystals is common. Bronzite forms



Figure 20. Crosslamination in Norite I, subzone 2 (A), ruler is 17.8 cm, and in Gabbronorite I, subzone 3 (B), pen is 13.5 cm.

subhedral to euhedral crystals with overgrowths that extend outward into the plagioclase framework in a spiderweb pattern (fig. 26). The amount of spiderweb overgrowth tends to increase as modal plagioclase increases. Augite is interstitial and commonly forms oikocrysts, locally replacing part of the bronzite overgrowth. These textural relations suggest that plagioclase began to crystallize first and was followed by bronzite while both crystallized to form the crystal pile. Both continue to crystallize, forming the overgrowth, especially the spiderweb textures, and were joined by the precipitation of augite. Phlogopite, amphibole, quartz, and sulfide minerals were last to crystallize.

A comparison of the cumulus modes of plagioclase-bronzite cumulates with total rock modes is shown in figure 27. From Figure 27A, it is obvious that plagioclase and bronzite rarely occur in cotectic proportions but range from 22 to 95 percent plagioclase. Figure 27B shows that as plagioclase content increases the amount of interstitial augite increases. This relation is also reflected in the highly significant correlation ($r=-0.9$) between the contents of bronzite and augite.



Figure 21. Wispy layering near contact of subzone 2 with subzone 3 of Norite I zone.

Plagioclase-Bronzite-Augite Cumulate

The most common rock type of the Gabbronorite I zone is plagioclase-bronzite-augite cumulates. Morphology of the cumulus phases varies with modal proportions. As a general rule, the less voluminous a given cumulus phase is the more likely it will form overgrowths that are interstitial to or poikilitic on the other phases. Plagioclase occurs in three habits. In rocks with more than about 40 percent cumulus plagioclase, crystal forms tend to be subhedral and tabular with angular to sutured mutual boundaries, much like those in plagioclase-bronzite cumulates. In rocks with less than about 40 percent plagioclase, plagioclase overgrowths become interstitial to the pyroxene framework and commonly poikilitically enclose pyroxene crystals (fig. 28). In extremely mafic samples, intercumulus plagioclase overgrowth greatly exceeds cumulus plagioclase, which may even be absent on the scale of individual thin sections. The

third habit of plagioclase is as inclusions of small euhedral crystals with rounded corners and simple albite and Carlsbad twins in bronzite and augite.

Augite occurs as xenomorphic cumulus crystals, commonly enclosed in bronzite, and as anhedral interstitial material in the plagioclase framework. Interstitial augite is largely restricted to plagioclase-bronzite-clinopyroxene cumulates with less than about 30 percent cumulus augite. Generally bronzite forms subhedral cumulate crystals having spiderweblike overgrowths similar to those in the plagioclase-bronzite cumulates that locally enclose cumulus augite. In exceedingly mafic samples, bronzite tends to have euhedral habits. Phlogopite, amphiboles, and sulfide minerals are accessory phases.

Textural changes with modal proportions imply that modal graded layers are also texturally graded. Textural grading was noted in the detailed study of core DS-2/WD-6 of subzone 4 of the Gabbronorite I zone (fig. 29). In felsic

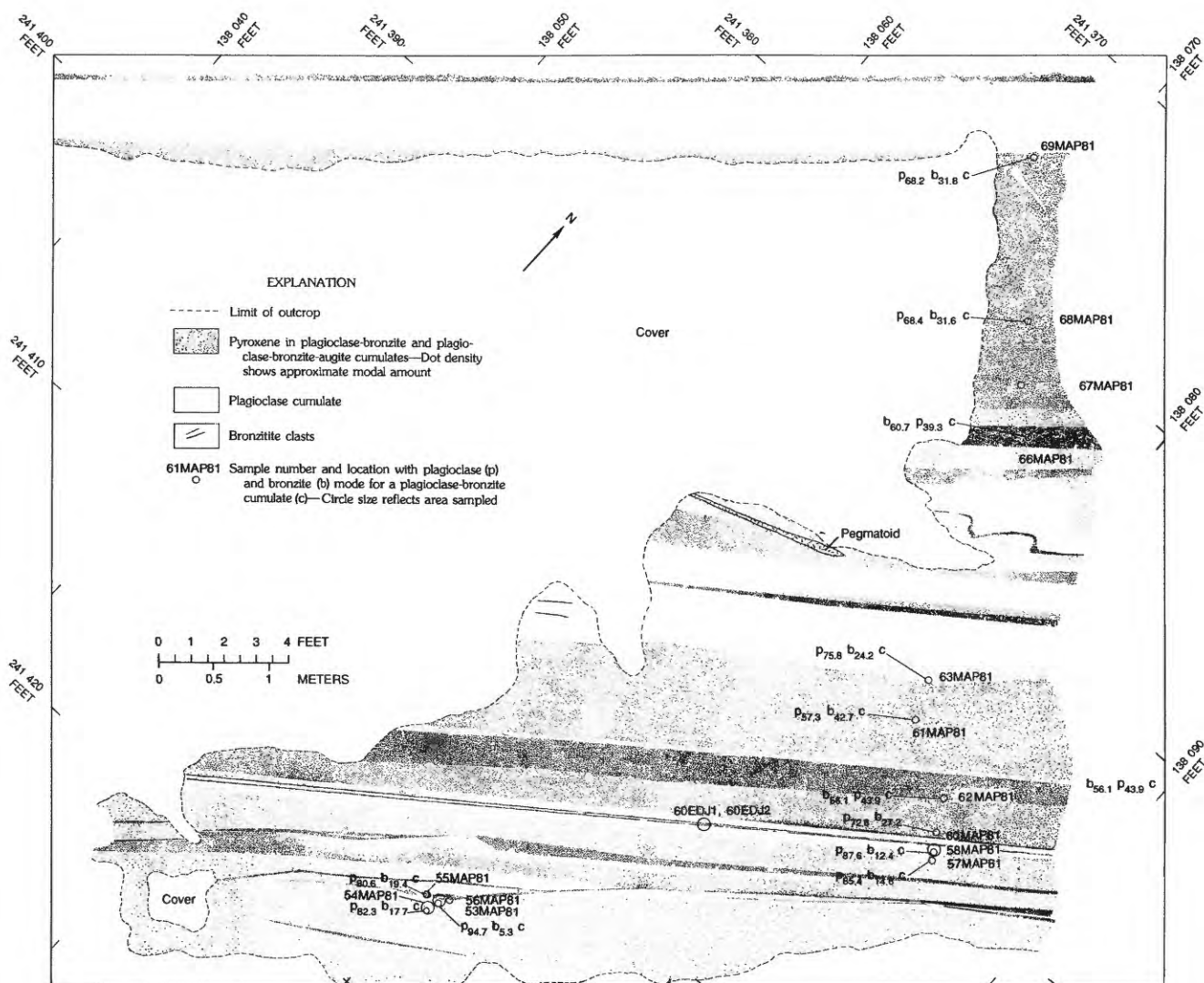


Figure 22. Schematic sketch map of "Snoopy's Doghouse" showing proportions of modal pyroxene in part of Gabbronorite I zone. Coordinates from Anaconda Minerals Company. Location of map shown on plate 1.



Figure 23. Bronzite-plagioclase and plagioclase cumulate layers in basinlike structure in "Snoopy's Doghouse" area. Notebook is 21 cm long.

to mafic sections, that is, with changing color index, textural grading occurs in plagioclase-bronzite-augite cumulates by the loss of interstitial augite followed by the occurrence of poikilitic plagioclase. Between a color index of about 17 and 60, augite is not an interstitial phase, and between a color index of 64 and 75, overgrowth plagioclase encloses cumulate pyroxenes. These variations in texture are shown schematically in figure 30 as textural categories.

Textural evidence suggests that cumulus plagioclase crystallized first, with cumulus augite crystallizing next or at the same time as plagioclase. This stage was followed by the crystallization of cumulus bronzite and the development of embayed margins of augite, perhaps by reaction or resorption with the magma. After establishing a cumulus framework, bronzite formed overgrowths on itself, augite, or both while plagioclase continued to crystallize as overgrowth material. Rare augite crystals with fractures infilled with postcumulus plagioclase suggest that all overgrowth did not occur until after some compaction of the pile.

Cumulus modes of plagioclase-bronzite-augite cumulates and total rock modes are compared in figure 31A and 31B. These diagrams indicate that eutectic proportions of



Figure 24. Ramp structure at locality A on plate 1. Knife is 9.5 cm.



Figure 25. Slump structure at "Snoopy's Doghouse" area. Pen is 12 cm long.



Figure 26. Cross-polarized light photomicrograph of bronzite with spiderweb overgrowth in plagioclase-bronzite cumulate.

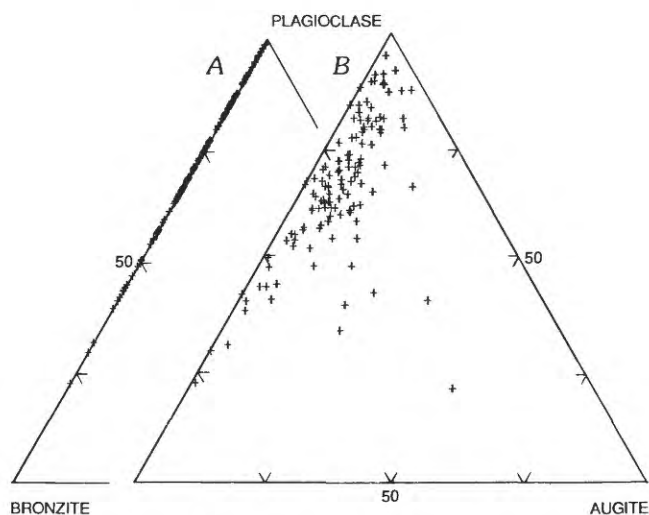


Figure 27. Triangular diagrams of mode of bronzite, augite, and plagioclase for plagioclase-bronzite cumulates. A, Cumulus mode. B, Total rock mode.

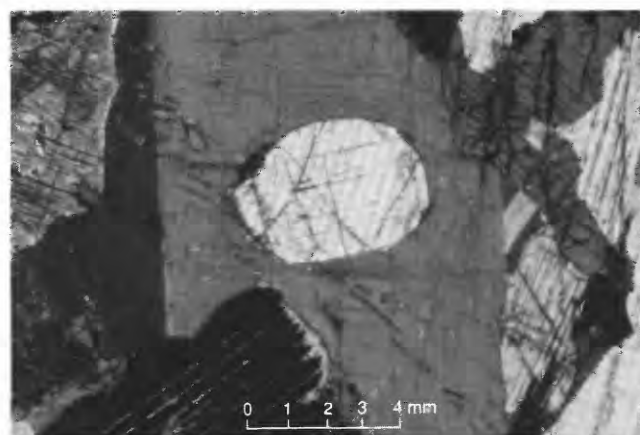


Figure 28. Photomicrograph of plagioclase overgrowth poikilitically enclosing augite in plagioclase-bronzite-augite cumulate.

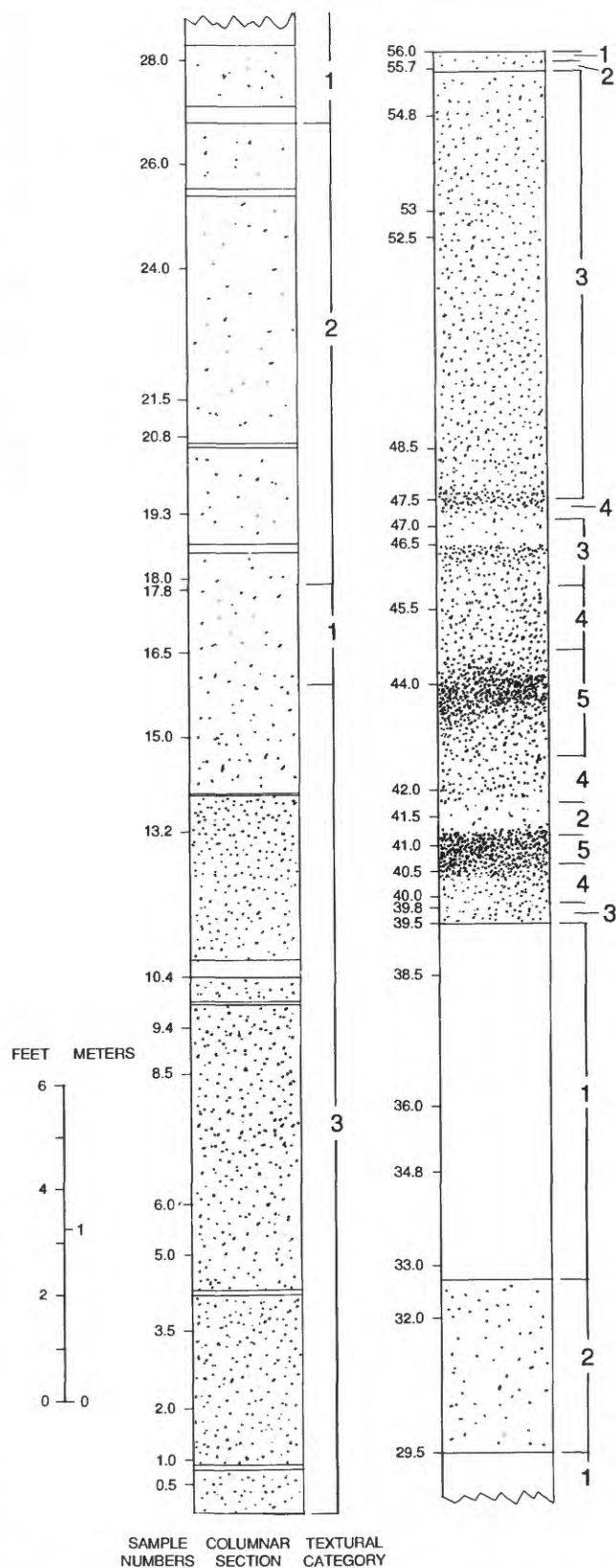


Figure 29. Columnar section based on core from drill hole DS-2/WD-6 showing textural grading. Unpatterned, plagioclase cumulate; dots proportional to pyroxene mode. Textural numbers correspond with those shown in figure 30.

the three phases rarely occur. The plot of cumulus modes in figure 31A indicates that rocks that can be distinguished by the presence or absence of intercumulus augite tend to plot in mutually exclusive fields, whereas modes of rocks with poikilitic plagioclase partially overlap with those without interstitial augite.

Plagioclase-Bronzite-Chromite Cumulate

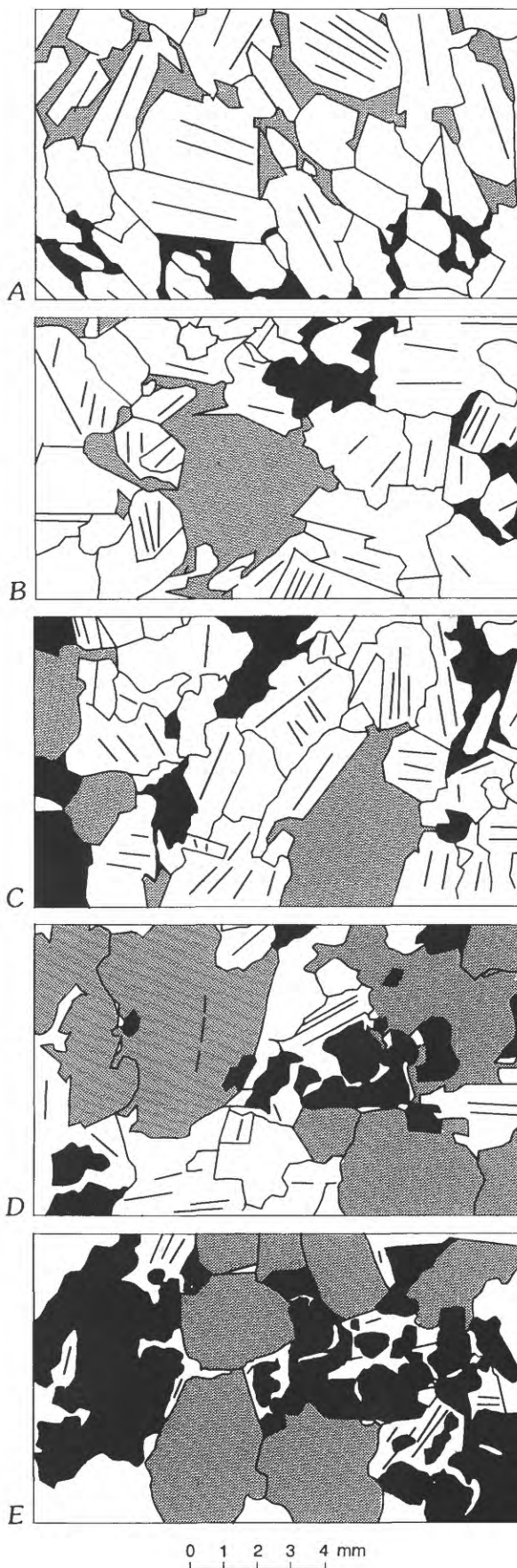
Plagioclase-bronzite-chromite cumulates were observed only in the lower 15 m of subzone 1 in the Norite I zone. Their mineralogy and texture are similar to plagioclase-bronzite cumulates except for the occurrence of euhedral crystals of chromite as much as 1 mm in diameter. The chromite forms as much as 2 percent of the rock and is present in disseminated patches and lenses. The texture of a plagioclase-bronzite-chromite cumulate is shown in figure 32.

Modal Mineralogy

Modal averages for rocks from the Norite I, Gabbronorite I, and Norite II zones were calculated by two methods, (1) simple averages of all samples collected and (2) weighted averages based on the linear percentage in the columnar sections (figs. 5, 7–10, 12–14) represented by each phase. The weighted averages are a more accurate representation of the overall composition of the units (table 2). The simple averages are useful to compare modes of individual lithologies, as it was not readily possible to calculate weighted averages for each lithology.

The overall weighted average composition of the Norite I, Gabbronorite I, and Norite II zones exclusively is 66.1 percent plagioclase, 23.9 percent bronzite, and 10.0 percent augite. Weighted subzone averages are listed in

Figure 30. Textural categories and their variations shown schematically, as defined in core DS-2/WD-6. Plagioclase shown as white with twinning lines inside; bronzite shown as light pattern; augite shown as dark pattern. *A*, Category 1. Plagioclase cumulate; intergrown cumulus plagioclase and poikilitic bronzite and augite. *B*, Category 2. Plagioclase-bronzite cumulate with cumulus plagioclase and bronzite with spiderweb overgrowths and intercumulus augite. *C*, Category 3. Plagioclase-bronzite-augite cumulate with intergrown cumulus plagioclase and cumulus bronzite with moderate overgrowth extending into the plagioclase framework and xenomorphic cumulus augite with intergranular overgrowth where not surrounded by cumulus or overgrown bronzite. *D*, Category 4. Plagioclase-bronzite-augite cumulate with overgrown cumulus plagioclase that poikilitically encloses augite locally, blocky cumulus bronzite with moderate overgrowth, and xenomorphic cumulus augite. *E*, Category 5. Augite-bronzite cumulate with cumulus augite, blocky cumulus bronzite, and poikilitic plagioclase.



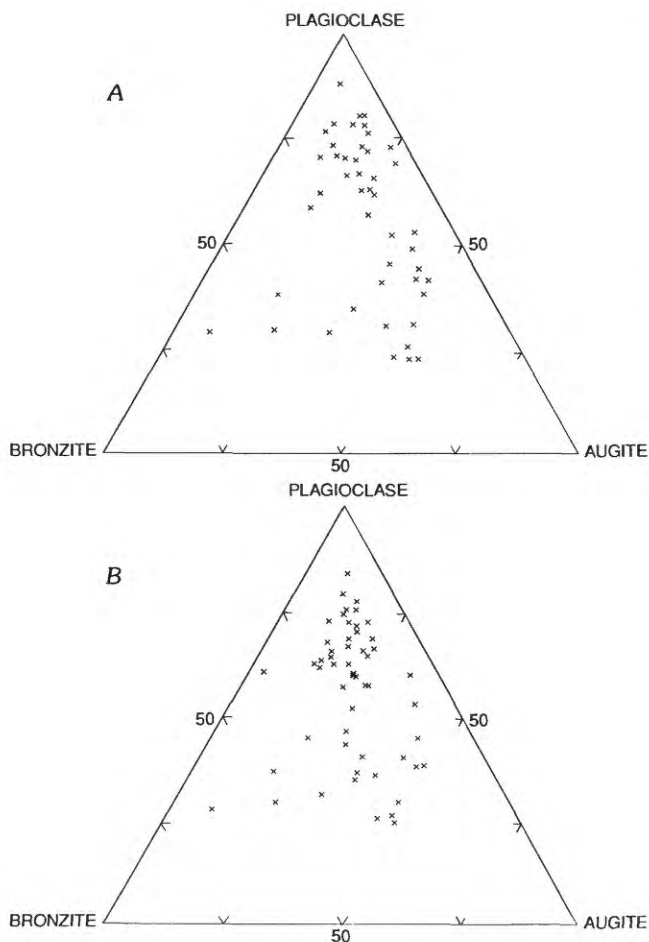


Figure 31. Triangular diagrams of plagioclase-bronzite-augite cumulates. *A*, Cumulus mode. *B*, Total rock mode.

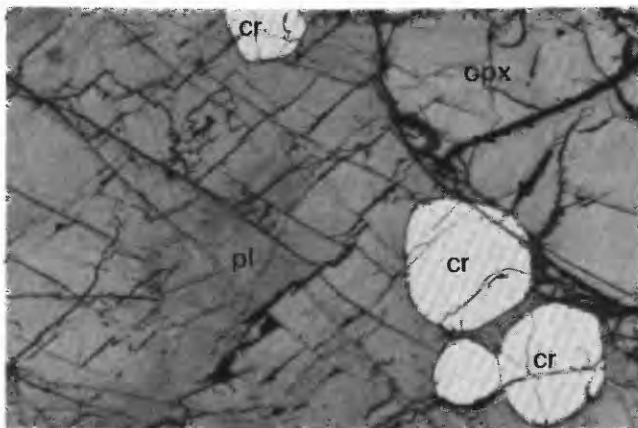


Figure 32. Photomicrograph in reflected light of plagioclase-bronzite-chromite cumulate from subzone 1 of Norite I zone. opx, bronzite; cr, chromite; pl, plagioclase. Field of view is 1.6 mm wide.

Table 2. Weighted-average modes by subzone and zone

Zone and subzone	Plagioclase	Bronzite	Augite	Number of samples
Norite I, subzone 1	66.8	29.0	9.2	48
Norite I, subzone 2	67.0	27.0	6.0	20
Norite I, subzone 3	68.1	24.7	7.2	11
Gabbronorite I, subzone 1	65.2	14.1	20.7	11
Gabbronorite I, subzone 2	49.9	24.4	25.7	24
Gabbronorite I, subzone 3	60.6	21.1	18.3	11
Gabbronorite I, subzone 4	75.6	16.3	9.1	65
Norite II	63.3	28.5	8.2	23
All rocks	66.1	23.9	10.0	213

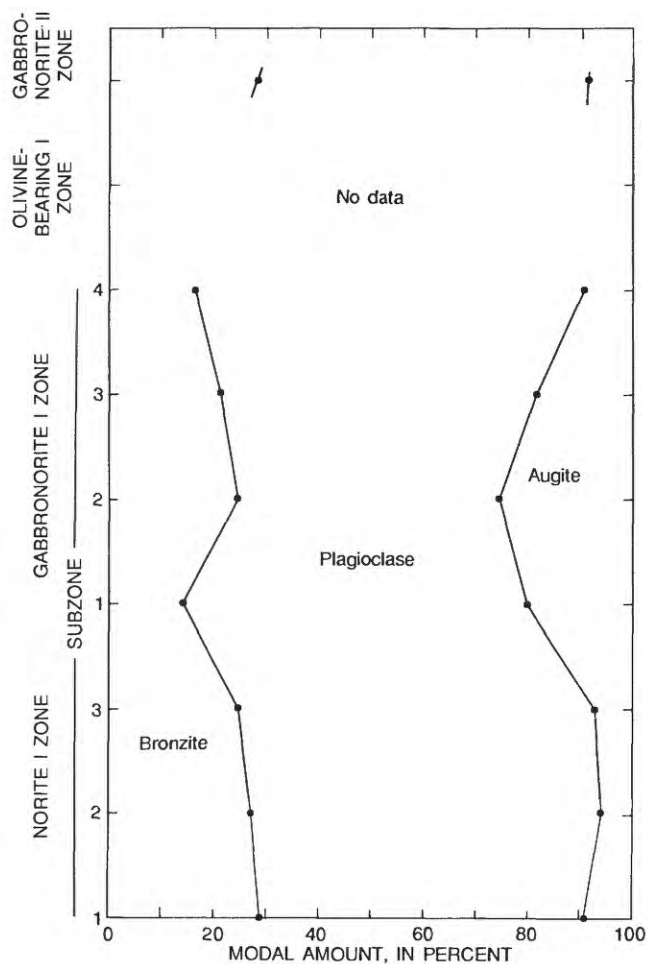


Figure 33. Weighted-average plagioclase, bronzite, and augite modes plotted by subzone and zone.

Table 3. Average total and cumulus modes for plagioclase-bronzite cumulates by subzone and zone

Zone and subzone	Total mode			Cumulus mode		Number of samples
	Plagioclase	Bronzite	Augite	Plagioclase	Bronzite	
Norite I, subzone 1	68.0	27.0	5.0	71.6	28.4	45
Norite I, subzone 2	63.4	26.7	9.9	70.4	29.6	21
Norite I, subzone 3	67.2	24.7	8.1	73.1	26.9	10
Gabbronorite I, subzone 1	68.4	20.1	11.5	77.3	22.7	2
Gabbronorite I, subzone 2	70.0	24.4	5.6	74.1	25.9	12
Gabbronorite I, subzone 3	55.0	37.7	6.4	59.7	40.3	4
Gabbronorite I, subzone 4	78.1	16.9	5.0	82.2	17.8	18
Norite II	60.2	33.1	6.7	64.5	35.5	19
All rocks	67.1	26.5	6.5	72.3	27.7	131

table 2 and plotted in figure 33. This figure shows a general decrease upsection in modal bronzite with the exception of the change from subzone 1 to subzone 2 of the Gabbronorite I zone. Augite increases slowly through subzone 3 of the Norite I zone and sharply at subzone 1 of the Gabbronorite I zone, commensurate with the appearance of abundant cumulus clinopyroxenite. Modal augite then decreases from subzone 2 through subzone 4 of the Gabbronorite I zone but shows little change from subzone 4 of the Gabbronorite I zone to the Norite II zone in spite of the disappearance of cumulus augite. Notably in subzones 1 through 3 of the Norite I zone, which are almost wholly composed of plagioclase-bronzite cumulates, augite increases with the upsection decrease in bronzite, yet where cumulus clinopyroxene is abundant in the Gabbronorite I zone, pyroxene modes have a positive correlation.

Plagioclase-bronzite cumulates (including plagioclase-bronzite cumulates with accessory cumulus chromite) vary in cumulus mode from rocks with as much as 77 percent bronzite to others with less than 5 percent (fig. 27A). Interstitial augite varies from nearly absent to more than 20 percent of the total rock mode and tends to show an increase with increasing plagioclase (fig. 27B).

Overall total mode averages of the 131 plagioclase-bronzite cumulate samples are plagioclase 67.1 percent, bronzite 26.5 percent, and augite 6.5 percent, whereas cumulus mode averages are 72.3 percent plagioclase and 27.7 percent bronzite. These modes can be compared to McCallum and others' (1980) estimate of cotectic proportions for norite of 60–64 percent plagioclase and 36–40 percent bronzite, which were inferred from Irvine's (1970) phase diagrams. The average cumulus modes probably represent a good approximation of the cotectic proportion of plagioclase and bronzite for Stillwater norites; however, this ratio is biased in favor of plagioclase due to the difficulty in distinguishing plagioclase overgrowth from cumulus plagioclase. Average modes for the plagioclase-bronzite cumulates of each subzone and zone are listed in table 3 and plotted in figure 34.

The composition of plagioclase-bronzite-augite cumulates ranges considerably. Modes range from 84 per-

cent to 21 percent for plagioclase, from 50 percent to 6 percent for bronzite, and from 52 percent to 6 percent for augite. In the most mafic samples, cumulus plagioclase may locally be absent on a thin-section scale. Unit to unit variation of average modes for plagioclase-bronzite-augite cumulates are listed in table 4. Simple average modes for 65 rocks sampled are 53.5 percent plagioclase, 21.1 percent

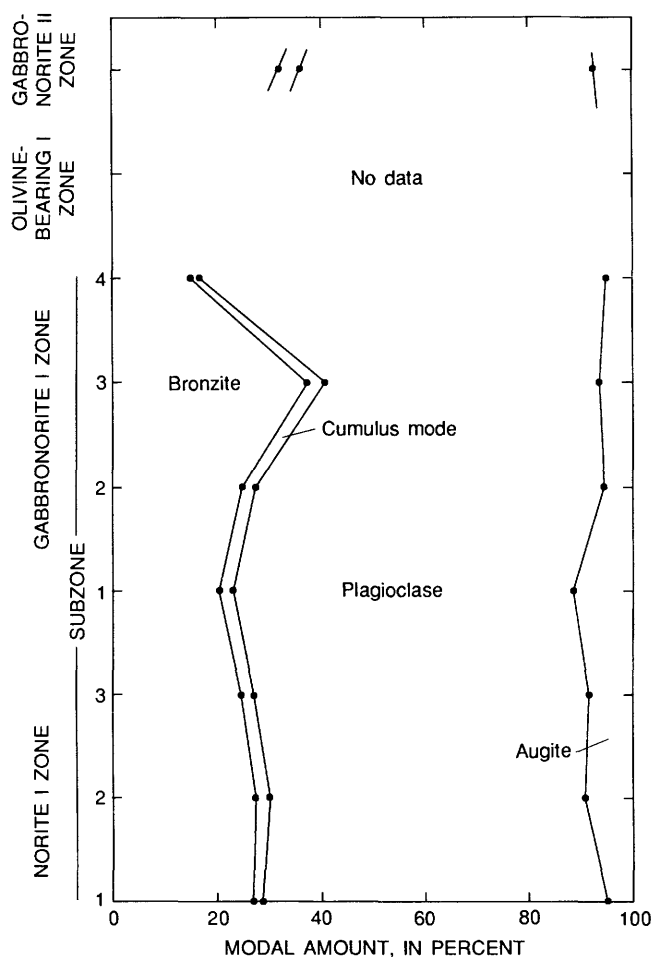


Figure 34. Average total and cumulus modes for plagioclase-bronzite cumulate plotted by subzone and zone.

Table 4. Average total and cumulus modes for plagioclase-bronzite-augite cumulates by subzone and zone

Zone and subzone	Plagioclase	Bronzite	Augite	Number of samples
Norite I, subzone 1	42.4	32.2	25.4	1
Norite I, subzone 3 ¹	37.5	15.8	46.7	1
Gabbronorite I, subzone 1	51.8	19.1	29.2	9
Gabbronorite I, subzone 2	43.8	26.4	29.8	11
Gabbronorite I, subzone 3	56.7	22.1	21.2	7
Gabbronorite I, subzone 4	56.5	19.5	24.0	35
Norite II	63.6	20.8	15.6	1
All rocks	53.3	21.1	25.6	65

¹One sample of a 4-cm-thick layer.

bronzite, and 25.6 percent augite. These may be compared with 55–60 percent plagioclase, 15–20 percent augite, and 20–25 percent orthopyroxene estimated as cotectic proportions for gabbronorite (McCallum and others, 1980). The agreement in estimates is almost perfect. Unit to unit average modes of all plagioclase bronzite-augite cumulate are listed in table 4 and shown in figure 35.

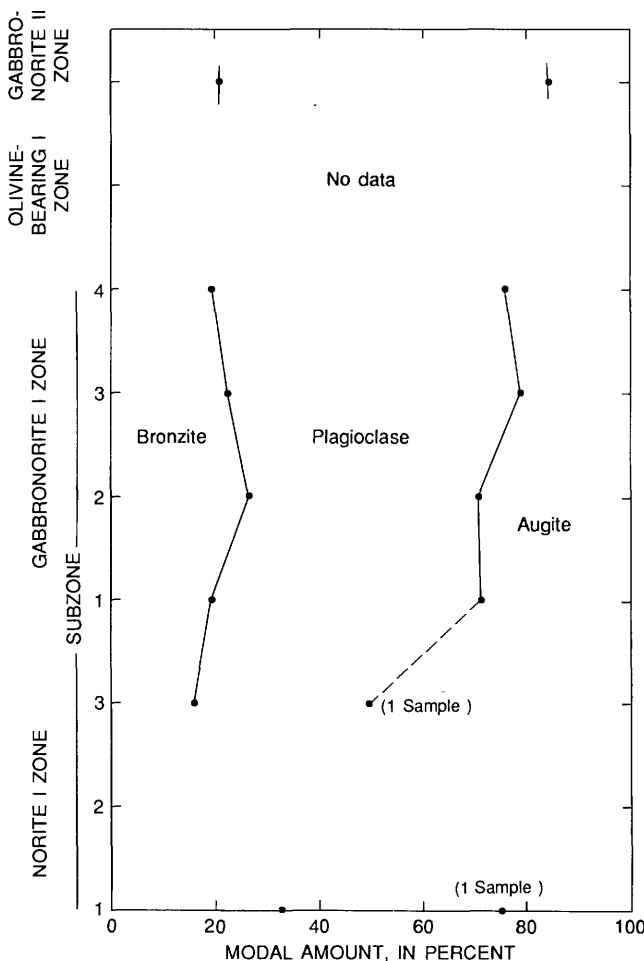


Figure 35. Average mode of plagioclase-bronzite-augite cumulates plotted by subzone and zone. Dashed line represents uncertainty.

Mineral Composition

Mineral compositions of 200 plagioclase and 198 bronzite samples were determined using the X-ray diffraction techniques of Jackson (1960) and Himmelberg and Jackson (1967). For all samples analyzed, plagioclase ranged from An₈₄ to An₆₃ and averaged An_{80.3}, and bronzite ranged from En₈₆ to En₅₇ and averaged En_{77.3}. Compositional data for each subzone and zone are listed in table 5. Interunit changes for average plagioclase and bronzite compositions are shown in figure 36.

Vertical variation within subzone and zone for plagioclase and bronzite compositions of individual samples varies by as much as 13 percent An and 26 percent En (table 4). However, the columnar sections of each subzone and zone (figs. 5, 7–10, 12–14) suggest that these variations are not strictly random but display various trends. In general, massively layered sections show relatively little variation in mineral compositions, whereas significant perturbations are common through more thinly layered sections. Trends of mineral compositions that underlie the perturbations associated with layering suggest several patterns. In subzone 1 of the Norite I zone (fig. 5), percentage An of two of the three columns increases upsection while percentage En tends to decrease. The third column shows little systematic change for either An or En content. In subzone 2 of the Norite I zone (fig. 7), both An and En content decrease upsection in the western column but show little change in the eastern column. In subzone 3 of the Norite I zone (fig. 8), both An and En tend to decrease upward in both columns. Subzones 2 and 3 of the Gabbronorite I zone (figs. 10 and 12) show a slight upsection decrease of En contents but little change in An content. In subzone 4 of the Gabbronorite I zone (fig. 13), widely spaced surface samples suggest that both An and En contents decrease upsection with little variation. However, detailed analysis from core DS-2/WD-6 indicates that the En content of bronzite varies considerably and that these variations have significant correlations at the 1 percent level with bronzite crystal size ($r=0.465$) and mode ($r=0.620$). In the Norite II zone (fig. 14), both An and En content tend to decrease slightly upsection.

In summary, in three units (subzone 1 of the Norite I zone and subzones 2 and 3 of the Gabbronorite I zone), En content decreased and An content either increased or remained approximately the same (fig. 37). In four sections (subzones 2 and 3 of the Norite I zone, subzone 4 of the Gabbronorite I zone, and the Norite II zone), both An and En contents tended to decrease upsection. In subzone 1 of the Gabbronorite I zone the En content increased slightly while An content remained approximately constant.

Average mineral compositions (fig. 36) for the units range from An_{81.1} to An_{78.2} for plagioclase and from En_{81.4} to En_{75.7} for bronzite. In general, both trends tend to decrease upsection; however, an analysis of variance of the

Table 5. Average, range, and standard deviations of mineral compositions of plagioclase and bronzite by subzone and zone

Zone and subzone	Average An or En ¹	Range		Standard deviation	Number of samples
		High	Low		
PLAGIOCLASE					
Norite I, subzone 1	81.1	88.9	76.2	2.0	49
Norite I, subzone 2	80.3	82.1	71.6	2.2	21
Norite I, subzone 3	81.0	87.5	77.5	2.7	11
Gabbronorite I, subzone 1	81.2	82.9	79.3	1.1	11
Gabbronorite I, subzone 2	80.5	82.5	78.5	1.2	25
Gabbronorite I, subzone 3	80.4	83.4	79.0	1.3	11
Gabbronorite I, subzone 4	79.9	83.0	74.0	1.8	62
Norite II	78.2	81.6	75.6	1.5	21
BRONZITE					
Norite I, subzone 1	77.7	83.2	72.1	2.6	45
Norite I, subzone 2	78.9	86.0	73.6	3.5	19
Norite I, subzone 3	77.2	81.2	73.6	2.7	11
Gabbronorite I, subzone 1	77.1	80.4	72.4	2.5	11
Gabbronorite I, subzone 2	71.3	83.3	68.4	3.2	27
Gabbronorite I, subzone 3	76.9	81.0	71.0	2.7	11
Gabbronorite I, subzone 4	75.7	83.0	57.0	4.5	55
Norite II	76.8	85.0	72.7	2.5	19

¹An, anorthite content for plagioclase; En, enstatite content for bronzite.

data indicates that only the average An content of the Norite II zone differs significantly from the values of other units.

Average mineral compositions for plagioclase cumulates, plagioclase-bronzite cumulates, and plagioclase-bronzite-augite cumulates are shown in figure 36. In general there is no consistent difference in An content between the three lithologies. Average bronzite composition, however, is always enriched in magnesium in plagioclase-bronzite-augite cumulate and in iron in the interstitial bronzite of the plagioclase cumulate. An analysis of variance of the data shows that only the iron enrichment in the plagioclase cumulates is significant at the 1 percent level for the entire section. On a smaller scale, the difference in En content for the three lithologies is significant in subzones 4 and 7 of the Gabbronorite I zone.

Sulfide Mineral Variation in Subzone 4 of the Gabbronorite I Zone

Most thin sections examined contained opaque minerals, which were preliminarily identified as sulfide minerals as well as oxides. Because sulfide minerals appeared to be present in most samples, the drill core (DS- 2/WD-6) in subzone 4 of the Gabbronorite I zone was selected for study of sulfide mineral distributions using polished thin sections. In addition, any patterns in sulfide mineralization could be related to patterns in the silicate mineral characteristics, as these were also studied in detail.

Sulfide minerals are present as both single-phase and polyphase grains as inclusions in silicate cumulus minerals, interstitially at silicate mineral boundaries, interstices, and triple junctions, and as veins. For those occurring as

inclusions, about 82 percent are enclosed in plagioclase, 14 percent in bronzite, 1 percent in clinopyroxene, and the remainder in epidote, an alteration mineral of plagioclase. Plagioclase-plagioclase grain boundaries predominate as the locations for interstitial sulfide minerals; minor amounts are at triple junctions and interstices formed by combinations of plagioclase and two pyroxenes. Commonly, small amounts of hornblende and phlogopite are associated with the sulfide minerals by occurring in the same interstitial space. About 20 percent of the sulfide grains have alteration minerals from plagioclase and pyroxene associated with them. The most common mineral is epidote, locally sericite, and rarely chlorite. The veins are usually less than a couple of millimeters long and 5 to 20 μm wide and probably represent remobilized primary sulfide minerals.

The most common shape of the sulfide grains approximates a rectangle which may be in part a function of the crystallographic habit of plagioclase. Next most common are elliptical shapes. Triangular, polygonal, and irregular

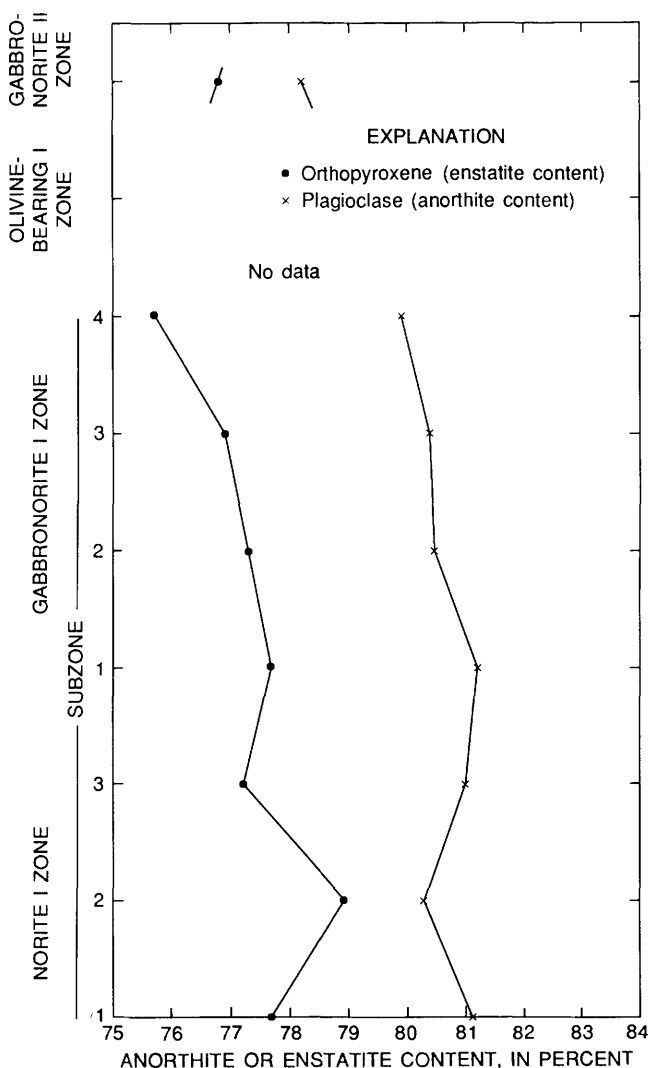


Figure 36. Average plagioclase and bronzite compositions plotted by subzone and zone.

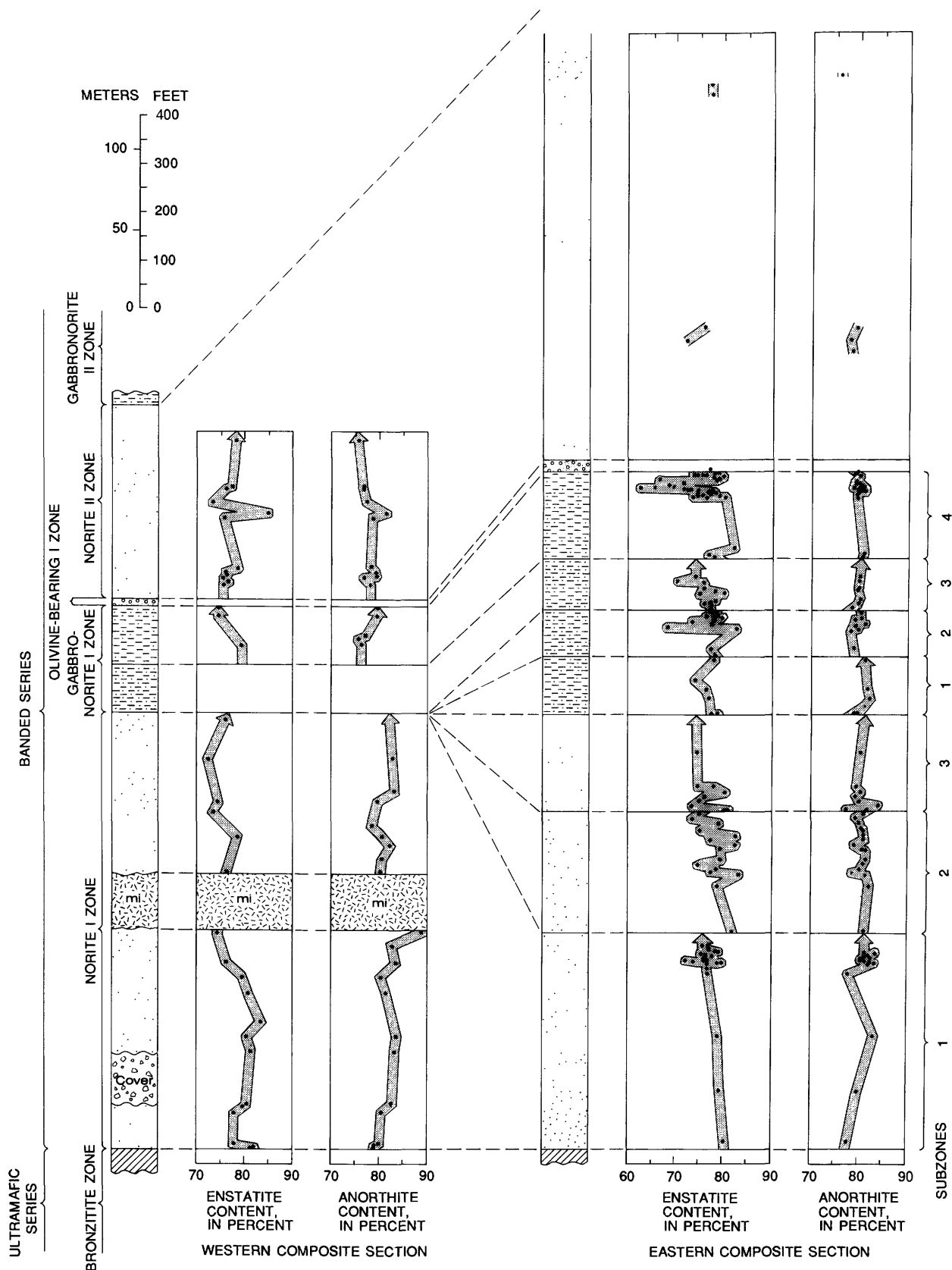


Figure 37. Generalized composite columnar sections for lower part of Banded series in Mountain View area, showing correlation of units and variation in bronzite and plagioclase compositions; mi, mafic intrusive rock. Dots, compositions of minerals in individual samples. Arrow shows projected trend in mineral compositions.

shapes of the sulfide grains are the least common. Sizes of the grains vary from 1 to 2 μm in average dimension (length + width/2) to about 220 μm and average about 52 μm .

The volume percent sulfide in the samples varies from about 0.001 percent to 0.016 percent as determined by measuring the area of the polished thin section and determining the total area occupied by sulfide grains. Such calculations probably only represent an order of magnitude and are similar to the 0.01 and 0.007 volume percent sulfide minerals found in the G and H chromitite zones of the Ultramafic series (Page, 1971b). Pyrrhotite, pentlandite, and chalcopyrite are the most abundant phases; magnetite is rare. Grains of one, two, three, and four phases were observed both as inclusions and interstitial material; however, pentlandite was not observed as single-phase grains. Proportions of sulfide minerals in three- or two-phase grains are highly variable. Vein fillings are predominantly pyrrhotite and chalcopyrite.

In order to estimate sulfide abundances through the section of subzone 4 of the Gabbronorite I zone, the number of polyphase sulfide grains was counted in polished thin sections. A group of these samples in which the sulfide and total area of the section were measured showed that the number of polyphase grains is proportional to the volume of sulfide minerals present, so that the more rapid technique of counting polyphase grains provides a reasonable estimate of the amount present. The sulfide abundance is compared with the silicate stratigraphy in the upper part of subzone 4 of gabbronorite I zone below the J–M Reef (fig. 38). Four polyphase grains per thin section equal approximately 0.006 percent by volume sulfide minerals, and nine grains approximate 0.013 percent sulfide minerals. The number of polyphase sulfide mineral grains per thin section tends to decrease upward in subzone 4 as the Olivine-bearing I zone is approached, with fairly wide fluctuations (fig. 38B). The use of a three-point running average smooths out some of the fluctuation but shows a similar pattern (fig. 38C).

The presence of sulfide minerals as polyphase grains in inclusions within cumulus plagioclase, the first cumulus phase to crystallize, suggests that immiscible sulfide liquid droplets were present when plagioclase crystallized. This also implies that the magma from which the plagioclase crystallized was saturated with respect to sulfide.

ROCK GEOCHEMISTRY OF SUBZONE 4 OF THE GABBRONORITE I ZONE

In order to characterize the geochemical environment in rocks immediately below the Olivine-bearing I zone, which contains the J–M Reef, core samples spaced approximately 30 to 60 cm apart were selected from drill hole DS–2/WD–6 for chemical analysis. The elements Ti, Mn, Ag, Co, Cr, Cu, Mo, Ni, Pb, Sn, V, and Zn were analyzed using quantitative emission spectroscopy, and Pt, Pd, and Rh were analyzed by fire assay-graphite furnace-atomic

absorption. The results are given in table 6. Five elements were not found above their detection limits: Ag (0.4 ppm), Mo (4 ppm), Sn (4 ppm), Zn (50 ppm), and S (0.01 weight percent). Rhodium was detected in two samples and Pb in three samples. The remaining elements were found at or above their detection limits with the distribution of concentrations in rocks for each element approaching log-normal values. Correlations for log-transformed concentrations between the trace elements are listed in table 7. Except for a weak correlation between themselves, Pt and Pd have no significant correlations with any of the detected elements. The remaining elements are moderately to highly correlated at better than the 1 percent level.

Average concentrations for cumulus rock types, shown in table 8, demonstrate that the elements Ti, Mn, Co, Cr, Cu, Ni, and V are related to rock type. Plagioclase-bronzite-augite cumulates on the average contain larger amounts of these elements than do plagioclase-bronzite or plagioclase cumulates. As these elements normally reside in mafic silicate, oxide, or sulfide minerals, such a relation should be expected. Further, correlations between log-transformed concentrations, total pyroxene mode, and En content of bronzite (table 9) emphasize this conclusion. Highly significant, moderate to high correlations exist between Ti, Mn, Cr, Co, Ni, and V and total mode; these elements also show moderate correlations with the En content of bronzite at the 1 percent level.

To investigate variations or changes in concentration levels not associated with the changes in total pyroxene mode, regressions of Ti, Mn, Co, Cr, Ni, and V against the total pyroxene mode were calculated. The residuals from these regressions were then plotted against stratigraphic height (fig. 39). These diagrams show individual samples that differ from the expected element concentration that would be predicted from the total pyroxene mode and (or) any chemical trends related to stratigraphic position. Deviations from predicted concentrations of elements based on total pyroxene mode reflect the occurrence of accessory minerals, such as oxide and sulfide minerals, or changes in trace element content of the pyroxenes related to magmatic differentiation. The divisions, I through IV, shown on figure 39 are layering packages that have pyroxene-enriched bases and grade to plagioclase-rich tops. The layering sequences defined in this way form repetitive cycles or units.

Residuals for Ti, Mn, Co, Cr, Ni, and V show strong excesses at or just above the boundary between the first and second layering package within the core section (samples 39.5–40.0). Near the boundaries between layering packages II and III and between III and IV, both excesses and depletions occur. Little significant difference or change is noted between layering packages II and III, but the top of layering package III is depleted in Mn, Co, Ni, and V and enriched in Ti. The residuals near the contact of subzone 4 of the Gabbronorite I zone with the Olivine-bearing I zone show increases in residuals similar or greater than those

between layering packages I and II. Residuals of Ni, Cr, and perhaps Co and the concentrations of Cu and Pt (table 6) show moderate to slight increases from the lower part of cyclic layering package I to the Olivine-bearing I zone. The increase in residual Cr upward through the core above layering package I agrees with observations of Barnes and Naldrett (1985) that Cr content in bronzite from the lower part of the Gabbronorite I zone ranges from 1,600 to 2,200 ppm and increases to 1,500 to 3,400 ppm at the boundary between the Gabbronorite I zone and the Olivine-bearing I zone. The range of Cr content in bronzite is greater (1,800–4,200 ppm) in the Olivine-bearing I zone. The

upward decrease in residual Cr within layering package I appears to be controlled by the upward decrease of the ratio of clinopyroxene to bronzite.

In summary, much of the variation in trace-element content in rocks below the Olivine-bearing I zone is explained by variation in the amounts of modal pyroxene. The residuals, the variation not ascribable to total pyroxene modal variations, in some situations can be ascribed to magmatic differentiation; however, rapid changes in the residuals are more probably related to variations in the amounts of accessory minerals, such as oxides and sulfide minerals.

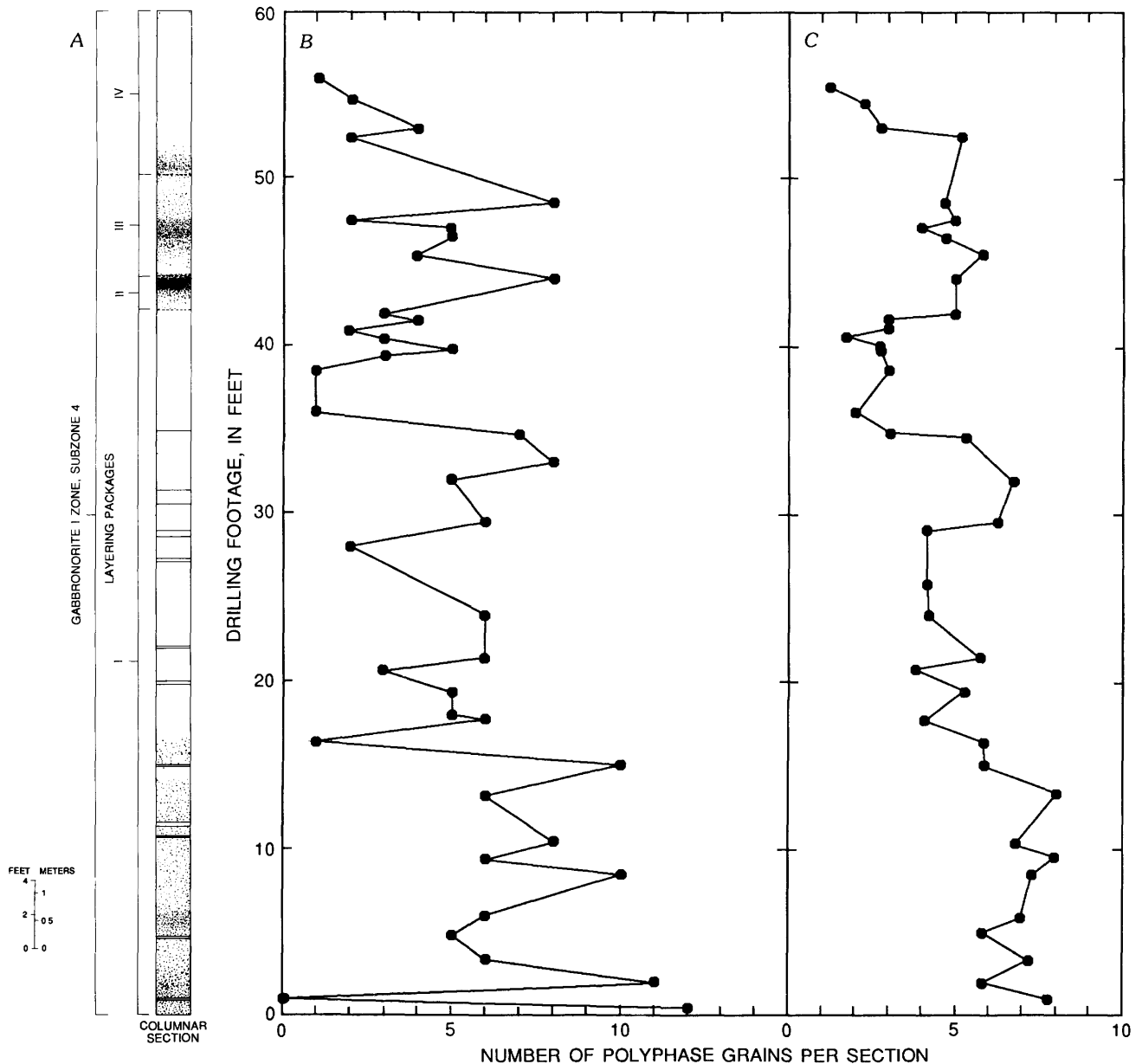


Figure 38. Estimated sulfide mineral abundance compared with silicate stratigraphy in subzone 4 of Gabbronorite I zone. Samples from DS-2/WD-6 core. A, Silicate stratigraphy. Dot density shows approximate modal amount of pyroxene. B, Number of polyphase sulfide grains per section. C, Three-point moving average of number of polyphase sulfide grains per section.

Table 6. Trace element analyses of rock samples from subzone 4 of the Gabbronorite I zone

[Values are given in parts per million. Samples from core DS-2/WD-6 and sample numbers are drilling footages. Ti, Mn, Co, Cr, Cu, Pb, Ni, and V by quantitative emission spectroscopy; analysts: J Kent and C. Heropoulos; Pd, Pt, and Rh by fire assay-graphite furnace-atomic absorption; analysts: J. McDade and S. Wilson; *, insufficient sample]

Sample No.	Ti	Mn	Co	Cr	Cu	Pb	Ni	V	Pd	Pt	Rh
0.5	0.05	780	38	1500	14	<14	170	110	0.009	0.025	<0.001
1	.05	720	28	1600	18	<14	160	150	.01	.018	<.001
2	.04	670	28	1400	15	<14	150	120	.009	.019	<.001
3.5	.05	810	41	1600	17	<14	200	140	.002	.014	.001
4.9	.06	790	41	1700	24	<14	220	150	.008	.017	<.001
6	.05	670	27	1400	15	<14	140	120	.006	.014	<.001
8.5	.05	590	25	1100	19	<14	120	100	.009	.018	<.001
9.4	.05	660	29	1400	19	<14	150	130	*	*	*
10.4	.04	380	15	620	13	<14	69	71	.012	.017	<.001
13.2	.04	500	21	590	20	<14	100	70	.005	.027	<.001
15	.05	590	22	980	22	<14	140	98	.004	.015	<.001
16.5	.03	300	10	150	21	<14	55	43	.004	.2	<.001
17.8	.03	420	12	160	16	<14	67	37	*	*	*
18	.04	370	15	430	15	<14	87	76	.001	.026	<.001
19.2	.04	420	16	290	17	<14	96	63	.01	.018	<.001
20.5	*	*	*	*	*	*	*	*	*	*	*
21.5	.04	350	13	230	18	<14	63	62	.007	.064	<.001
24	.04	330	14	190	20	<14	68	62	.008	.025	<.001
26	.04	360	15	290	18	<14	82	72	.008	.027	<.001
28	.03	320	11	280	17	<14	54	64	.007	.032	.001
29.5	.03	360	14	210	17	<14	70	52	.007	.027	<.001
32	.04	410	17	200	17	43	74	64	.005	.025	<.001
33	.05	360	10	140	25	41	58	72	.012	.031	<.001
34.8	.04	250	9.7	85	18	83	52	53	.005	.018	<.001
36	.05	330	11	62	14	<14	43	65	.001	<.01	<.001
38.6	.04	330	8.5	170	4.9	<14	42	46	.004	.02	<.001
39.5	.04	660	23	430	26	<14	154	73	*	*	*
39.8	.09	1200	57	3000	49	<14	390	240	.005	.019	<.001
40	.1	1300	72	3200	60	<14	430	380	.003	.013	<.001
40.5	.1	1400	71	2700	21	<14	410	260	.001	.011	<.001
41	.09	1400	72	3200	26	<14	420	220	.009	.028	<.001
41.5	.06	850	36	1400	42	<14	170	130	*	*	*
42	.06	980	62	2500	32	<14	350	160	.015	.033	<.001
44.5	.1	1100	69	3200	38	<14	430	210	.007	.124	<.001
45.5	.07	1100	67	3100	39	<14	400	200	.008	.017	<.001
46.5	.04	1100	60	2600	32	<14	330	190	.016	.024	<.001
47	.08	310	11	440	27	<14	73	60	.004	.027	<.001
47.5	.08	1000	59	2800	24	<14	330	180	.012	.03	<.001
48.5	.05	1000	59	2900	52	<14	360	190	.01	.024	<.001
52.5	.06	730	37	1800	31	<14	240	110	.031	.033	<.001
53	.05	820	42	1900	33	<14	280	110	.027	.029	<.001
54.8	*	*	*	*	*	*	*	*	*	*	*
55.7	.05	710	44	1900	41	<14	290	110	.011	.021	<.001
56	.05	660	25	225	29	<14	130	78	.012	.093	<.001

ENVIRONMENTS OF MAGMATIC ACCUMULATION BELOW THE J-M REEF

The stratigraphic, mineralogic, and petrologic observations discussed and tabulated for cumulus rocks below the Olivine-bearing I zone and above the Bronzite zone describe two extremes of depositional environments for the cumulates. One environment produces cumulates with monotonous-appearing characteristics that vary only slightly over relatively large distances; the other produces cumulates that have highly variable characteristics over

relatively short distances. Within and between subzones there is an interplay between both environments that appears predominantly with stratigraphic position but which is also present along strike. In addition, there are petrologic constraints imposed by examining the average characteristics of the zones and subzones as whole units excluding the variability. It is these different features that must be addressed by genetic models for the formation of the Norite I and Gabbronorite I zones.

Characteristics of the monotonous-appearing cumulates include relatively thick modal and phase layers within

Table 7. Correlation coefficients of log-transformed concentrations of selected trace elements in rocks from subzone 4 of the Gabbronorite I zone

[Values are significant at the 1 percent level when the correlation coefficient is greater than 0.400]

	Pd	Pt	Ti	Mn	Co	Cr	Cu	Ni
Pt	0.427	—	—	—	—	—	—	—
Ti	.093	0.203	—	—	—	—	—	—
Mn	.175	.214	0.722	—	—	—	—	—
Co	.210	.198	.715	0.978	—	—	—	—
Cr	.258	.319	.672	.915	0.933	—	—	—
Cu	.284	.073	.553	.617	.659	0.567	—	—
Ni	.237	.201	.728	.968	.987	.935	0.707	—
V	.059	.322	.796	.930	.934	.903	.626	0.921

Table 8. Average concentrations of selected trace elements in rocks from subzone 4 of the Gabbronorite I zone based on analyses in table 5

[ppm, parts per million; ppb, parts per billion]

Element	Plagioclase-bronzite-augite cumulate	Plagioclase-bronzite cumulate	Plagioclase cumulate
Ti, wt pct	0.065	0.043	0.040
Mn, ppm	858	517	391
Co, ppm	44	23	14
Cr, ppm	1968	728	206
Cu, ppm	28	25	19
Ni, ppm	253	130	73
V, ppm	153	80	62
Pd, ppb	6.5	7.5	6.6
Pt, ppb	21.6	22.5	35.7

Table 9. Correlation coefficients of log-transformed concentrations of selected elements, total pyroxene mode, and En content of bronzite for rocks from subzone 4 of the Gabbronorite I zone

[Values are significant at the 1 percent level when the correlation coefficient is greater than 0.40]

Element	Total pyroxene mode	En content
Ti	0.67	0.49
Mn	.84	.59
Co	.85	.67
Cr	.90	.38
Cu	.42	.59
Ni	.83	.54
V	.86	.58

which there is slight variation in the modal composition of the cumulates. Nevertheless, within the thick layers the slight changes in modal composition are exhibited by pyroxene-rich bases and plagioclase-enriched tops to the layers, thus producing overall large-scale mineral-graded layers. Within layers, bronzite and plagioclase compositions are relatively constant showing only small changes in En and An content; that is, there is little cryptic layering. Textural layering is also sparse.

In the environment that produces cumulates with highly variable features, the characteristics of the rocks include relatively thin modal and phase layers (thin as one crystal thick). Modal compositions of the cumulates are highly variable, as are the plagioclase and bronzite compositions. Mineral, size, and cryptic layering are well developed. Textural layering is common. Syndepositional structures and irregular layering are characteristic features of the cumulates formed in this environment. In addition, the features change relatively rapidly (over distances of outcrop scale) along strike.

Both environments tend to be constrained to specific positions in the stratigraphic sections (compare figure 34 with the detailed sections figures 5, 7–10, and 12–14). The bases of the subzones of the Norite I and Gabbronorite I

zones contain the more monotonous-appearing cumulates, whereas the tops of the subzones contain the cumulates with highly variable characteristics. There are exceptions to this observation, and along strike within a subunit, the environment does change locally. The general pattern implies that during the deposition of subzones, the environment or the processes producing that environment changed during the period of deposition.

Excluding the variability and examining only the overall characteristics of the plagioclase-pyroxene cumulates below the Olivine-bearing I zone also imposes constraints on the processes that produced the two extreme environments. Although few individual samples of plagioclase-bronzite or plagioclase-bronzite-augite cumulate have the hypothetical modal eutectoid compositions for basaltic liquids, the average modal compositions of the cumulates approach both of the eutectoid compositions. Layers, subzones, and zones tend to have decreasing modal amounts of bronzite and clinopyroxene upward, as emphasized in figure 31. Another overall characteristic is the change from either plagioclase-bronzite or plagioclase-bronzite-augite to plagioclase cumulate upward in the stratigraphic section. Relatively small changes in average En and An content of bronzite and plagioclase are observed,

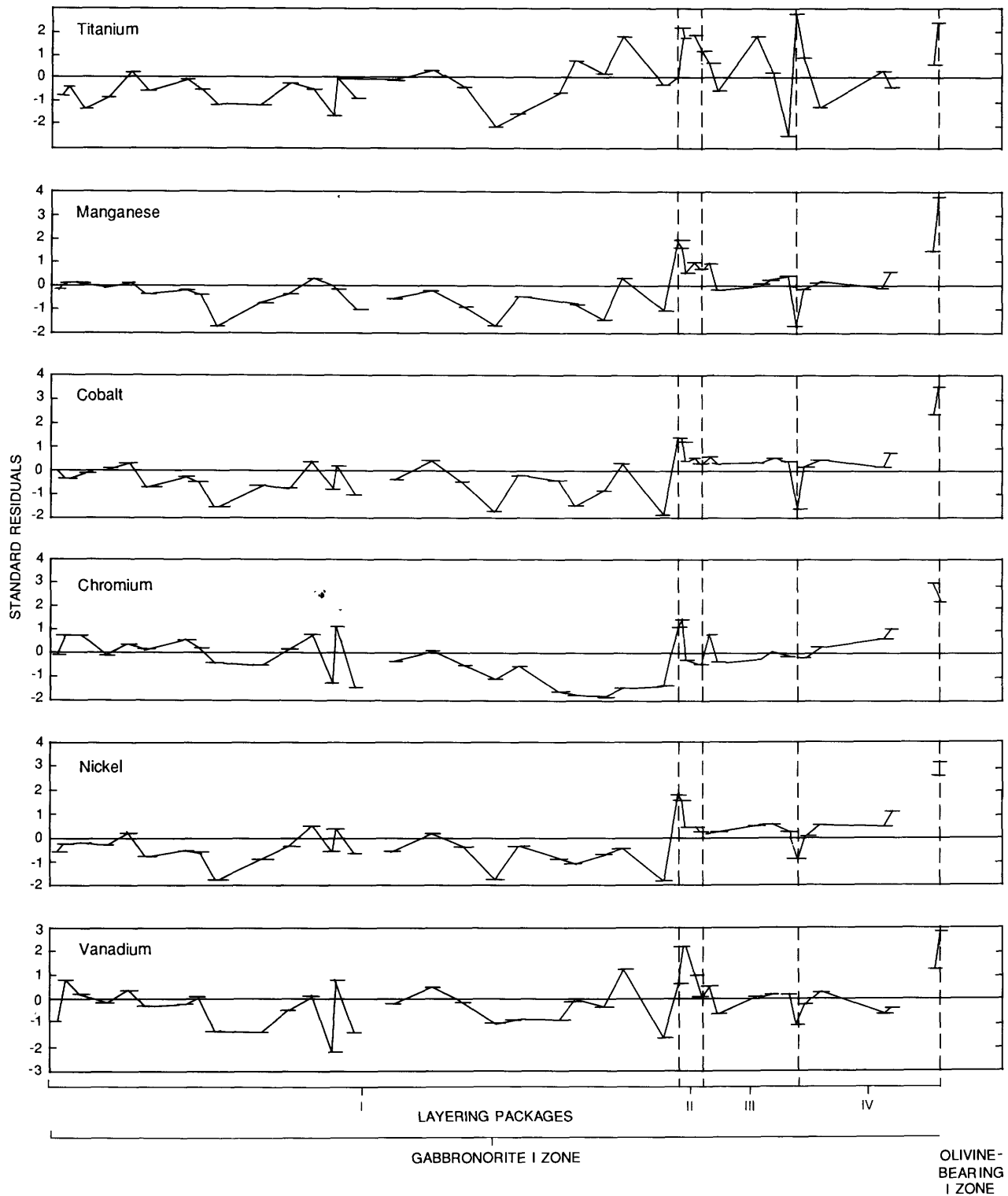


Figure 39. Standard residuals from regressions of titanium, manganese, cobalt, chromium, nickel, and vanadium against total pyroxene mode, plotted against stratigraphic position, in subzone 4 of Gabbronorite I zone.

although the compositions do change toward lower En and An contents upward through the subzones in a relatively regular fashion. The final characteristic that needs consideration is the overall dominance of the monotonous-type cumulates in the lower subzones of the Norite I zone and the progressively increasing dominance of the variable-type cumulates in the subzones of Gabbronorite I just below the Olivine-bearing I zone with the return to the more monotonous-type cumulates in the Norite II zone.

DISCUSSION AND DEVELOPMENT OF A MODEL FOR THE GENESIS OF THE NORITE I AND GABBRONORITE I ZONES

A wide range and variety of processes and models have been put forward and defended to explain the development of cumulate rocks and their repetitive layering in specific and general examples. These include (1) crystal settling under the influence of gravity or in convection currents as discussed by Hess (1960) and Wager and Brown (1968), who also recognized the potential for crystals floating, accreting to walls or the roof of an intrusion and upward or inward in-place growth of crystals from the floor or walls, (2) in-place crystallization from stagnant batches of magma with the potential for crystals settling only short distances (Jackson, 1961a, and refined by Campbell, 1978), (3) crystallization concurrently of whole sequences of cumulus layers by downdip accretion from magma layers of varying compositions separated by diffusive interfaces (Irvine and others, 1983), (4) magma replenishment or influxes and mixing (Brown, 1957; Raedeke and McCallum, 1984), and (5) various other processes dependent upon changes in pressure (Osborn, 1980; Cawthorn, 1982), compaction and expulsion of pore magma (Irvine, 1980), diffusion-controlled crystal growth and oscillatory nucleation (McBirney and Noyes, 1979), and contamination by crustal materials. The purpose of this brief and incomplete review is not to decide the merits of one or the other of the hypotheses, but to credit some of the sources that influenced the model presented below.

The small and relatively regular changes in the average composition of bronzite and clinopyroxene upward through the Norite I and Gabbronorite I zones suggest that magmas of similar compositions related by normal differentiation were the source of the cumulates. The development of subzones within the zones that have more plagioclase-rich tops than bottoms suggests that the magmas, in a generalized way, crystallized in batches, subzone by subzone. The existence of local unconformities at subzone boundaries also supports crystallization individually and in the sequence of the subzones. However, the crystallization of a subzone is more complicated, and these complications are represented by the two extreme environments of deposition.

The homogeneity exhibited by the composition of bronzite and plagioclase within the monotonous-appearing

parts of the subzones could be explained by nucleation and equilibrium crystallization with the crystals suspended in the batch of magma from which they originated. Such a process also accounts for the overall approach of the cumulates to modal compositions resembling hypothetical eutectoid proportions. As crystallization proceeded, pyroxene and plagioclase must have adjusted their position in the suspension under the influence of gravity by pyroxene settling, plagioclase floating, or both to enrich the bases in pyroxene and the tops in plagioclase. Because there is little evidence for large amounts of size sorting of either plagioclase or bronzite, the crystals must not have traveled great distances. This also implies that the thickness of magma from which a monotonous-appearing part of a subzone crystallized was probably not much thicker than those cumulates. After the cumulus crystals formed an interlocking pile of crystals, postcumulus processes could and did modify the cumulates, but the result did not produce textural layering, suggesting that broad-scale interchange of magma within the pore spaces did not happen.

Near the tops of subzones, the monotonous-appearing cumulates are followed by cumulates that vary rapidly in modal mineral composition, crystal size, and textural and structural characteristics. Although the characteristics change rapidly, they correlate well one with another and imply that modal amount, mineral composition, crystal size, and textural category are interrelated. The structural features in these thinner cumulate layers imply an environment of higher energy involving currents and changes in orientation of the floor. Specifically, the onlap and offlap relations of cumulate layers are evidence that the orientation of the floor changed during deposition, and slump and ramp structures imply that the crystal pile was poorly cemented and that movements of the floor may have triggered the instability of the cumulates. Unconformities, scours, channels, and current structures suggest local erosion and deposition by moving magma. The rapidly varying modes, mineral compositions, and crystal size suggest that accumulation of cumulus material involved gravity, currents, and perhaps variations in magma composition. The stratigraphic and structural relations of the thin cumulate layers suggest that the cumulus crystals did not settle great distances under the influence of gravity and settled perhaps no farther than the thickness of the layer that contains them. Even in this environment, there are regular changes within layers of cumulates, such as plagioclase enrichment upward, and regular sequences of layers from bronzite-plagioclase to plagioclase cumulates or bronzite-augite-plagioclase to bronzite-plagioclase to plagioclase cumulates. After deposition, the pore-filling magma must have been much more active than in the monotonous-appearing cumulates to have produced the textural changes that produce textural layering. At the top of the cumulates that formed in the more active environment is a sharp boundary, usually an unconformity or at least locally an unconformity, above which monotonous-appearing cumu-

lates were deposited. This boundary appears critical in the interpretation of processes and probably represents the arrival of a new batch of magma at this particular position in the chamber. The precursor events to this, as shown by the structures in the cumulates with variable characteristics, seem to be changes in the orientation of the floor, production of current features, and perhaps production of variable composition magmas. There are several ways of interpreting the boundary. One is that new magma of slightly different composition, but with a composition that could be produced from the underlying magma by normal basaltic fractionation, was introduced either from an exterior source or from the Stillwater chamber itself, perhaps by variable depth convection as outlined by Jackson (1961a). Another interpretation is that the rocks immediately below the boundary represent a zone of magma mixing either in a density-composition stratified magma chamber or from the introduction of a batch of new denser magma and that the rocks above represent the return to normal crystallization. For the subzones within the Norite I and Gabbronorite I zones, we believe that the evidence favors the former interpretation.

The observation that cumulates with variable characteristics progressively become more dominant as the Olivine-bearing I zone is approached is intriguing. Did the development of these rocks act as a signal or precursor to major change in the Stillwater magma chamber? Most investigators of the J-M Reef or Olivine-bearing I zone agree that its formation represents the introduction of new magma of different composition than the rest of the magma chamber. Such an event could involve a period of structural preparation of the conduits, country rocks, and chamber that might have been reflected in the change of environment from low-energy, almost stagnant conditions to a high-energy environment.

REFERENCES CITED

- Barnes, S.J., 1982, Investigations of the Stillwater Pt/Pd horizon, Minneapolis adit areas: Stratigraphic relations, geochemistry and genesis, *in* Walker, D., and McCallum, I.S., eds., Workshop on magmatic processes of early planetary crusts: Magma oceans and stratiform layered intrusions: Lunar and Planetary Institute, Houston, Tex., LPI Technical Report 82-01, p. 45-48.
- Barnes, S.J., Campbell, I.H., and Naldrett, A.J., 1982, Mineral composition variations associated with platinum mineralization in the Stillwater Complex, Montana [abs.]: Geological Association of Canada-Mineralogical Association of Canada Joint Annual Meeting, Program with Abstracts, v. 7, p. 37.
- Barnes, S.J., and Naldrett, A.J., 1983, Mineral composition variations associated with the J-M Reef of the Stillwater Complex: Constraints on magma compositions [abs.]: Geological Society of America Abstracts with Programs, v. 15, p. 521.
- , 1985, Geochemistry of the J-M (Howland) Reef of the Stillwater Complex, Minneapolis adit area; I, Sulfide chemistry and sulfide-olivine equilibrium: *Economic Geology*, v. 80, p. 627-645.
- Boudreau, A.E., 1982, The main platinum zone, Stillwater Complex, MT-Evidence for bimetasomatism and a secondary origin for olivine, *in* Walker, D., and McCallum, I.S., eds., Workshop on magmatic processes of early planetary crusts: Magma oceans and stratiform layered intrusions: Lunar and Planetary Institute, Houston, Texas, LPI Technical Report 82-01, p. 59-61.
- Bow, C., Wolfgram, D., Turner, A., Barnes, S., Evans, J., Zdepski, M., and Boudreau, A., 1982, Investigations of the Howland reef of the Stillwater Complex, Minneapolis adit area: Stratigraphy, structure, and mineralization: *Economic Geology*, v. 77, p. 1481-1492.
- Cabri, L.J., 1981, Relationship of mineralogy to the recovery of PGE from ores, *in* Cabri, L.J., ed., Platinum-group elements: Mineralogy, geology, recovery: Canadian Institute of Mining and Metallurgy Special Volume 23, p. 233-250.
- Campbell, I.H., 1978, Some problems with the cumulus theory: *Lithos*, v. 11, p. 311-323.
- Carlson, C.A., and Moring, B.C., 1985, ENSTA: A program to calculate orthopyroxene compositions from X-ray data: U.S. Geological Survey Open-File Report 85-104, 8 p.
- Casella, C.J., 1969, A review of the Precambrian geology of the eastern Beartooth Mountains, Montana and Wyoming, *in* Larsen, L.H., Prinz, M., and Manson, V., eds., Igneous and metamorphic geology: Geological Society of America Memoir 115, p. 53-71.
- Cawthorn, R.G., 1982, An origin of small-scale fluctuations in bronze composition in the lower and critical zones of the Bushveld Complex, South Africa: *Chemical Geology*, v. 36, p. 227-236.
- Coffrant, D., Tatsumoto, M., and Obradovich, J.D., 1980, Sm-Nd age of the Stillwater Complex [abs.]: International Geological Congress, 26th, Abstracts, v. 2, p. 768.
- Conn, H.K., 1979, The Johns-Manville platinum-palladium prospect, Stillwater Complex, Montana, U.S.A., *in* Naldrett, A.J., ed., Nickel-sulfide and platinum-group-element deposits: Canadian Mineralogist, v. 17, p. 463-468.
- Czamanske, G.K., and Scheidle, D.L., 1985, Characteristics of the Banded-series anorthosites, *in* Czamanske, G.K., and Zientek, M.L., eds., The Stillwater Complex, Montana: Geology and guide: Montana Bureau of Mines and Geology Special Publication 92, p. 334-345.
- Czamanske, G.K., and Zientek, M.L., eds., 1985, The Stillwater Complex, Montana: Geology and guide: Montana Bureau of Mines and Geology Special Publication 92, 396 p.
- DePaolo, D.J., and Wasserburg, G.J., 1979, Sm-Nd age of the Stillwater Complex and the mantle evolution curve for neodymium: *Geochimica et Cosmochimica Acta*, v. 43, p. 999-1008.
- Foose, M.P., 1985, Primary structural and stratigraphic relations in Banded-series cumulates exposed in the East Boulder Plateau-Contact Mountain area, *in* Czamanske G.K. and Zientek, M.L., eds., The Stillwater Complex, Montana: Geology and guide: Montana Bureau of Mines and Geology Special Publication 92, p. 305-324.
- Foose, R.M., Wise, D.U., and Garbarini, G.S., 1961, Structural geology of the Beartooth Mountains, Montana and Wyo-

- ming: Geological Society of America Bulletin, v. 72, p. 1143–1172.
- Fuchs, W.A., and Rose, A.W., 1974, The geochemical behavior of platinum and palladium in the weathering cycle in the Stillwater Complex, Montana: *Economic Geology*, v. 69, p. 332–346.
- Hess, H.H., 1936, Plagioclase, pyroxene and olivine variation in the Stillwater Complex: *American Mineralogist*, v. 21, p. 198–199.
- 1938a, Primary banding in norite and gabbro: *American Geophysical Union Transactions*, part I, p. 264–268.
- 1938b, A primary peridotite magma: *American Journal of Science*, 5th series, v. 35, p. 231–344.
- 1939, Extreme fractional crystallization of a basaltic magma: The Stillwater Igneous Complex: *American Geophysical Union Transactions*, part III, p. 430–432.
- 1940, An essay review: The petrology of the Skaergaard Intrusion, Kangerdlugssuaq, East Greenland: *American Journal of Science*, v. 238, p. 372–378.
- 1941, Pyroxenes of common mafic magmas: *American Mineralogist*, v. 26, part 1, p. 515–535, part 2, p. 573–594.
- 1960, Stillwater igneous complex, Montana—A quantitative mineralogical study: *Geological Society of America Memoir* 80, 230 p.
- Hess, H.H., and Phillips, A.H., 1938, Bronzites of the Bushveld type: *American Mineralogist*, v. 23, p. 450–456.
- 1940, Optical properties and chemical composition of magnesian bronzites: *American Mineralogist*, v. 25, p. 271–285.
- Himmelberg, G.R., and Jackson, E.D., 1967, X-ray determinative curve for some orthopyroxenes of composition Mg_{48-85} from the Stillwater Complex, Montana in *Geological Survey Research 1967*: U.S. Geological Survey Professional Paper 575-B, p. B101–B102.
- Howland, A.L., 1933, Sulphide and metamorphic rocks at the base of the Stillwater Complex, Montana: Princeton, N.J., Princeton University, Ph.D. thesis, 81 p.
- Howland, A.L., Peoples, J.W., and Sampson, E., 1936, The Stillwater igneous complex and associated occurrences of nickel and platinum metals: *Montana Bureau of Mines and Geology Miscellaneous Contribution* 7, 15 p.
- Humphreys, R.H., 1983, The characterization of the sulfide component in layered igneous and metasedimentary rocks in the Mouat block of the Stillwater Complex: San Jose, Calif., San Jose State University, Master's thesis, 44 p.
- Irvine, T.N., 1970, Crystallization sequences in the Muskox intrusion and other layered intrusions—I. Olivine-pyroxene-plagioclase relations: *Geological Society of South Africa Special Publication* 1, p. 441–475.
- 1980, Magmatic infiltration metasomatism, double-diffusive fractional crystallization, and adcumulus growth in the Muskox intrusion and other layered intrusions, in Hargroves, R.B., ed., *Physics of magmatic processes*: Princeton, N.J., Princeton University Press, p. 325–382.
- 1982, Terminology for layered intrusions: *Journal of Petrology*, v. 23, p. 127–162.
- Jackson, E.D., 1960, Primary textures and mineral associations in the Ultramafic zone of the Stillwater Complex, Montana: Los Angeles, Calif., University of California, Ph.D. thesis, 307 p.
- 1961a, Primary textures and mineral associations in the Ultramafic zone of the Stillwater Complex, Montana: U.S. Geological Survey Professional Paper 358, 106 p. [Reprinted 1984, Montana Bureau of Mines and Geology, Reprint 4.]
- 1961b, X-ray determinative curve for some natural plagioclases of composition An_{60-85} , in *Short papers in the geologic and hydrologic sciences*: U.S. Geological Survey Professional Paper 424-C, p. C286–C288.
- Jones, W.R., Peoples, J.W., and Howland, A.L., 1960, Igneous and tectonic structures of the Stillwater Complex, Montana: U.S. Geological Survey Bulletin 1071-H, p. 281–340.
- Lambert, D.D., 1982, Geochemical evolution of the Stillwater Complex, Montana: Evidence for the formation of platinum-group element deposits in mafic layered intrusion: Golden, Colo., Colorado School of Mines, Ph.D. thesis, 274 p.
- Lambert, D.D., Unruh, D.M., and Simmons, E.C., 1985, Isotopic investigations of the Stillwater Complex: A review, in Czamanske, G.K., and Zientek, M.L., eds., *The Stillwater Complex, Montana: Geology and guide*: Montana Bureau of Mines and Geology Special Publication 92, p. 46–54.
- Leonard, B.F., Desborough, G.A., and Page, N.J., 1969, Ore microscopy and chemical composition of some laurites: *American Mineralogist*, v. 54, p. 1330–1346.
- LeRoy, L.W., 1985, Troctolite-Anorthosite zone I and the J-M Reef: From Pondadit and Graham Creek area, in Czamanske, G.K., and Zientek, M.L., eds., *The Stillwater Complex, Montana: Geology and guide*: Montana Bureau of Mines and Geology Special Publication 92, p. 325–333.
- Mann, E.L., Lin, C.P., 1985, Geology of the West Fork adit, in Czamanske, G.K., and Zientek, M.L., eds., *The Stillwater Complex, Montana: Geology and guide*: Montana Bureau of Mines and Geology Special Publication 92, p. 247–252.
- Mann, E.L., Lipin, B.R., Page, N.J., Foote, M.P., and Loferski, P.J., 1985, Guide to the Stillwater Complex exposed in the West Fork area, in Czamanske, G.K., and Zientek, M.L., eds., *The Stillwater Complex, Montana: Geology and guide*: Montana Bureau of Mines and Geology Special Publication 92, p. 231–246.
- McBirney, A.R., and Noyes, R.M., 1979, Crystallization and layering of the Skaergaard intrusion: *Journal of Petrology*, v. 20, p. 487–554.
- McCallum, I.S., Raedeke, L.D., and Mathez, E.A., 1980, Investigations of the Stillwater Complex: Part I. Stratigraphy and structure of the Banded zone: *American Journal of Science*, v. 280-A (The Jackson Volume), p. 59–87.
- Moring, B.C., and Carlson, C.A., 1985, ANORTH: A program to calculate plagioclase compositions from X-ray data: U.S. Geological Survey Open-File Report 85–103, 7 p.
- Mueller, P.A., Wooden, J.L., Henry, D.J., and Bowes, D.R., 1985, Archean crustal evolution of the eastern Beartooth Mountains, Montana and Wyoming, in Czamanske, G.K., and Zientek, M.L., eds., *The Stillwater Complex, Montana: Geology and guide*: Montana Bureau of Mines and Geology Special Publication 92, p. 9–20.
- Nunes, P.D., 1981, The age of the Stillwater Complex—A comparison of U-Pb zircon and Sm-Nd isochron systematics: *Geochimica et Cosmochimica Acta*, v. 45, p. 1961–1963.
- Nunes, P.D., and Tilton, G.R., 1971, Uranium-lead ages of minerals from the Stillwater igneous complex and associ-

- ated rocks, Montana: Geological Society of America Bulletin, v. 82, p. 2231-2249.
- Osborn, E.F., 1980, On the cause of the reversal of normal fractionation trend—An addendum to the paper by E.N. Cameron: *Economic Geology*, v. 75, p. 872-875.
- Page, N.J., 1971a, Comments on the role of oxygen fugacity in the formation of immiscible sulfide liquids in the H chromitite zone of the Stillwater Complex, Montana: *Economic Geology*, v. 66, p. 607-610.
- , 1971b, Sulfide minerals in the G and H chromitite zones of the Stillwater Complex, Mont.: U.S. Geological Survey Professional Paper 694, 20 p.
- , 1972, Pentlandite and pyrrhotite from the Stillwater Complex, Montana: Iron-nickel ratios as a function of associated minerals: *Economic Geology*, v. 67, p. 814-818.
- , 1977, Stillwater Complex, Montana; Rock succession, metamorphism and structure of the complex and adjacent rocks: U.S. Geological Survey Professional Paper 999, 79 p. [Reprinted in 1983.]
- , 1979, Stillwater Complex, Montana; Structure, mineralogy, and petrology of the Basal zone with emphasis on the occurrence of sulfides: U.S. Geological Survey Professional Paper 1038, 69 p.
- Page, N.J., and Jackson, E.D., 1967, Preliminary report on sulfide and platinum-group minerals in the chromitites of the Stillwater Complex, Montana, in *Geological Survey Research 1967*: U.S. Geological Survey Professional Paper 575-D, p. D123-D126.
- Page, N.J., and Nokleberg, W.J., 1974, Geologic map of the Stillwater Complex, Montana: U.S. Geological Survey Miscellaneous Investigation Series I-797, 5 sheets, scale 1:12,000.
- Page, N.J., Riley, L.B., and Haffty, Joseph, 1969, Platinum, palladium, and rhodium analyses of ultramafic and mafic rocks from the Stillwater Complex, Mont.: U.S. Geological Survey Circular 624, 12 p.
- , 1971, Lateral and vertical variation of platinum, palladium, and rhodium in the Stillwater Complex, Montana [abs.]: *Geological Society of America Abstracts with Programs*, v. 3, p. 401.
- , 1972, Vertical and lateral variation of platinum, palladium, and rhodium in the Stillwater Complex, Montana: *Economic Geology*, v. 67, p. 915-923.
- Page, N.J., Rowe, J.J., and Haffty, Joseph, 1976, Platinum metals in the Stillwater Complex, Montana: *Economic Geology*, v. 71, p. 1352-1363.
- Page, N.J., Shimek, Richard, and Huffman, C.J., 1972, Grain-size variations within an olivine cumulate, Stillwater Complex, Montana, in *Geological Survey Research 1972*: U.S. Geological Survey Professional Paper 800-C, p. C29-C37.
- Page, N.J., and Zientek, M.L., 1985, Geologic and structural setting of the Stillwater Complex, in Czamanske G.K., and Zientek, M.L., eds., *The Stillwater Complex, Montana: Geology and guide*: Montana Bureau of Mines and Geology Special Publication 92, p. 1-8.
- Page, N.J., Zientek, M.L., Lipin, B.R., Raedeke, L.D., Wooden, J.L., Turner, A.R., Loferski, P.J., Foose, M.P., Moring, B.C., and Ryan, M.P., 1985, Geology of the Stillwater Complex exposed in the Mountain View area and on the west side of the Stillwater Canyon, in Czamanske, G.K., and Zientek, M.L., eds., *The Stillwater Complex, Montana: Geology and guide*: Montana Bureau of Mines and Geology Special Publication 92, p. 147-209.
- Peoples, J.W., 1932, The geology of the Stillwater igneous complex: Princeton, N.J., Princeton University, 180 p.
- , 1933, Stillwater igneous complex, Montana: *American Mineralogist*, v. 18, p. 117.
- , 1936, Gravity stratification as a criterion in the interpretation of the structure of the Stillwater Complex, Montana: *International Geological Congress, 16th, 1933, Report*, v. 1, p. 353-360.
- Scheidle, D.L., 1983, Plagioclase zoning and compositional variation in Anorthosite I and II along the Contact Mountain traverse, Stillwater Complex, Montana: Stanford, Calif., Stanford University, 112 p.
- Segerstrom, Kenneth, and Carlson, R.R., 1979, Faulting in banded upper zone of the Stillwater Complex, in *Geological Survey Research 1979*: U.S. Geological Survey Professional Paper 1150, p. 6.
- , 1982, Geologic map of the banded upper zone of the Stillwater Complex and adjacent rocks, Stillwater, Sweet Grass, and Park Counties, Montana: U.S. Geological Survey Miscellaneous Investigations Series Map I-1383, 2 sheets, scale 1:24,000.
- Todd, S.G., Keith, D.W., LeRoy, L.W., Schissel, D.J., Mann, E.L., and Irvine, T.N., 1982, The J-M platinum-palladium Reef of the Stillwater Complex, Montana: I. Stratigraphy and petrology: *Economic Geology*, v. 77, p. 1454-1480.
- Turner, A.R., Wolfgram, D., and Barnes, S.J., 1985, Geology of the Stillwater County sector of the J-M Reef, including the Minneapolis adit, in Czamanske, G.K., and Zientek, M.L., eds., *The Stillwater Complex, Montana: Geology and guide*: Montana Bureau of Mines and Geology Special Publication 92, p. 210-230.
- Wager, L.R., and Brown, G.M., 1968, Layered igneous rocks: Edinburgh, Oliver and Boyd, 588 p.
- Wager, L.R., Brown, G.M., and Wadsworth, W.J., 1960, Types of igneous cumulates: *Journal of Petrology*, v. 1, p. 73-85.
- Zientek, M.L., 1983, Petrogenesis of the Basal zone of the Stillwater Complex, Montana: Stanford, Calif., Stanford University, Ph.D. thesis, 246 p. Also *Dissertation Abstracts International*, v. 45, p. 105B-106B.
- Zientek, M.L., Czamanske, G.K., and Irvine, T.N., 1985, Stratigraphy and nomenclature of the Stillwater Complex, in Czamanske, G.K., and Zientek, M.L., eds., *The Stillwater Complex, Montana: Geology and guide*: Montana Bureau of Mines and Geology Special Publication 92, p. 21-32.

